The Dissertation Committee for Sook Kyung Park Certifies that this is the approved version of the following dissertation:

Studies of Natural Vitamin E Forms and Their Synthetic Derivatives for Potential Anticancer Application in Human Breast Cancer Cell Lines and Mouse Mammary Tumor Models

Committee:

Bob G. Sanders, Co-Supervisor

Kimberly Kline, Co-Supervisor

Stephen D. Hursting

Phillip Tucker

Carla L. Van Den Berg

Studies of Natural Vitamin E Forms and Their Synthetic Derivatives for Potential Anticancer Application in Human Breast Cancer Cell Lines and Mouse Mammary Tumor Models

by

Sook Kyung Park, B.S., M.S.

Dissertation

Presented to the Faculty of the Graduate School of

The University of Texas at Austin

in Partial Fulfillment

of the Requirements

for the Degree of

Doctor of Philosophy

The University of Texas at Austin

August, 2010

Dedication

To my husband, Hak Joong Kim for sharing every minute of my life with compassion, love, and inspiration.

And to my family and parents-in-law for their unconditional love, unwavering cheering, and fullest support.

Acknowledgements

I would like to sincerely thank my supervisors, Dr. Bob G. Sanders and Dr. Kimberly Kline for their continued encouragement, mentoring, academic guidance, and belief in me with patience from the beginning to the end of my graduate career. I would also like to thank my committee members, Drs. Stephen D. Hursting, Philip Tucker, and Carla Van Den Berg for sharing their scientific perspectives on my projects and generously spending their precious time to finalize this dissertation. I am truly grateful to the past and current members of Kline/Sanders lab. Special thanks to Dr. Weiping Yu for her candid advice on my research projects as well as on my career as a scientist; to Drs. Jing Li and Paul Latimer for sharing ups and downs of life in the laboratory; to Dr. Wenbin Chen for synthesizing novel vitamin E derivatives; to Richa Tiwari, Ailian Xiong, Archana Gopalan, and Na Lu for giving their hands to my studies whenever I needed; and to Marla Menchaca for her willingness to help and assist animal studies. And last but not least, I am sincerely thankful to Hak Joong Kim, a medicinal chemist as well as life-time partner who constantly challenges and inspires me.

Studies of Natural Vitamin E Forms and Their Synthetic Derivatives for Potential Anticancer Application in Human Breast Cancer Cell Lines and Mouse Mammary Tumor Models

Publication No._____

Sook Kyung Park, Ph.D.

The University of Texas at Austin, 2010

Supervisors: Bob G. Sanders and Kimberly Kline

Vitamin E is a group of naturally occurring fat soluble compounds which consists of eight distinct forms of tocopherols and tocotrienols. Although a well-defined physiological function of vitamin E is as an antioxidant, beneficial effects of individual vitamin E compounds on chronic human diseases such as cancer need to be better understood. Studies in this dissertation investigated potential application of γ-tocopherol (γ-T), γ-tocotrienol (γ-T3) or synthetic derivatives of tocotrienols as anticancer agents in comparison to α-tocopherol (α-T), its redox-silent acetic acid derivative (α-TEA) or α-tocotrienol (α-T3). Redox-silent derivatives of α- and γ-T3; namely α-T3EA and γ-T3EA exhibited potent anti-proliferative and proapoptotic activities in a murine mammary

cancer cell line as well as in human breast cancer cell lines. Moreover, studies using human vascular endothelial cells in cell culture showed that the tocotrienol derivatives exhibited strong antiangiogenic activities which were markedly improved over those of the parent compounds. An antitumor efficacy study using the 66cl-4-GFP syngeneic mouse mammary tumor model showed that each tocotrienol derivative, when delivered in the diet, significantly suppressed mammary tumor growth; however serum and tissue concentrations of these novel compounds were lower than those of α-TEA, suggesting that the next generation of vitamin E derivatives will need to be modified to improve bioavailability. On the other hand, some natural-source vitamin E forms, especially γ-forms, display anticancer activities without any chemical modification in both *in vitro* cell culture studies and *in vivo* animal models. Dietary delivery of γ-T3 suppressed tumor growth in a syngeneic implantation mouse mammary cancer model by inhibiting cell proliferation and inducing apoptosis. Cell culture studies using human breast cancer cells showed that γ-T3 triggered apoptosis by inducing endoplasmic reticulum (ER)-stress mediated by acid sphingomyelinase (ASMase) action. Activation of stress-activated mitogen-activated protein kinases (MAPKs), JNK and p38, was associated with γ-T3-induced ER stress followed by upregulation of extrinsic death receptor-5 (DR5) expression in a CHOP transcription factor dependent manner. γ-T also triggered extrinsic apoptosis signaling by increasing DR5 mRNA, protein and cell surface expression levels followed by mitochondria-dependent apoptotic signaling. In agreement with *in vitro* studies, γ-T delivered in the diet suppressed the tumor growth of MDA-MB-231-GFP

human breast cancer cells in a *xenograft* model but the antitumor activity of γ-T was hampered by co-administration of α-T. The preferential tissue retention of α-T over γ-T could be overcome by use of sesamin, a dietary source of human cytochrome P450 inhibitor. Based on data presented, γ-T and γ-T3 show preclinical potential for cancer treatment either as single agents or in combination with other agents.

Table of Contents

List of Tables

List of Figures

Chapter 1. Introduction

1.1. An overview of natural vitamin E

1.1.1. Structures and biological functions of natural vitamin E

Vitamin E refers a group of fat-soluble natural compounds that share a chromanol ring and an aliphatic side chain. Based on the degree of saturation of the side chain, vitamin E is divided into two subgroups called tocopherols and tocotrienols. Each subgroup includes α-, β-, γ- and δ-forms based on the number and location of methyl groups on the chroman head (Figure 1.1). Both subgroups are further diversified by stereoisomers: tocotrienols have one chiral center at the C2 position on the chroman head, whereas tocopherols have the C2 chiral center plus two more at the 4′ and 8′ positions on the phytyl tail. All naturally existing vitamin E forms have only *R* configurations. Although different forms of natural vitamin E exist, the term vitamin E is most frequently used to refer to *R,R,R*-α-tocopherol (α-T), the vitamin E form preferentially retained in humans (1). Commercially available vitamin E supplements may contain naturally isolated α-T or synthetic forms or derivatives of α-T. Based on clinical reports regarding vitamin E supplementation, vitamin E is associated with decreased risk of chronic diseases such as cardiovascular diseases, atherosclerotic progression, and neurodegenerative diseases (2). Although a well-defined physiological function of vitamin E is as a fat-soluble antioxidant, various forms of vitamin E have been reported to possess unique biological properties such as anti-inflammatory, anti-thrombotic and

anticancer properties (3, 4). In this regard, tocotrienols have gained attention due to distinctive functions not shared by α-T, such as neuroprotective, anticancer, and cholesterol-lowering activities (4). Another unique property of tocotrienols is the inhibition of angiogenesis which is believed to be a major therapeutic target for various human disorders including cancer, diabetic retinopathy, and rheumatoid arthritis (5, 6). Therefore, a better cellular and mechanistic level understanding of the various forms of vitamin E would be beneficial in establishing more targeted *in vivo* applications as therapeutic agents.

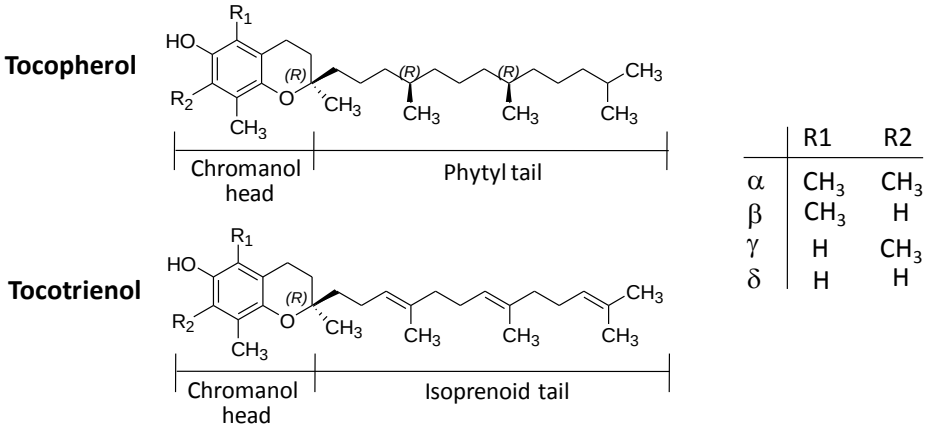

Figure 1.1. Structure of tocopherols and tocotrienols. Naturally occurring tocopherols contain *R*-configurations at the C2 position of the chromanol ring, and C4′ and C8′ position of the phytyl tail, whereas tocotrienols have a *R*-configuration at the C2 position of the chromanol ring.

1.1.2. Absorption and metabolism of vitamin E

The absorption of vitamin E after dietary ingestion is dependent on fat absorption processes (7). Ingested vitamin E is emulsified and mixed into micelles in the small intestine with the aid of bile acids, pancreatic lipases and esterases. The micelles are then transported into the intestinal enterocytes and transferred to the lymphatic fluids in chylomicrons which are delivered to other lipoproteins and tissues (7). In the liver, tocopherol transfer protein (TTP) discriminates between different forms of vitamin E for enrichment of α-T into nascent very low density lipoprotein (VLDL) which is subsequently transformed to low-density lipoprotein (LDL), the major α-T carrier in blood (7). Studies in TTP deficient patients suggest that α-TTP is required for normal α-T absorption and transportation (8). The other vitamin E compounds have lower affinity for TTP and are selectively metabolized in the liver resulting lower circulating and tissue levels (7). Interestingly, animal studies using TTP-deficient mice fed tocotrienols suggest that tocotrienols can be distributed into vital organs via TTP-independent pathway(s) and eliminate α-T deficient symptoms, such as neurological disorders and female infertility (9).

Elimination of absorbed vitamin E involves ϖ-hydroxylation of the phytyl side chain by cytochrome P450 enzyme-dependent processes followed by several steps of β-oxidation (8). Tocotrienols and α-T have been shown to activate pregnane X-receptor, a nuclear receptor that induces gene expression of drug metabolizing enzymes such as CYP3A4

(10). Indeed, CYP3A4 and CYP4F2 are known to be the major P450 enzymes that are involved in vitamin E metabolism (8), which implies that the elimination of vitamin E is tightly regulated after vitamin E ingestion to prevent toxic accumulation. Carboxyethyl-hydroxychroman (CEHC) is the major metabolite of all vitamin E compounds and excreted largely in the urine (Figure 1.2).

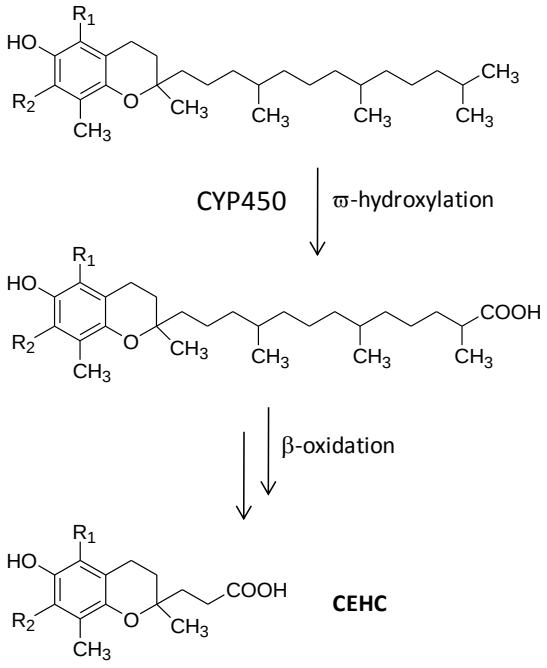

Figure 1.2. Scheme of vitamin E metabolic process to form metabolic products, 2-(2′-carboxyethyl)-6-hydroxychromans (CEHCs) through CYP-mediated ϖ-hydroxylation and multiple steps of β-oxidation (adopted from (7)**).**

1.1.3. Anticancer activities of natural vitamin E

Major efforts have been made to demonstrate a chemopreventive role for vitamin E in cancer; however, neither preclinical nor clinical studies support a beneficial effect of α-T, α-T derivative (*R,R,R*-α-tocopheryl acetate) or synthetic vitamin E acetate derivative (*all-racemic*-α-tocopheryl acetate) on human cancer development (3). Most recently, a randomized, placebo-controlled Selenium and Vitamin E Cancer Prevention Trial (SELECT) was conducted to determine whether 200 μg of selenium or 400 IU of synthetic vitamin E as *all-rac*-α-tocopheryl acetate, or combination of both could prevent prostate cancer and other diseases in healthy men. This trial which started in 2001 and was planned to continue for 12 year was discontinued early in 2008 because there was no evidence of benefit from either agent (11). On the other hand, studies using γ-tocopherol (γ-T) or tocotrienols have demonstrated potent anticancer effects of these compounds in various systems. Although not many clinical or observation studies using these molecules are available, the CLUE studies epitomize the possible chemopreventive effect of γ-T in human prostate cancer (12, 13). The subjects of these studies were male residents of Washington County, Maryland who donated blood in 1974 and 1989. In these subjects, higher serum γ-T level was associated with reduced risk of developing prostate cancer (13). Cell culture studies using various human cancer cells also support anticancer action of γ-T: in human prostate cancer cells, γ-T induced apoptosis by interrupting *de novo* sphingolipid synthesis pathways (14); in human colon cancer cells, γ-T induced apoptosis

in a caspase-8 dependent manner (15); and in human breast cancer cells, γ-T induced death receptor 5 (DR5)-mediated apoptotic signaling by increasing the expression level of DR5 (16). In previous animal studies in our lab, both liposomal and dietary delivery of γ-T reduced tumor burden in a syngeneic 66cl-4-GFP mouse mammary tumor model as well as in the MDA-MB-231-GFP human breast cancer *xenograft* model (17, 18). Notably, anticancer action of γ-T was antagonized by co-treatment with α-T perhaps due to the selective metabolism of γ-T by hepatic cytochrome P450 (CYP) enzymes (18). Tocotrienols had not been studied extensively for their possible benefits to human health due to their limited amounts in natural sources until tocotrienol-rich fraction (TRF) was obtained from palm oil as 68% tocotrienols and 32% α-T (19). Although the exact anticancer mechanism of TRF or individual forms of tocotrienols need to be better understood, a possible therapeutic application of tocotrienols in human cancers has been evaluated using various cancer types including breast cancer, colorectal cancer, gastric adenocarcinoma, liver cancer, lung carcinoma, pancreatic cancer, and prostate cancer (20-26). Possible mechanisms of tocotrienol-mediated inhibition of cell proliferation or apoptosis induction have been proposed in neoplastic murine mammary epithelial cells or human breast cancer cells. Note should be taken that highly malignant mammary epithelial cells are more sensitive to anti-proliferative and apoptotic effects of tocotrienols than preneoplastic cells (27). In malignant mammary epithelial cells, γ-tocotrienol (γ-T3) antagonizes phosphatidyl inositol-3 kinase (PI-3K)/Akt and nuclear factor-κB (NF-κB) signaling pathways, and also induces caspase-8 and -3 mediated

apoptosis (28, 29). δ-tocotrienol (δ-T3) triggers apoptosis which is mediated by upregulation of transforming growth factor-β receptor II (TGF-βRII) and TGF-β-, Fas/CD95-, and c-Jun N-terminal kinase (JNK)-signaling pathways in human breast cancer cells (30). δ-T3 also reduces phosphorylation of retinoblastoma protein (Rb) as well as the expression of cyclin D1/cyclin dependent kinase 4 (CDK4), all of which induces G0/G1 cell cycle arrest (31). In a human breast cancer *xenograft* model, oral gavage of 1 mg/day/mouse of TRF reduces tumor incidence and the area of tumor surface (32) and the dietary delivery of δ-T3 at 62.5 mg/kg bodyweight significantly inhibits the weight of murine melanoma tumors in a syngeneic model (33). In liver or lung carcinogenic studies, oral delivery of a tocotrienol mixture in drinking water suppressed the incidence of spontaneous liver tumor formation or glycerol-induced lung carcinogenesis, suggesting that daily intake of tocotrienols can prevent cancer incidence (24). Tocotrienols are also known to inhibit angiogenesis; thus, have been explored for an application to suppress tumor malignancy (5, 6). Because of the aforementioned advantages to human health, tocotrienols have gained substantial attention during the last decade.

1.2. Synthetic vitamin E derivatives and their anticancer activities

1.2.1. Redox-silent vitamin E derivatives and their anticancer activities

Vitamin E was first discovered in 1922 as a dietary factor required for reproduction in rats (2). Due to the essential nature of vitamin E as a micronutrient, total syntheses of vitamin E or purification from natural sources were of great economic importance (34). To date, the largest amount of manufactured vitamin E is the acetate derivative of synthetic vitamin E, namely, *all-racemic*-α-tocopheryl acetate (*all-rac*-α-T-Ac) which is more resistant to oxidative destruction (35). Another synthetic form that is less common but also commercially available and resistant to oxidation is *R,R,R*-α-tocopheryl succinate (α-TOS) in which succinic acid is coupled to the C6 on the chroman head via an ester bond. After oral intake, these pro-vitamin E forms are liberated into active free α-T or *all-rac*-α-T by pancreatic enzymes in the intestine (36). Intriguingly, the succinate derivative but not the acetate form of α-T exhibits strong apoptogenic activity *in vitro* and anti-tumor/anti-metastatic effects *in vivo* (reviewed by (37)). Although α-TOS exhibits tumor suppressive activity in various preclinical animal studies, its clinical use is hindered due to hydrolysis of the critical succinyl moiety by cellular or intestinal esterases yielding α-T and succinic acid, neither of which has anticancer properties (38). To circumvent the hydrolytic inactivation of the active moiety in α-TOS, the ester-linked succinate moiety at the C6 position of the chroman head was exchanged for an ether-linked acetate moiety to generate a non-hydrolysable α-T derivative, 2,5,7,8-tetramethyl-

2*R*-(4′*R*,8′*R*,12′-trimethyltridecyl)-chroman- 6-yloxy acetic acid (α-tocopheryloxyacetic acid or α-TEA) (Figure 1.3). Consequently, α-TEA is stable as an inducer of apoptosis, while α-TOS is less effective in several cancers that highly express esterases such as ovarian and cervical cancer cells (38). Both α-TOS and α-TEA display pleiotropic anticancer actions selectively to malignant cells: activation of apoptosis, blockage of cell survival and cell proliferation, induction of differentiation, blockade of metastasis, and sensitization of tumor cells to other chemotherapeutic agents (3).

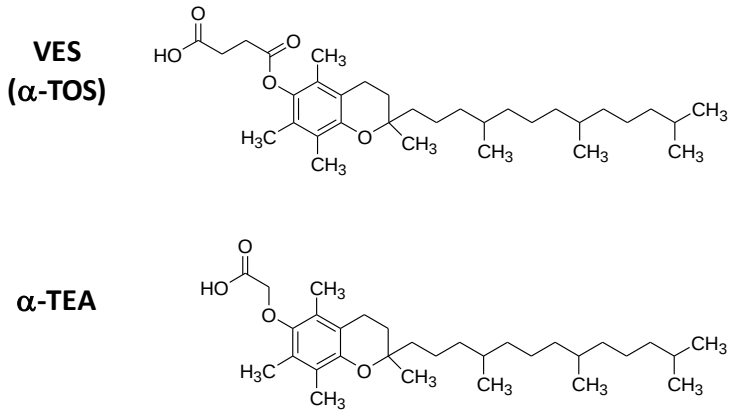

Figure 1.3. Structure of *R,R,R*-α-tocopherol derivatives. *R,R,R*-α-tocopheryl succinate, namley VES or α-TOS, is an ester-linked succinic acid derivative and *R,R,R*-α-tocopheryloxyacetic acid (α-TEA) is an ether-linked acetic acid derivative.

1.2.2. Anti-tumor effects of α-TEA in animal studies

α-TEA has been shown to suppress the growth of tumors in both syngeneic mouse mammary tumor models using highly metastatic 66cl-4-GFP and 4T1 cells as well as in *xenograft* models using immune compromised mice transplanted with human breast cancer cells (MDA-MB-435-GFP), human prostate cancer cells (PC3-GFP) or cisplatin-resistant human ovarian cancer cells (A2780-cp70-GFP) (39-43). α-TEA also showed preventive effects on skin-tumor development in mice exposed to ultraviolet (UV) for 24-weeks (44). Combinational treatment of α-TEA with other cancer therapeutics, such as 9-nitrocamptothecin, celecoxib (a cyclooxygenase-2 inhibitor), cisplatin, and paclitaxel, showed better outcomes than single treatments (41, 43, 45, 46). Since α-TEA is a yellow crystalline chemical which is insoluble in water, delivery of α-TEA in animals has been tried in several different ways. The first animal study was conducted using 87.5% peanut oil with 12.5% ethanol as a solvent for oral gavage of α-TEA. Mice bearing murine mammary tumors received 5 mg/mouse/day for 13 days but no tumor growth inhibition was observed (40). On the other hand, liposomal formulation of α-TEA delivered by aerosol suppressed tumor growth effectively and also reduced lung metastases (40). The estimated amount of aerosolized α-TEA delivered per each mouse/day was 36 μg. Not only aerosol delivery but also the oral gavage of α-TEA (5 to 6 mg/mouse/day) formulated in liposomes exhibited tumor suppressive and metastases inhibitory effects in different animal studies (42, 47), suggesting liposomal formulation

can be an effective way to deliver lipophilic α-TEA. Another approach to α-TEA administration was by incorporating it into a diet. Hahn *et al.* (39) showed that dietary delivery of α-TEA at a concentration of 3.3 g of α-TEA/kg diet (approximately 5 mg/mouse/day) significantly suppressed the growth of 4T1 mammary tumors in mice. In our studies, 250 mg α-TEA/kg diet significantly reduced the mammary tumor growth by 40% compared to the control diet, suggesting that α-TEA can be easily translated to the clinic as a dietary treatment (39).

To investigate *in vivo* antitumor mechanism of α-TEA in mouse models, tumor tissue sections were analyzed for several different cellular markers including Ki-67 for cell proliferation, TUNEL assay for apoptosis, and CD31 for blood vessel formation. Based on several studies, α-TEA increased the percentage of tumor cells undergoing apoptosis and decreased the number of tumor cells undergoing proliferation. Neither CD31 positive cell numbers nor blood volume in tumor showed significant differences from control groups (45), indicating that α-TEA exerts tumor suppressive effects by directly acting on tumor cells rather than targeting blood vessel formation in the tumor.

1.2.3. Anticancer mechanism of α-TEA in cancer cells

Since α-TEA induces tumor cell apoptosis and inhibits tumor cell proliferation in animal studies, efforts have been made to identify possible cellular target(s) of α-TEA using a wide variety of human cancer cell lines. Anderson *et al.* showed that normal human mammary or prostate epithelial cells or non-tumorigenic breast cells did not respond to

α-TEA action to induce apoptosis, but various types of human cancer cells including breast, cervical, ovarian, endometrial, prostate, colon and lung cancer cells underwent apoptosis in a dose- and time-dependent manner after α-TEA treatment (38). Since then, most of the studies in our lab have focused on indentifying tumor-selective anticancer mechanisms of α-TEA using various types of human cancer cells including cisplatin-sensitive and resistant human ovarian cancer cells in cell culture. Cisplatin is a platinum-based DNA-damaging agent that is used as a first line chemotherapeutic for ovarian cancer patients; however, its side effects and intrinsic or acquired resistance limits its use in clinical practice (43). Although cisplatin-resistant A2780/CP70 cells are less sensitive to α-TEA treatment, α-TEA works as a proapoptotic agent in both cisplatin sensitive and resistant human ovarian cancer cells (48). Therefore, α-TEA can be used as a potential therapeutic agent that can substitute for or as an adjuvant to the first line chemotherapeutic approach. In these ovarian cancer cells, α-TEA activates caspase-dependent proapoptotic pathway by enhancing a cell surface death receptor, Fas signaling followed by caspase-8 activation, tBid translocation to the mitochondrial fraction, cytochrome C release, caspase-9 activation; as well as caspase-3 activation and PARP cleavage (48). α-TEA also inhibits prosurvival pathways through the downregulation of extracellular signal-regulated kinase (ERK1/2) and protein kinase B (Akt) (48). Further studies showed that the expression of epidermal growth factor receptors (EGFR) and anti-apoptotic proteins such as cellular FLICE-like inhibitory protein (FLIP, a caspase 8 inhibitor) and survivin were down-regulated following α-TEA treatment (49).

Overexpression of EGFR family members and the activation of downstream proteins such as Akt, FLIP, and survivin is frequently observed in many types of human cancer and directly associated with poor prognosis. Therefore, the ability of α-TEA to induce apoptosis selectively in cancer cells by activating pro-apoptotic death receptor signaling as well as by downregulating pro-survival and anti-apoptotic signaling pathways in cancer cells makes α-TEA an important candidate as an anticancer drug.

Since increases in Fas expression at both mRNA and protein levels after α-TEA treatment was observed in various cancer cell types, the role of Fas signaling in α-TEA-induced apoptosis was studied using human breast and prostate cancer cells. Fas-neutralizing antibodies or silencing Fas or Fas ligand (FasL) using small interfering RNA (siRNA) partially protect cells from the apoptosis induced by α-TEA treatment (48, 50). Several studies reported that c-Jun N-terminal kinase (JNK), a stress-activated protein kinase, plays a critical role in α-TEA-induced apoptosis in various cancer cell types (30, 48, 50); however the exact target of JNK activated by α-TEA was not very clear until Jia *et al*. found the link between JNK activation and Fas signaling (50). In human prostate cancer cells, Fas not only activates caspase 8 through the classical death receptor signaling pathway followed by caspase 9 and 3 activations, but also associates with Daxx, a death domain associated protein which leads to the activation of JNK after α-TEA treatment. Interestingly, c-Jun activated by JNK upon α-TEA treatment directly binds to

the promoter region of Fas and Fas L suggesting the possibility of a positive feedback loop that further amplifies the apoptotic response triggered by α-TEA in cancer cells (50).

cDNA microarray analyses of human breast cancer cell-line, MDA-MB-435 treated with α-TEA added more insights into understanding the pleiotropic anticancer activities of α-TEA in cancer cells (51). Over 400 genes were modulated after α-TEA treatment and 34 genes have been further classified for their functions regarding involvement in apoptosis, cell-cycle regulation, signal transduction, transcriptional regulation, cell adhesion and motility, and membrane trafficking (51). Among these genes, the gene coding for NOXA, a pro-apoptotic and BH3-only member of the Bcl-2 family has been shown to be upregulated in a JNK-dependent manner after α-TEA treatment of human breast cancer cells (51). In these cells, JNK also regulated the expression of p73, a member of the p53 family which can recognize p53 response elements. It is still unclear whether p73 directly binds to the promoter region of NOXA; however data suggest that the activation of JNK is required for the upregulation of p73 which affects increased NOXA level as well as the apoptotic response after α-TEA treatment (51). Based on these cellular studies, proposed anticancer action of α-TEA in cancer cells is summarized in Figure 1.4.

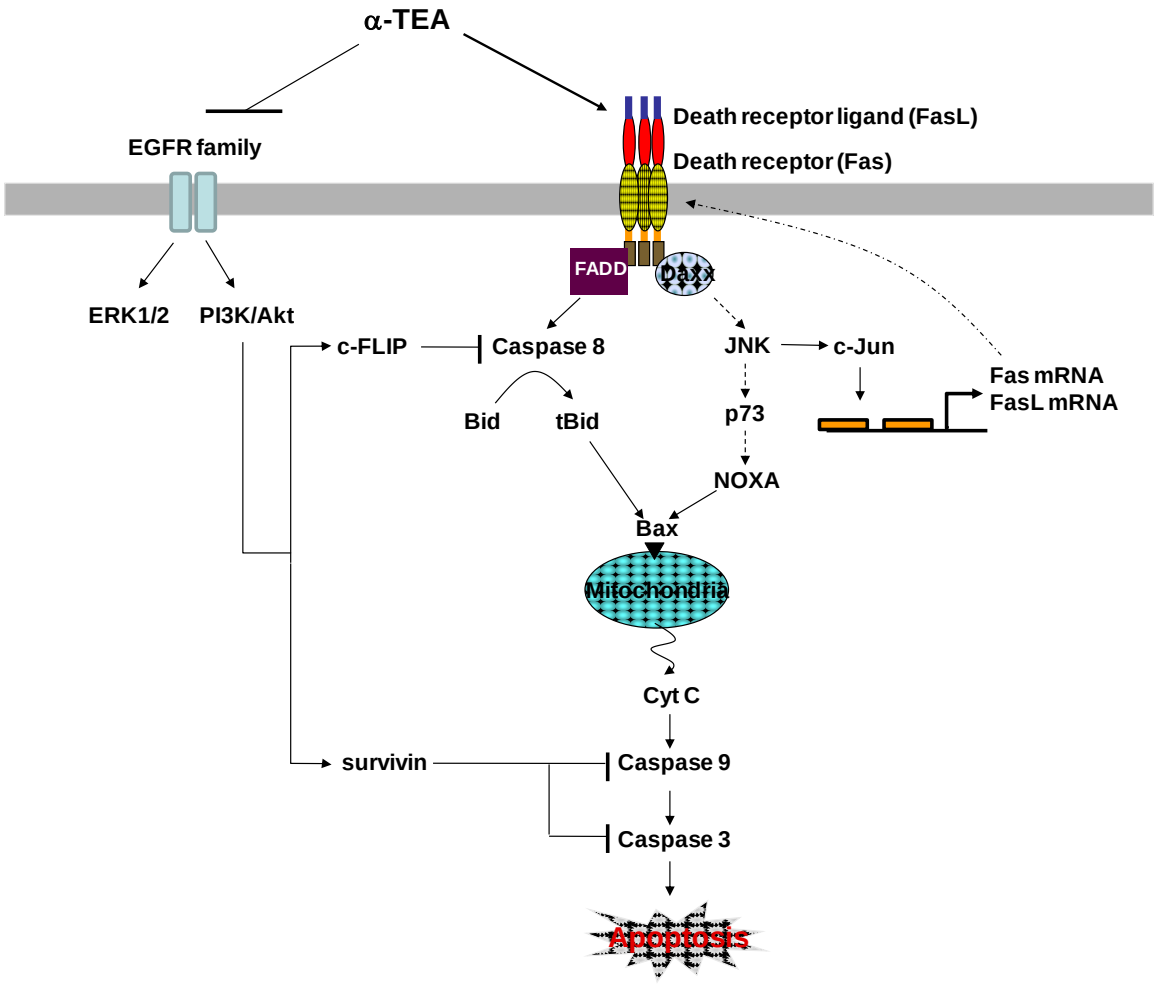

Figure 1.4. Schematic diagram of anticancer action of α-TEA via inhibiting pro-survival pathways as well as enhancing death receptor signaling pathways in human cancer cells. α-TEA decreases the protein level of EGFR family members; downregulates the phosphorylation of ERK1/2 and Akt; and also reduces expression of inhibitors of apoptosis, such as c-FLIP and survivin. At the same time, α-TEA activates Fas/FasL mediated apoptosis signal transduction followed by caspase 8 activation which eventually causes mitochondria-mediated caspase 9 activation. Fas signaling enhanced by α-TEA induces activation of JNK and c-Jun which directly increase gene expression of Fas and FasL; as well as protein levels of p73 and NOXA, all of which amplify the apoptotic response.

1.3 Endoplasmic reticulum stress and effects on cell fate

1.3.1. Unfolded protein response

The endoplasmic reticulum (ER) serves critical functions in synthesis and folding of secreted, membrane-bound, or organ targeted proteins and their transport; metabolic processing of lipids, steroids and carbohydrates; as well as, regulation of intracellular calcium concentration in eukaryotic cells (52, 53). Disruption of ER functions under various cellular stresses such as hypoxia, glucose deprivation, depletion of calcium ions, or viral infection can increase unfolded or misfolded protein build-up within the ER causing further ER stress followed by activation of the unfolded protein response (UPR). The lumen of the ER contains a chaperon, called glucose-regulated protein of 78 kDa (GRP78) also known as BiP, that is a critical regulator of intracellular signaling pathways under ER stress. In unstressed cells, GRP78 physically interacts with three ER resident transmembrane transducers: pancreatic ER kinase-like ER kinase (PERK), inositol-requiring enzyme 1 (IRE1), and activating transcription factor 6 (ATF6) (54). When unfolded proteins accumulated in the ER, GRP78 is redirected to aid protein folding thereby releasing these transducers, which allows their activation. Through the UPR, cells can adapt to environmental changes by enhancing protein folding capacity; activate NF-κB signaling pathway that induces genes required for host defense and survival; and ultimately triggers apoptosis if the stress is excessive or prolonged (52).

1.3.2. Mediators of UPR

Under ER stress, global gene expression is halted at the translational level by PERK, a Ser/Thr kinase that accumulates and is activated after its detachment from GRP78. The major substrate of PERK is eukaryotic translation initiation factor 2 (eIF-2) which becomes phosphorylated by PERK and is thereby rendered unable to deliver initiator met-tRNA to the translational machinery (55). Certain proteins such as activating transcription factor 4 (ATF4) gain advantage by the inactivation of eIF-2. ATF4 is a basic leucine zipper (bZIP) transcription factor which targets genes involved in the restoration of cellular redox homeostasis and protein folding including ER chaperons, GRP78 and GRP94 (53).

IRE1, the other transducer oligomerized upon release from GRP78, contains both a Ser/Thr kinase domain and an endoribonuclease domain (52). The Ser/Kinase domain of IRE1 autophosphorylates itself, which not only activates its endoribonuclease activity but also recruits adaptor protein, tumor necrosis factor receptor associated receptor-associated factor-2 (TRAF2) followed by apoptosis-signal-regulating kinase 1 (ASK1) recruitment (56). ASK1, an upstream kinase of JNK and p38 MAPK, is activated by various stress signals including oxidative stress and calcium overload (57). The major consequence of ASK1 activation under ER stress is activation of cell death signaling pathways mainly via JNK which modulates activity of BCL2 protein family members (58). Although a role for p38 MAPK in ER-stress mediated apoptosis is yet to be confirmed, overexpression and knockout studies showed that ASK1 plays a pivotal role

in ER-stress mediated apoptosis (58). While IRE1 transduces cell death signaling via TRAF2-ASK1-JNK, the endonuclease activity of IRE1 processes the mRNA encoding X-box-binding protein (XBP1) to generate a splice variant encoding an active transcription factor which regulates expression of several genes involved in ER-associated degradation (ERAD) and proper protein folding (58, 59).

GRP78 also releases ATF6, a b-ZIP family member transcription factor, similar to ATF4. When detached from ER membrane, ATF6 translocates to the Golgi apparatus for proteolytic processing of a juxtamembrane site resulting in an active transcription factor. The active form of ATF6 is released into the cytosol and translocates to the nucleus (53). Target genes of ATF6 include XBP1, GRP78 and protein disulfide isomerate (PDI), all of which regulate ER homeostasis by increasing ER chaperon activity and degradation of misfolded proteins (53).

1.3.3. C/EBP homologous protein (CHOP), a component of ER stress-mediated apoptosis

CHOP, also known as growth arrest- and DNA damage-inducible gene 153 (GADD153), is a 29 kDa transcription factor upregulated at multiple levels during ER stress (60). The promoter region of CHOP has at least four distinct *cis*-acting elements to which ATF4, ATF6 and XBP-1 bind (61). In addition, p38 MAPK, one of the downstream kinases activated by IRE1 under ER stress phosphorylates Ser78 and Ser 81 of CHOP thereby

enhancing CHOP transcriptional activity (61). Thus, CHOP is a key transcription factor that is highly induced and activated during ER stress.

The role of CHOP upregulation during ER stress has been studied in various systems. A dominant negative form or targeted disruption of CHOP delays ER stress-induced cell death, whereas overexpression of CHOP markedly reduces cell viability (62, 63), suggesting that CHOP connects persistent and overwhelming ER stress to the onset of cellular apoptosis. Target genes of CHOP related to UPR include the mammalian homolog of yeast ER oxidase (ERO1α) that is responsible for the accumulation of reactive oxygen species in ER-stressed cells; and GADD34, a regulatory protein that is required to reverse the early translational repression during various cellular stresses including UPR (60). CHOP also regulates gene expression of BCL2 protein family members: Bcl-2, an anti-apoptotic protein, is down-regulated by CHOP although it is not clear if CHOP directly binds to the promoter sites of Bcl-2; and Bim, a proapoptotic BH3 only member of the BCL2 family is transcriptionally induced by CHOP (64, 65).

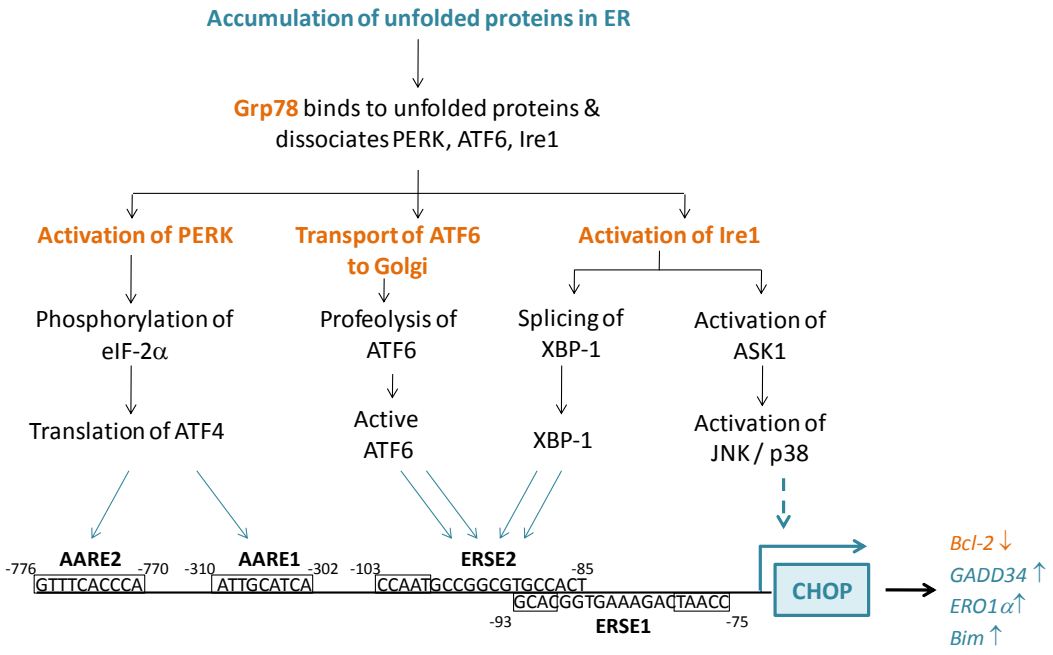

Figure 1.5. Schematic diagram of transcriptional induction of CHOP/GADD153 under ER stress. When unfolded or misfolded proteins accumulated in the ER, GRP78, an ER chaperon relocates to promote protein folding and dissociates from three transducers, PERK, ATF6, and IRE1 followed by activation of the UPR response. When released from GRP78, PERK phosphorylates eIF-2α which induces global translational suppression and the induction of ATF4. IRE1 has both a kinase activity as well as an endoribonuclease activity. While ASK1 phosphorylated and activated by IRE1 further activates downstream kinases, *Xbp-1* mRNA is processed by endoribonuclease acvitiy of IRE1 and is translated into a stable transcription factor. ATF6 is translocated from ER to Golgi for proteolytic processing and then localized into the nucleus for transcriptional regulation. All transcription factors, ATF4, ATF6 and XBP-1, directly bind to the *cis*-acting elements of *CHOP* and induce its expression (adapted from (61)).

1.4. Role of TNF-related apoptosis inducing ligand (TRAIL) in apoptosis

1.4.1. Pathways of apoptosis

Apoptosis, a well characterized process of programmed cell death, occurs during embryogenesis and metamorphosis, and helps to maintain tissue homeostasis (66, 67). Unlike necrosis which is generally mediated by external factors such as injuries or infection and subsequent inflammation, apoptosis is a highly ordered process regulated by complex and sophisticated pathways which eventually lead to characteristic morphological changes of a cell: dense cytoplasmic organelles, DNA fragmentation, chromatin condensation, cellular blebbing and shrinkage (67, 68).

Biochemically, apoptotic pathways involve hierarchical activation of cysteine-dependent aspartate-directed proteases (caspases), and this sequential proteolytic cascade amplifies the apoptotic signal leading to rapid cell death (67, 69). Caspases are synthesized as inactive zymogens with prodomains which are bound to regulatory proteins preventing unregulated activation (68). Upon apoptotic triggers, initiator caspases such as caspase-8 or -9 are recruited to upstream adaptor molecules which provide a platform for initiation of autocatalytic cleavage of their prodomains followed by proteolytic activation of effector caspases such as caspase-3 or -7 resulting in the execution steps of apoptosis (70).

Depending on the origin of apoptotic cue, initiator caspases can be activated by two main pathways: the intrinsic pathway activated by DNA damage and the extrinsic pathway involving interaction between transmembrane death receptors and extracellular ligands (67). The intrinsic pathway is a mitochondrial-initiated multi-step process activated by

various cellular stresses including UV radiation, chemotherapy, starvation, and hypoxia (68). Members of the Bcl-2 protein family control and regulate mitochondrial membrane permeability (67). Loss of mitochondrial membrane potential and permeability promotes release of factors into the cytoplasm forming a protein complex; namely, the apoptosome that activates initiator caspase-9 and effector caspases (68). The extrinsic pathway involves engagement of cell surface death receptors (DR) with the tumor necrosis factor (TNF) family of cytokines including TNF, Fas ligand (FasL), and TNF-related apoptosis-inducing ligand (TRAIL) (71). This ligand-receptor interaction induces formation of the death inducing signaling complex (DISC) comprised of multimerized death receptors and death domain (DD)-containing adaptor proteins such as Fas-associated death domain, FADD (72). DISC recruits procaspase-8, and activates caspase-8 and other effector caspases subsequently. Crosstalk between extrinsic and intrinsic pathways is mediated by the proapoptotic Bcl-2 homology 3 (BH3)-only protein, Bid, when it is cleaved by extrinsic pathway activated-caspase 8 (72). Truncated Bid (tBid) translocates to mitochondrial membrane and promotes intrinsic apoptotic signaling pathway by employing proapoptotic Bcl-2 family proteins, Bax and Bak resulting in mitochondrial membrane permeabilization and formation of the apoptosome.

1.4.2. TRAIL and death receptors

TRAIL, also known as Apo2L, is a transmembrane protein and a member of the TNF superfamily which shares conserved C-terminal domains required for receptor binding (68). A soluble form of TRAIL has been found in serum following proteolytic cleavage of its extracellular domain by activated monocytes and neutrophils (73). So far, two agonistic receptors (TRAIL-R1/DR4 and TRAIL-R2/DR5) and three antagonistic receptors (TRAIL-R3/DcR1, TRAIL-R3/DcR2 and osteoprotegerin/OPG) have been reported to interact with human TRAIL (74). Both DR4 and DR5 are type I transmembrane proteins containing an extracellular cysteine-rich domain and a cytoplasmic death domain (DD). The crystal structure of TRAIL and DR5 revealed that the trimeric ligand is interdigitated with three monomeric receptors (73). Trimerized receptor death domains recruit FADD through its own DD at the C-terminus followed by the recruitment of procaspase-8 via N-terminus death effector domain (DED). On the other hand, antagonistic receptors, DcR1 or DcR2 lack functional death domains; and thus, impair the downstream apoptotic signaling cascade (74).

1.4.3. TRAIL in cancer therapy

TRAIL mRNA and protein are present in a diverse range of tissues; however, cell surface expression of TRAIL is not observed in resting normal cells which express high level of decoy receptors, DcR1 or DcR2, sequestering TRAIL (68). Some subsets of macrophages, lymphocytes and dendritic cells when activated by proinflammatory cytokines or virally

infected fibroblasts upregulate their cell surface expression of TRAIL and/or death receptors, implicating a possible role of TRAIL in innate immunity (68). Importantly, studies have shown that some types of cancer cells express high levels of DR4 or DR5 and low levels of decoy receptors (68). Therefore, TRAIL has been recognized as a potential anti-tumor therapeutic with the major advantage that it will trigger apoptosis selectively in cancer cells producing little to no toxicity in normal cells (74). The first attempt to use recombinant soluble TRAIL as an anticancer agent in clinical studies failed to show promising effects due to its short half-life and rapid clearance from circulation (75). Nevertheless, different formulations of TRAIL as well as alternative approach to targeting TRAIL signaling are currently in phase I/II clinical studies (75). Trials using recombinant human TRAIL (rhTRAIL), a receptor-selective variant of TRAIL, as well as DR4- and DR5-selective agonistic antibodies as single agents or in combination therapy are being tested for ability to improve patient disease free survival (75).

1.4.4. Cancer cell resistance of TRAIL

One of obstacles of targeting TRAIL signaling as an anticancer approach is that numerous tumors are not responsive to TRAIL-induced apoptosis due to several different inhibitory mechanisms (73). One of the proposed inhibitory mechanisms is that decoy receptors (DcR) in cancer cells may compete with agonistic death receptors for TRAIL binding; therefore, the ratio of DRs/DcRs at the cell membrane may determine sensitivity to TRAIL in some cancers that express both DRs and DcRs (74). Defective DRs may also

contribute to TRAIL-resistance. Best known examples are breast cancer cells that generally express very low level of DcRs but display resistance to TRAIL due to defective DR4 expression and/or loss of cell surface DRs (76). In addition to low or deficient DR4 expression, polymorphic DR4 death domains contribute to TRAIL insensitivity in several different types of cancer cells (77). Another important determinant is the presence of or defective internal regulators. Cells with inactive caspase-8 due to epigenetic silencing fail to transmit TRAIL-induced apoptotic signaling (78); and elevated expression of c-FLIP (FLICE-inhibitory protein), an inhibitor of caspase-8 activation, also shows correlation with TRAIL-resistance (77). High expression of inhibitor-of-apoptosis proteins (IAP), such as X-linked IAP (XIAP) or anti-apoptotic Bcl-2 proteins are also linked to TRAIL resistance (75). Therefore, various strategies are currently being tested using chemotherapeutics as well as natural compounds to restore TRAIL sensitivity in TRAIL-resistant cancer cells as summarized in Figure 1.6.

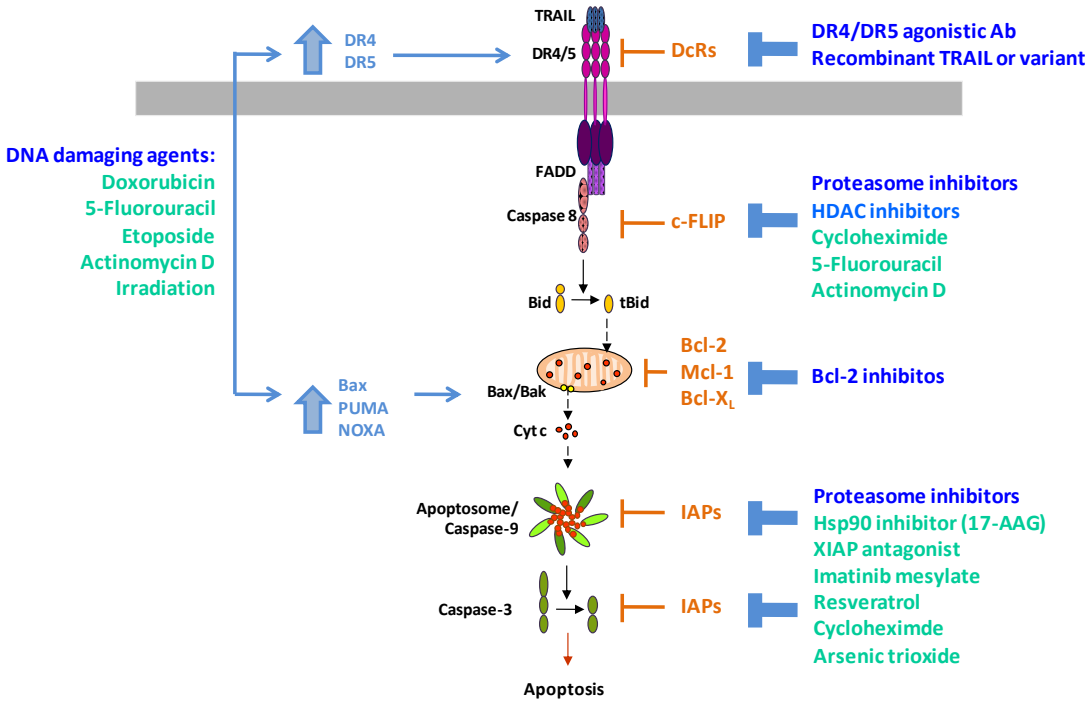

Figure 1.6. Mechanisms of TRAIL resistances (in orange color) and therapeutic strategies to restore TRAIL sensitivity (in blue color). Binding of TRAIL to DR4/DR5 triggers apoptosis in tumor cells by recruiting FADD to form the death inducing signaling complex (DISC) which attracts procaspase-8 and initiates its activation. Active caspase-8 can directly activate execution caspases and/or cleave Bid to tBid which translocates to mitochondrial membranes leading to the formation of Bax/Bak pores in the outer mitochondrial membrane. Mitochondrial membrane permeability is increased and cytochrome *c* is released into the cytosol triggering formation of apoptosomes and activation of caspase-9 followed by activation of executioner caspases (caspase-3 or -7). Decoy receptors (DcRs) can block the activation of DR4/DR5 when expressed at high levels in some tumor cells. Novel therapies using DR4/DR5 selective TRAIL variant or receptor specific agonistic antibodies are currently under investigation. Several DNA damaging reagents are also known to induce increases of DR4/DR5 levels on the cell surface membrane thereby potentiating TRAIL induced apoptosis. Downstream signaling of DR4/DR5 can be blocked by c-FLIP which can be targeted by several chemotherapeutic agents shown to down-regulate c-FLIP. Anti-apoptotic Bcl-2 family proteins (Bcl-x_L, Mcl-1 and Bcl-2) can block the delivery of apoptotic signals, which can be overcome by small molecule Bcl-2 inhibitors. Inhibitor of apoptosis proteins (IAP) are another class of downstream inhibitors of TRAIL-induced apoptosis. Several natural compounds and therapeutic agents are proposed to re-sensitize cells displaying IAPs-mediated TRAIL resistance. In p53 expressing tumor cells, DNA damaging agents and radiation therapy can sensitize cells to TRAIL-induced apoptosis by up-regulating several genes including DR4/DR5, and the BH3-only proteins Bax, Puma and Noxa (adapted from (75)).

1.5. Objective and specific aims

Studies in our lab have been focused on the therapeutic potential of a non-hydrolyzable ether derivative of α-T (α-TEA: 2,5,7,8-tetramethyl-2*R*-(4′*R*,8′*R*,12′-trimethyltridecyl)-chroman-6-yloxy acetic acid or α-tocopheryloxyacetic acid) which has an acetic acid moiety attached via an ether-linkage at the C6 position of the α-TEA chroman head (3, 37). α-TEA displays pleiotropic anticancer actions selectively to malignant cells: induction of apoptosis, blockage of cell survival, inhibition of cell proliferation, induction of differentiation, blockade of metastasis, and sensitization of tumor cells to other anticancer drugs (3). Considering that α-TEA exhibits a broad spectrum of anticancer activity while the parent compound α-T has modest to no anticancer activity and lacks any consistent documentation of anticancer activity in humans, modification of tocotrienols known to have beneficial effects on inhibiting cancer cell growth posses an intriguing possibility for the development of more effective vitamin E-derived therapeutic drugs. In addition, characterization of the anticancer mechanism of different forms of natural vitamin E as well as the interactions between/among various forms of natural vitamin E during metabolism need to be investigated to identify the most beneficial vitamin E form for anticancer approach, as well as to increase public understanding of the advantages and disadvantages of vitamin E supplementation.

Thus, my studies focused on the following: 1) define the potential of tocotrienol derivatives to serve as potent anticancer drugs; 2) identify the anticancer mechanisms of

the parent tocotrienol compounds to better understand their mode of action; and 3) evaluate the anticancer effects of γ-T, the most abundant form of vitamin E in US diet, and define its mechanism(s) of action. Through these studies, we have gained important insights into the development of novel vitamin E derivatives as cancer therapeutics, and also obtained a better understanding of the anticancer mechanisms of action of different forms of natural vitamin E.

Contents in Chapter 1 have focused on background information and review of the literature. Chapter 2 is focused on the development of novel tocotrienol derivatives and their effects on human breast cancer cells and mouse mammary tumor cells in cell culture. Antitumor effects of each derivative in a syngeneic mouse mammary tumor model are also addressed. Chapter 3 describes anticancer mechanisms of tocotrienols in breast cancer cells in cell culture and the role that endoplasmic reticulum (ER)-stress plays in tocotrienol-mediated apoptosis. Chapter 4 documents the anticancer effect of γ-T in human breast cancer cells and in a mouse *xenograft* tumor model. Chapter 5 summarizes the studies and discusses future directions for research.

Chapter 2. Anti-cancer and antiangiogenic effects of novel tocotrienol derivatives

Breast cancer is the most common cancer diagnosed in US women. Even though early diagnosis has reduced the rate of metastasis and mortality, breast cancer still ranks as the second leading cause of death from cancer in US women. There is a need for better chemotherapeutic agents for this disease. Previous studies in our lab have characterized the anticancer efficacy of a novel non-hydrolysable ether derivative of *R,R,R*,-alpha-tocopherol, namely α-TEA (2,5,7,8-tetramethyl-2R-(4R,8R,12-trimethyltridecyl) chroman-6-yloxy acetic acid). In this study, non-hydrolysable ether derivatives of other forms of vitamin E; namely, α-tocotrienol (α-T3) and γ-tocotrienol (γ-T3) were synthesized and tested for their anticancer activities in comparison to α-TEA. These novel tocotrienol agents exhibited strong anti-proliferative and proapoptotic activities in murine mammary cancer cells and in both estrogen receptor (ER) positive and negative human breast cancer cells. Notably, studies in human vascular endothelial cells (HUVECs) showed that tocotrienol derivatives exhibited strong antiangiogenic activities which were markedly improved over those of the parent compounds. An antitumor efficacy study using the 66cl-4-GFP syngeneic mouse mammary tumor model showed that each tocotrienol derivative, when delivered in the diet, significantly suppressed mammary tumor growth as much as α-TEA; however serum and tissue concentration of these novel derivatives were lower than those of α-TEA, which suggest that the next generation of vitamin E derivatives will need to be modified to improve bioavailability.

2.1. Introduction

Vitamin E refers to a group of natural compounds which share similar structure, a chromanol ring and an aliphatic side chain. Vitamin E is divided into two subgroups which consist of tocopherols and tocotrienols, and each subgroup includes four individual forms as α-, β-, γ- and δ-tocopherols and α-, β-, γ- and δ-tocotrienols respectively. Efforts to prove a possible role for vitamin E in cancer prevention have been made; however neither preclinical nor clinical studies support a beneficial effect of the major form of vitamin E (α-T), synthetic vitamin E (*all-rac*-α-tocopherol) or their acetate derivatives on human cancer development (3). On the other hand, the other subgroup of vitamin E, tocotrienols, although not as abundant as α-T, exhibits various distinctive functions not shared by α-T, such as neuroprotective, anticancer, and cholesterol-lowering activities (4). While α-tocotrienol (α-T3) has potential to prevent neurodegeneration, γ- and δ-tocotrienols (γ-T3, δ-T3) are reported to display potent anticancer properties (4, 20). Studies using human breast cancer cells or murine neoplastic mammary epithelial cells demonstrated that both γ-T3 and δ-T3 exert anti-proliferative and pro-apoptotic effects (28-30). The intracellular mechanisms of γ-T3-mediated growth inhibition is via antagonizing phosphatidyl inositol-3 kinase (PI-3K)/Akt and NF-κB signaling pathways. These pathways play a critical role in growth factor-induced cell growth and survival, and are frequently mutated or amplified in human cancers (29). Another unique property of tocotrienols is the inhibition of

angiogenesis which is believed to be the major therapeutic target against various human disorders including cancer, diabetic retinopathy, and rheumatoid arthritis (6).

Studies in our lab have been focused on the therapeutic potential of redox-silent vitamin E derivatives as anticancer agents (3, 37). To date, α-tocopheryl succinate (VES or α-TOS) and a non-hydrolyzable ether derivative of α-T (α-TEA: 2,5,7,8-tetramethyl-2*R*-(4′*R*,8′*R*,12′-trimethyl-tridecyl)chroman-6-yloxy acetic acid or α-tocopheryloxyacetic acid) are the most studied compounds. Although VES exhibits tumor suppressive activity in various preclinical animal studies, its clinical use is hindered by the hydrolysis of the critical succinyl moiety by cellular or intestinal esterases yielding α-T and succinic acid, neither of which have anticancer properties (38). In contrast, the C6 position of the α-TEA chroman head is attached to an acetic acid moiety via an ether-linkage which is stable in hydrolytic environments. Consequently, α-TEA is stable as an inducer of apoptosis while VES is less effective in several cancers that highly express esterases such as ovarian and cervical cancer cells (38, 43). Considering that both VES and α-TEA exhibit a broad spectrum of anticancer activities while the parent compound α-T has modest to no anticancer activity and lacks any consistent documentation of anticancer activity in humans, modification of the other natural vitamin E compounds known to have beneficial effects on cancer intervention posses an intriguing possibility for the development of more effective vitamin E-based therapeutic drugs.

In this study, we chemically modified α-T3 and γ-T3 to generate redox-silent tocotrienol derivatives. These novel compounds were tested for their anticancer and anti-angiogenic activities in murine mammary cancer cells, human breast cancer cells, and human umbilical vascular endothelial cells in cell culture. Finally, tumor-suppressive activities of novel tocotrienol derivatives compared to the parent compound or α-TEA were tested in the 66cl-4-GFP syngeneic murine mammary tumor model.

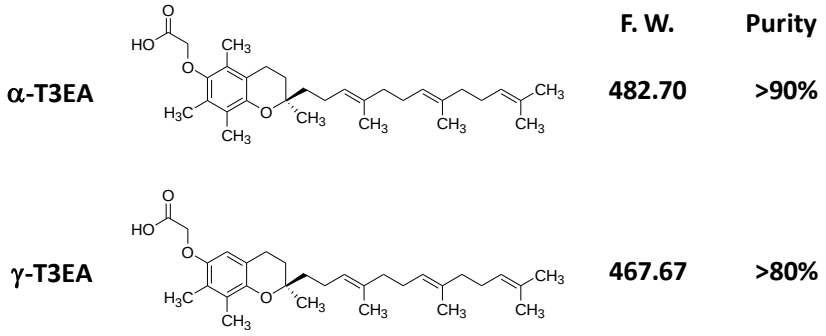

Figure 2.1. Structures of novel tocotrienol derivatives. The hydroxyl group at the C6 position of the chroman head of α-T3 and γ-T3 was modified to become an ether-linked acetic acid, generating *R*-α-tocotrienyl-oxyacetic acid (α-T3EA) and *R*-γ-tocotrienyloxyacetic acid (γ-T3EA), respectively. The purity of each compound was determined using NMR spectroscopy.

2.2. Materials and Methods

2.2.1. Chemicals

α-T3 and γ-T3 used to synthesize novel derivatives were kindly provided by the Malaysian Palm Oil Board (Malaysia). The ether-linked acetic acid derivative of α-T3, namely α-T3EA, was synthesized by Dr. Jeffrey Atkinson (Department of Chemistry, Brock University, St. Catharines, Ontario, Canada) and the derivative of γ-T3, namely γ-T3EA, was prepared by Dr. Hakjoong Kim (Department of Chemistry and Biochemistry, University of Texas at Austin, Austin, TX) based on the chemical synthesis of α-TEA as described previously (40). The purity of new derivatives was determined using NMR spectroscopy. The structure and the purity of each ether-linked acetic acid derivative are shown in Figure 2.1. Relatively low purity (>80%) of γ-T3EA is due to impurities in the parent compound, γ-T3. The major impurity (approximately 10%) in γ-T3 is considered to be β-T3 based on NMR analyses.

2.2.2. Cell culture and reagents

The source and culture conditions for 66cl-4-GFP murine mammary tumor cells were previously described (79). MDA-MB-231 and MCF-7 human breast cancer cells were obtained from the American Type Culture Collection (ATCC), cultured and maintained in MEM medium as previously described (18). All media were supplemented with 10% fetal bovine serum (HyClone Laboratories, Logan, UT), 100 U/ml penicillin, and 100

mg/ml streptomycin. Human mammary epithelial cells (HMEC; Cooperative Human Tissue Network, Birmingham, AL) were primary cultures of human mammary cells derived from normal mammoplasty specimens as described previously (80). For treatments, FBS was reduced to 2% to better mimic the *in vivo* low serum exposure of these cell types. Human umbilical vascular endothelial cells (HUVECs) were purchased from Lonza (Basel, Switzerland), cultured and maintained in EGM2 endothelial cell medium (Lonza) following manufacturer's instructions.

2.2.3. Cell proliferation assay (MTS assay)

Effect of novel derivatives on cell proliferation was assessed in cell culture. MDA-MB-231 or MCF-7 cells at $5X10^3$/well, 66cl-4 cells at 10^4/well and HUVECs at $2.5X10^5$/well were seeded in 96-well plates. Cells were treated with a range of concentrations from 5 to 40 µM of each compound. Control cells were treated with the vehicle (ethanol) at a final concentration of 0.1%. After 24 hrs, viable cells were measured using CellTiter 96® AQueous Non-Radioactive Cell Proliferation Assay (Promega, Corp., Madison, WI) following manufacturer's instructions. The percentage of viable cells at each concentration was calculated by dividing color absorbance (A490) of treated cells by that of control cells. The IC_{50} of each compound was determined using BioDataFit 1.02 (http://www.changbioscience.com/stat/ ec50.html).

2.2.4. Evaluation of apoptosis [Annexin V-FITC/Propidium iodide (PI) assay]

Percentage of apoptotic cells after treatments was determined using an Annexin V-FITC/PI assay as previously described (16). Briefly, cells were collected at indicated time points and resuspended in Annexin V binding buffer (10 mM HEPES (pH7.4), 150 mM NaCl, 5 mM KCl, 1 mM $MgCl_2$, 1.8 mM $CaCl_2$). Cells were incubated with Annexin V-FITC (Invitrogen, CA) for 8 minutes at room temperature. Cells were then diluted in PI solution (50 ng/mL in PBS) and fluorescence was measured with flow cytometer (FACSCalibur, BD Biosciences, San Jose, CA). Data were analyzed using CellQuest software (FACSCalibur, BD Biosciences).

2.2.5. *In vitro* wound healing assay

HUVEC migration was assessed using a wound healing assay as described by Staton *et al*. (81). Cells were seeded onto 24-well plates and permitted to reach confluence. Using a sterilized 500 μl pipet tip, a straight line clearance of cells was made through the cell monolayer. The wounded cell monolayer was treated with 2.5, 5 or 10 μM of each compound and incubated for 15 hrs. Wounded morphologies at time 0- and 15-hr of treatment were recorded with a digital camera (Olympus DP71) connected to an inverted microscope (Olympus 1X71). Treatments were performed in triplicate. The cell-free area was analyzed using ImageJ 1.38x software (NIH, USA). The degree of cell migration was calculated by subtraction of the cell-free area after treatment from the original wounded area.

2.2.6. *In vitro* tube formation assay

HUVEC tube formation was assessed as described by Yamagishi *et al.* (82). Wells of 96-well plates were coated with matrigel (30 μl/well) which was allowed to solidify for at least 1 hr at 37°C. HUVECs were prepared by trypsinization and seeded onto the matrigel-coated well with 5 μM of each vitamin E derivative. Control cells were treated with 0.1% ethanol. Treatments were performed in duplicate. After 18 hrs, each well was photographed and the tube formation was evaluated by counting the number of tube nodes manually.

2.2.7. Animal study

The animal study was conducted in accordance with "Guidelines for the humane treatment of animals" as designated by the University of Texas Institutional Animal Care and Use Committee. Female BALB/c mice at 6 weeks of age were purchased from Jackson Laboratories (Bar Harbor, ME). To exclude any possible interference from vitamin E supplementation, upon arrival, the animals were fed adjusted vitamin E diet (Harlan Teklad TD.08228, Madison, WI) which consisted of a tocopherol-stripped semi-purified AIN-76A diet with 30 IU/kg diet of *all-racemic*-α-tocopheryl acetate to meet the nutrient requirement of laboratory mice (83). 66cl-4-GFP cells were harvested and resuspended at a density of $2X10^5$ cells/100 μl cell medium without any serum or antibiotics. Mice were injected subcutaneously with $2X10^5$ cells in the inguinal area at a point equal distant between the fourth and fifth nipples on the right side. Tumor size was

measured using calipers and calculated according to the equation V= (X^2Y)/2, where V is the volume of each tumor, *X* is the smaller diameter, and *Y* is the larger one (79). When tumors reached an average volume of 1 mm^3, mice were randomly assigned to treatment groups (10 animals/group): Basal diet (vitamin E adjusted diet), α-TEA, α-T3, γ-T3, α-T3EA or γ-T3EA containing diets. Each group received their respective diets for 21 days. For α-TEA, α-T3, γ-T3, α-T3EA or γ-T3EA containing diets, each compound was incorporated into the adjusted vitamin E diet by Harlan Teklad at a concentration of 250 mg of each compound/kg diet. The average amount of food consumption during the study was 2.6±0.3 g/day/mouse, which provided approximately 0.65 mg of each compounds per mouse on a daily basis. This amount is the equivalent to a daily intake of 134 mg of each compound in humans based on body surface area equivalency (84). For reference, a typical soft gel capsule of vitamin E contains 268 mg of *R,R,R-α*-tocopherol (400 IU). Tumors were measured every other day and body weights were measured on a weekly basis. Animals were euthanized after 22 days of treatment.

2.2.8. Immunohistochemistry to detect endothelial cell maker (CD31)

Primary tumors from 5 individual mice in each group were collected at the time of animal sacrifice and fixed in 10% formalin. Samples were processed for immunohistochemical analyses by the Histological & Tissue Processing Facility Core 3 at the University of Texas M.D. Anderson Cancer Center-Science Park Research Division (Smithville, TX) as previously described (45). Briefly, deparaffinized tumor sections (5 μm) were

examined for blood vessel density using antibody to endothelial antigen CD31 as an indicator of small capillaries. Three fields (X100) per tumor were examined for CD31 stained microvessels. Quantification of vessels was performed using the ImageJ (http://rsbweb.nih.gov/ij) 'Analyze Particles' function without any manipulation in brightness or contrast as described by Vlahovic *et al*. (85).

2.2.8. Measurement of tissue concentration of tocotrienols or vitamin E derivatives

Primary tumors, liver, lung, heart and kidney from 5 individual mice in each group were collected at the time of animal sacrifice. Collected tissues were snap frozen in liquid nitrogen and stored at -80°C until analyzed. Lipids from each tissue were extracted as described previously (38). The concentration of each compound per gram tissue was measured by an internal standard method using reverse-phase HPLC with fluorometric detection. The mobile phase consisted of 96% methanol (HPLC grade; EMD Bioscience, NJ), 4% water, and 0.001% glacial acetic acid. Samples were separated on a Waters Spherisorb ODS-2 column (Alltech, IL). All compounds were detected at the excitation and emission wavelengths of 260 and 320 nm respectively. The amount of individual compounds per gram tissue was calculated based on the internal standard method using δ-T as the internal standard (38).

2.2.9. Determination of lung metastases

The number of metastatic foci in the left lung lobe was evaluated using fluorescence microscopy (X100) as previously described (41, 79). Metastatic foci on both sides of the

flattened tissue (10 tissues/group) were scored. Based on the typical 66cl-4-GFP cell size of 10 to 20 μm, only 10 μm or larger foci were counted.

2.2.10. Statistical analysis

Tumor growth was analyzed using one-way analysis of variance (ANOVA) with TUKEY's post-hoc test using SPSS software (SPSS Inc, Chicago, IL). Differences in number of TUNEL and Ki-67 positive cells were determined by *t-test* (two-tailed, non-paired) using Prism software version 4.0 (Graphpad, San Diego, CA). A level of $P<0.05$ was regarded as statistically significant. Student *t-test* (two-tailed, unpaired) was used to compare vehicle control versus treatment in all *in vitro* studies.

2.3. Results

2.3.1. Novel tocotrienol derivatives inhibited cell proliferation in murine mammary cancer cells and human breast cancer cells.

For comparison of anti-proliferative effects of new derivatives, murine mammary cancer cells (66cl-4) and human breast cancer cells (MCF-7 and MDA-MB-231) were treated with various concentrations of novel vitamin E derivatives, and assessed for cell growth inhibition using CellTiter 96® AQueous Non-Radioactive Cell Proliferation Assay (Promega, Corp., Madison, WI). Cell proliferation was inhibited in a dose-dependent manner after 2 days of treatment. Notably, IC_{50} values of new compounds for growth inhibition were significantly lower than that of α-TEA in all cell lines tested (Figure 2.2.A). In comparison to the parent compounds, α-T3EA had significantly lower IC_{50} value compared to α-T3 (*$p<0.01$, t-test*), while γ-T3EA and γ-T3 had similar growth inhibitory effects in human breast cancer cells (Figure 2.2.B). In human immortalized mammary epithelial cells (MCF-10A) and normal mammary epithelial cells (HMEC), the IC_{50} of each compound was higher than that in cancer cell lines (Table 2.1), which suggest that malignant cells are more sensitive to the growth inhibitory effects of natural vitamin E compounds and their derivatives.

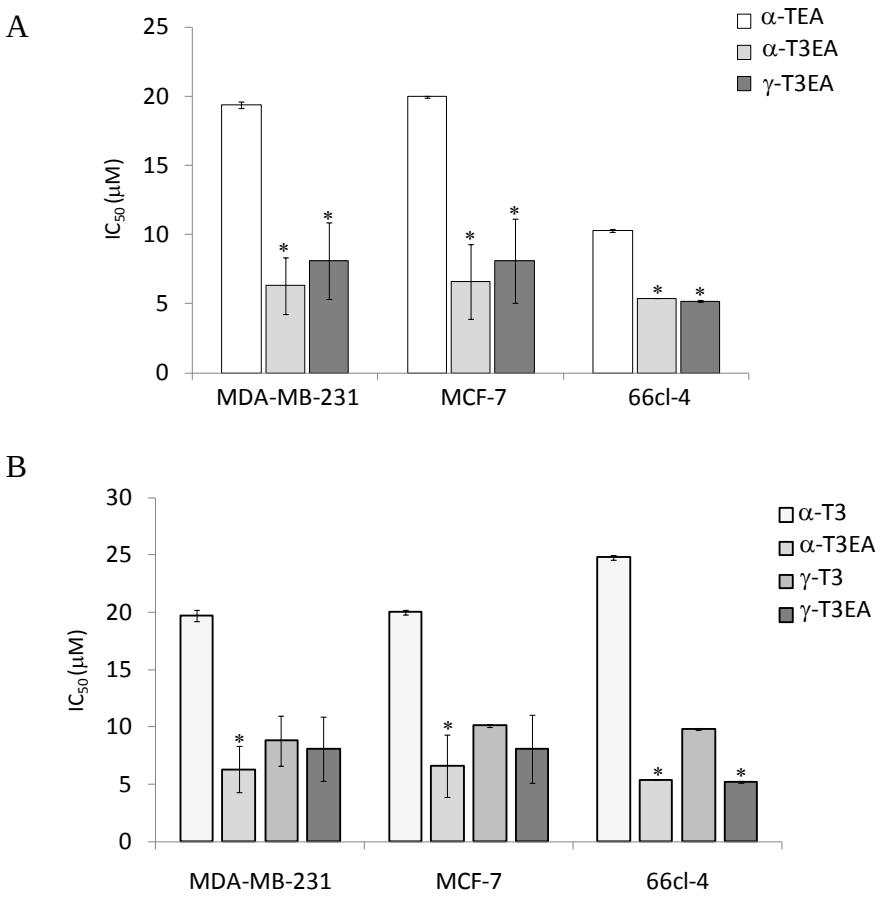

Figure 2.2. Comparison of IC_{50} for each novel compound to α-TEA (A) or to the parent tocotrienol (B). Cells were seeded in 96-well plates and treated with a range of concentrations from 0.6125 to 80 µM of α-TEA, α-T3EA, γ-T3EA, α-T3 or γ-T3 for 2 days. Control cells were treated with the vehicle (ethanol) at a final concentration of 0.1%. Viable cells were determined using CellTiter 96® AQueous Non-Radioactive Cell Proliferation Assay. Data are depicted as mean ± SD for three independent experiments. The asterisk (*) indicates significant difference from α-TEA treatment (A) or the parent compound of each derivative (B) in each cell line (*$p<0.01$, t-test*).

Table 1. Comparison of IC_{50} (μM) of natural vitamin E compounds and their derivatives using several different human cell lines and primary culture of human mammary epithelial cells (mean ± SD, n=2 or 3).

Compound	Cell lines			
	HMEC	**MCF-10A**	**MCF-7**	**MDA-MB-231**
α-T	N.I.[a]	N.I.	N.I.	N.I.
α-TEA	> 80 [b]	39.8 ± 0.5	20.0 ± 0.1	19.4 ± 0.3
α-T3	> 80	> 80	20.0 ± 0.2	19.7 ± 0.5
α-T3EA	19.8 ± 0.2	19.6 ± 0.3	6.6 ± 2.3	6.3 ± 2.0
γ-T3	19.7 ± 0.2	20.9 ± 0.3	10.1 ± 0.0	8.8 ± 2.1
γ-T3EA	20.4 ± 0.6	20.4 ± 0.3	8.1 ± 3.0	8.1 ± 2.8

[a] N.I.: No inhibition of cellular proliferation was observed at the highest concentration tested (100 μM) .

[b] Treatment of the cells for 2 days at the highest concentration (80 μM) failed to produce IC_{50}.

2.3.2. Novel tocotrienol derivatives induced apoptosis in human breast cancer cells.

Previous studies in our lab showed that α-TEA is a potent inducer of apoptosis in cancer cells. To test if tocotrienol-based derivatives also induce apoptosis, MCF-7 and MDA-MB-231 cells were used for apoptosis analyses using the Annexin V/PI assay. As shown in Figure 2.3, tocotrienol derivatives induced apoptosis in a dose-dependent manner more effectively than α-TEA.

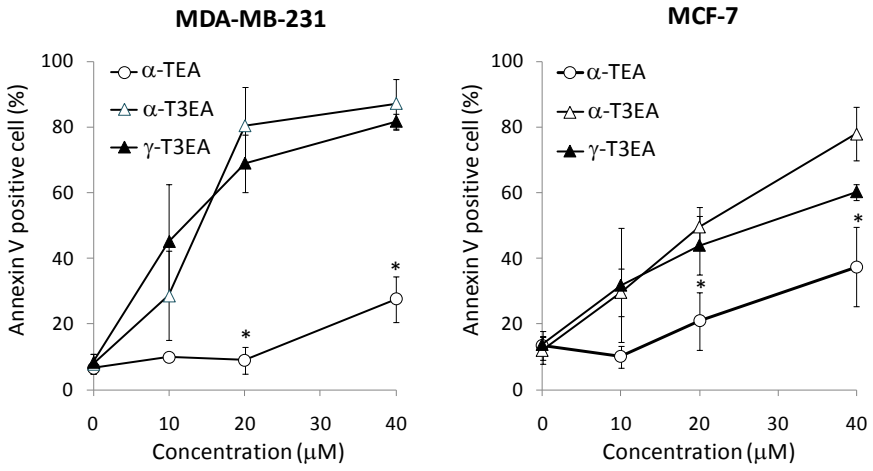

Figure 2.3. Comparison of apoptogenic activities of vitamin E derivatives. MCF-7 and MDA-MB-231 cells at $5X10^5$/well were seeded in 6-well plates. Cells were treated with 10, 20 or 40 μM of α-TEA, α-T3EA or γ-T3EA. Control cells were treated with vehicle at a final concentration of 0.1% ethanol. After 24 hrs, cells were collected and labeled with Annexin V/PI. The labeled cells were analyzed by flow cytometer (FACSCalibur, BD Biosciences, CA). Data are depicted as mean ± SD for three to six independent experiments (*significant difference from α-T3EA or γ-T3EA treatments at the same concentration, *P<0.05, t-test*).

2.3.3. Novel tocotrienol derivatives exhibited antiangiogenic properties in HUVECs.

Studies using natural tocotrienols have demonstrated that angiogenesis is suppressed by tocotrienol treatment both in endothelial cells in cultures and in animal models (6). To test if the new compounds can modulate angiogenic activity of endothelial cells in culture, cell properties required for new vessel formation; namely, cell proliferation, migration and differentiation, were examined (81). First, apoptogenic effect of novel compounds on actively proliferating human umbilical vein endothelial cells (HUVECs) was tested using the Annexin V/PI assay. As shown in Figure 2.4.A, both tocotrienol derivatives induced strong apoptotic response in proliferating HUVECs, and the percentage of apoptotic cells was significantly higher than in α-TEA treated cells. To test the effects of new compound on migration ability of endothelial cells at non-apoptotic concentrations, a wound healing assay was conducted as described by Staton *et al.* (81). While tocotrienols at 10 μM exhibited little to moderate inhibitory effects on endothelial cell migration, tocotrienol derivatives at 2.5 μM significantly inhibited the migration of endothelial cells (Figure 2.4.B & C). Further analyses using *in vitro* tube formation assays showed that the novel compounds inhibited capillary-like tubule formation by endothelial cells at a non-apoptotic concentration (Figure 2.4 D& E) and in a manner analogues to the migration inhibitory effect, higher concentrations (10 μM) of natural tocotrienols (α-T3 and γ-T3) exhibited only moderate to no inhibitory effects on tube formation. Taken together, these studies suggest improved chemotherapeutic potential for the tocotrienol-based derivatives

for these antiangiogenic parameters. Notably, α-TEA did not inhibit HUVEC migration at 2.5 μM or tube formation at 5 μM (data not shown).

2.3.4. Dietary administration of tocotrienol derivatives reduced tumor burden.

Anti-tumorigenic properties of α-T3EA or γ-T3EA in comparison to the parent compounds or α-TEA supplemented in basal vitamin E (*dl*-α-tocopheryl acetate) diets were evaluated using the 66cl-4-GFP mouse mammary tumor syngeneic model as shown in Fig. 2.5. The average tumor growth rates of α-TEA, α-T3EA and γ-T3EA supplemented diet groups were significantly attenuated compared to the basal diet group ($P<0.01$). Among the natural tocotrienols, only γ-T3 significantly suppressed tumor growth while the α-T3 group exhibited no tumor growth inhibitory effect. There was no difference observed in the tumor growth rate between γ-T3, α-TEA, α-T3EA and γ-T3EA groups. The average body weight of mice at the beginning of the experiment was 16.3 ± 0.2 grams and at the end of the experiment was 17.5 ± 0.3 grams. There was no significant difference in body weights among the groups (data not shown). The average food consumption was 2.6 ± 0.3 g, and no differences in the amount of food intake between groups was observed. Immunohistochemical analyses of CD31 positive cells in tumor sections showed no difference between treatment groups and the basal control diet group (data not shown), suggesting none of the compounds exhibited antiangiogenic activities.

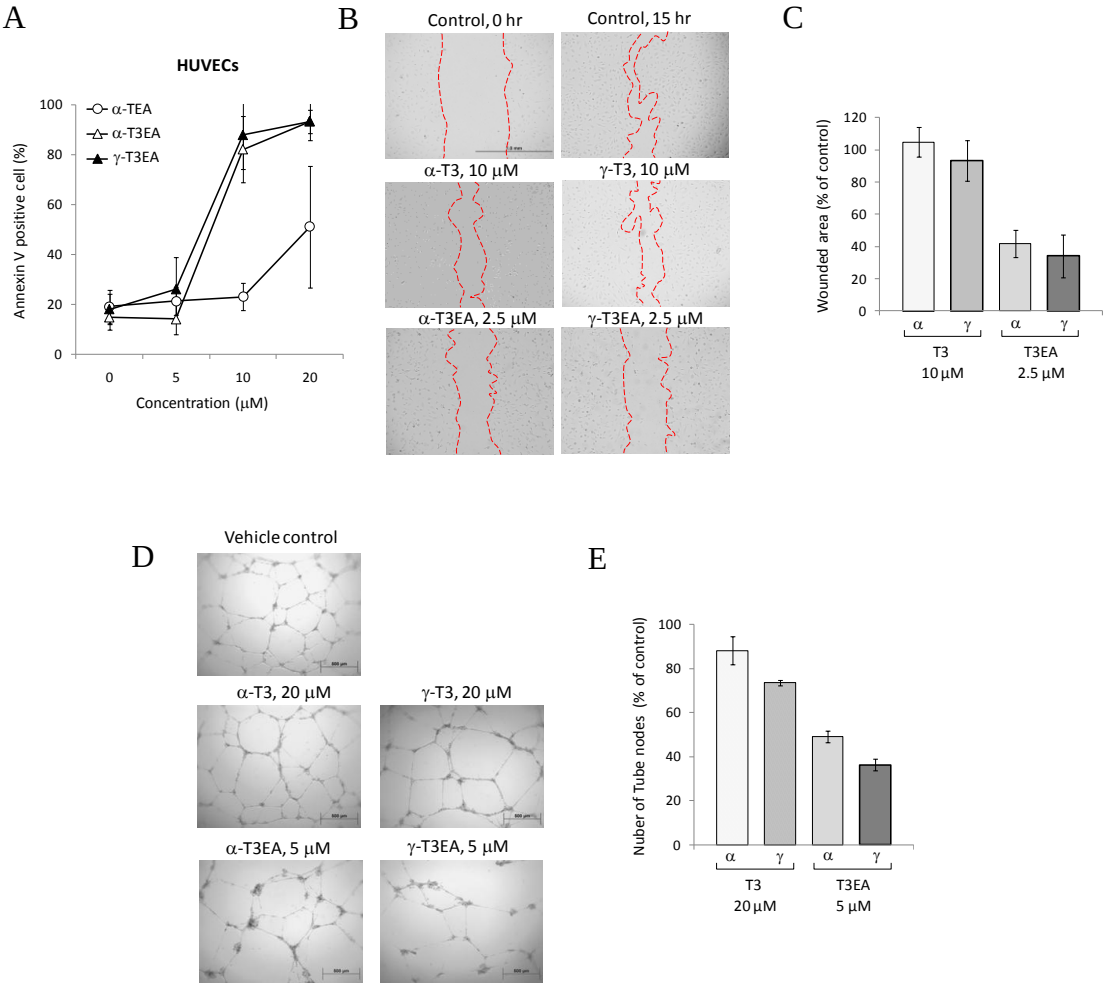

Figure 2.4. Antiangiogenic properties of tocotrienol derivatives in HUVECs. A, Cells were analyzed for apoptotic status using the Annexin V/PI assay after 24 hr treatments. Data are depicted as mean ± SD for at least three independent experiments. B & C, Cells were analyzed for migration ability after treatment. Confluent cell monolayers were wounded and then treated with various concentrations of each compound for 15 hrs. Figures in B depict representative examples of cell migration into the wounded area. The graph in C represents the average percentage of the area covered by the treated cells in comparison to the area covered by the vehicle control treated cells (Mean±SD, n=3). D & E, Cells were analyzed for the ability to form tubule-like structures. Cells were seeded in matrigel coated 96-well plates and treated with each compound. Control cells were treated with 0.1% ethanol. After 18 hrs, each well was photographed and the tube formation was evaluated by counting the number of tube nodes manually. The graph in E represents the average number of tubule nodes in treated samples compared to the vehicle control (Mean±SD, n=2).

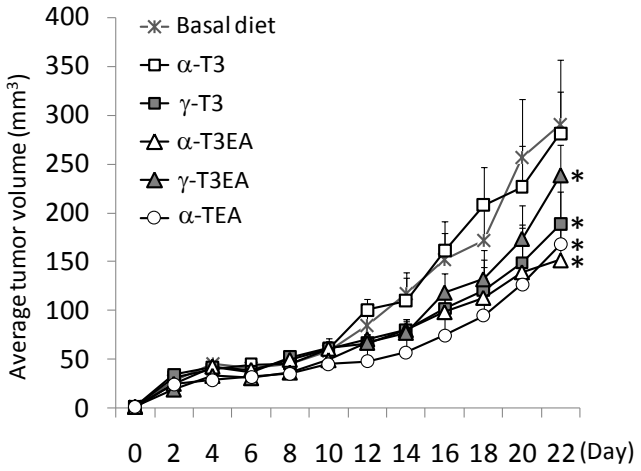

Figure 2.5. Average tumor volume (mean±SE) over time of BALB/c mice bearing 66cl-4-GFP tumor cells. Each compound was incorporated into the adjusted vitamin E diet at a concentration of 250 mg of each compound/kg diet (0.025%). Tumor volume was measured every other day as described in Materials and Methods. *Significant difference from basal diet by one-way ANOVA with TUKEY's post-hoc test (*$P<0.01$*).

2.3.5. Novel compounds were not retained in the liver as much as α-TEA.

Tissue concentration of each compound was analyzed using reverse-phase HPLC with fluorometric detection. Unfortunately, the novel compounds could only be detected in the liver. While α-forms of each compound retained in the liver (α-TEA, 55.1±8.7 nmol/g; α-T3, 27.3±5.5 nmol/g; and α-T3EA, 45.0±3.2 nmol/g), γ-T3 was retained at an approximately 8 times lower level than α-T3 (3.8±1.0 nmol/g tissue) and γ-T3EA was undetectable as shown in Figure 2.6. These results suggest that γ-forms were either less incorporated into the liver or more rapidly metabolized by the liver in comparison to the α-forms. While γ-T3EA was rapidly cleared from the body, α-T3EA was highly retained in the liver.

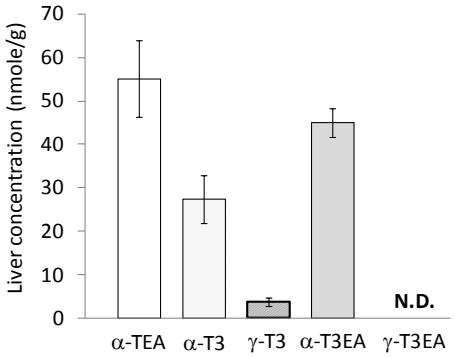

Figure 2.6. Concentrations of natural tocotrienols and vitamin E derivatives in the liver. The level of each compound was measured using reverse-phase HPLC with fluorometric detection at excitation and emission wavelength of 290 and 330 nm respectively. Data are depicted as mean ± SE (n=5). γ-T3EA was not detected in the liver (N.D.).

2.3.6. Lung metastases were not inhibited by either natural tocotrienols or vitamin E derivatives

Micrometastatic foci in lung were counted by observing green fluorescent protein (GFP) tagged tumor cells under fluorescence microscope. A reduction in the number of micrometastatic foci was observed in all treatment groups compared to the basal diet group, but no significant difference was observed (Figure 2.7.A). Likewise, there was no reduction in average lung weight between groups, which suggests no suppressive effects of these compounds on lung metastases at the treated dose (Figure 2.7.B).

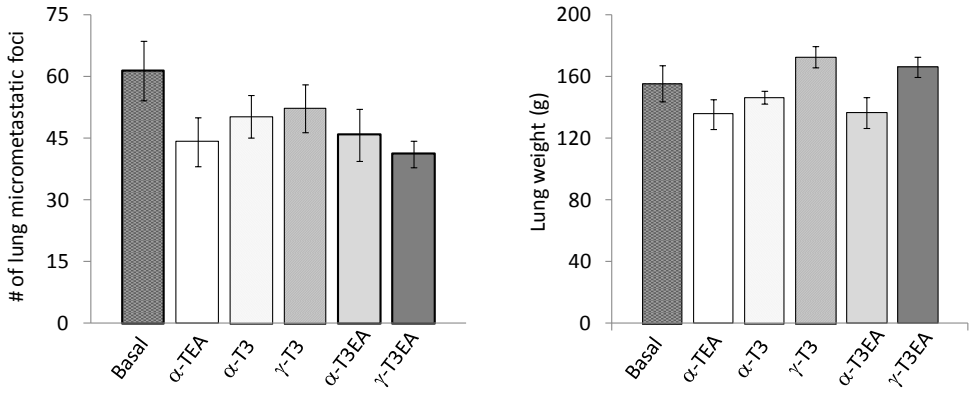

Figure 2.7. Effects of tocotrienols and vitamin E derivatives on lung metastasis. A, GFP-labeled metastatic lung foci were counted using fluorescence microscopy. Data are depicted as mean ± SE (n=10). B, Data represent average lung weight (mean ± SE, n=10).

2.4. Discussion

Non-hydrolyzable, redox-silent modification of *R,R,R*-α-tocopherol confers pleiotropic anticancer properties: anti-proliferative, apoptosis-inducing, pro-survival inhibitory and anti-metastatic effects which are not observed in the parent compound (3). In an effort to generate stronger anticancer therapeutics, natural α- and γ-tocotrienols were modified as redox-silent derivatives; namely α-T3EA and γ-T3EA. Data presented here demonstrated that: 1) α-T3EA and γ-T3EA reduced tumor cell viability and triggered a high degree of apoptosis in human breast cancer cells and mouse mammary tumor cells; 2) both α-T3EA and γ-T3EA exhibited strong antiangiogenic activities which included apoptosis induction, migration inhibition, and tubule formation inhibition in human umbilical cord endothelial cells; 3) both apoptogenic activity and antiangiogenic properties of tocotrienol derivatives were significantly better than those of α-TEA; 4) dietary delivery of α-T3EA and γ-T3EA at 250 mg/kg diet significantly suppressed the growth of 66cl-4-GFP mouse mammary tumor cells in a syngeneic mouse model; and 5) both γ-T3 and its derivative exhibited low bioavailability.

Modifications of natural vitamin Es aimed at improving proapoptotic activity of the parent compounds have been studied, especially after the discovery of proapoptotic and anti-neoplastic activities of α-tocopherol succinate (α-TOS) which has a hydrolysable succinic acid at the C6 position of the chroman head of α-T (Figure 1.3). Birringer *et al.* (86) studied structure-function relation of vitamin E modifications, and found that

succinylation of the C6-phenolic group of natural tocopherols or γ-T3 via an ester bond significantly improved apoptogenic activities in various human cancer cell lines, such as T lymphoma, breast carcinoma, and neuroblastoma cells, although the improved efficacy was not observed in some types of prostate cancer cells (87). Data presented here showed that a non-hydrolysable acetic acid modification at the C6-phenolic ring of α-T3, namely α-T3EA showed improved efficacy of cell proliferation inhibition as well as apoptosis induction compared to the parent compound. In contrast, creation of γ-T3EA did not confer any additional anticancer properties to its parent compound, γ-T3, when treated using estrogen receptor positive or negative human breast cancer cells. Similar results were observed with a succinate derivative of γ-T3 in some types of prostate cancer cells (87), suggesting that the anticancer efficacy of each natural vitamin E compound or its corresponding derivative may vary depending on cellular context.

One property of tocotrienols that distinguish them from tocopherols is antiangiogenic action which makes them a promising potential therapeutic agent for targeting specific cancers or various human diseases including age-related disorders (5, 88). In order to test if modification of tocotrienols can improve antiangiogenic activity of the parent compounds, several *in vitro* assays were conducted using HUVECs. Migration, proliferation, and differentiation of endothelial cells are critical elements of neovascularization (89). Both α- and γ-T3EA induced apoptosis in actively proliferating HUVECs. These novel derivatives also inhibited migration and the differentiation of

HUVEC. Antiangiogenic effect of α-TEA and α-TOS observed in endothelial cells in cell culture showed high correlation with *in vivo* tumor suppression as well as reduction of tumor vasculature (90). *In vitro* antiangiogenic properties of α- and γ-T3EA were markedly higher in comparison to either parent compounds or α-TEA, suggesting the novel derivatives may be promising therapeutic agents to target diseases reliant on angiogenesis.

Previous animal studies in our lab showed that dietary delivery of α-TEA at 250 mg/kg diet significantly reduced tumor growth in a *xenograft* model of MDA-MB-231-GFP human breast cancer cells transplanted into immune compromised nude mice (18). Based on this study, 250 ppm of the novel tocotrienol derivatives or natural tocotrienols supplemented in diets were delivered to syngeneic 66cl-4-GFP tumor transplanted mice. This amount of vitamin E compound is equivalent to a daily intake of 134 mg of each compound in humans based on body surface area equivalency (84), since the amount of average diet consumed was 2.6±0.3 g/mouse/day (0.65 mg/mouse/day). Dietary delivery of α-T3EA significantly inhibited tumor growth compared to the parent compound, but the effect was not better than α-TEA. The tumor growth rate of γ-T3EA group was significantly different from the control group; however, the average tumor weight at the end of the experiment (Day 22) was not different from the average control tumors. In fact, γ-T3, the parent compound of γ-T3EA, displayed better tumor suppressive effect than its derivative. Although α-TEA, α-T3EA, and γ-T3 attenuated tumor growth rate, examining

tumor sections for CD31 as a biomarker for blood vessels showed that these compounds did not affect blood vessel formation in this tumor model. This suggests that at the supplemental dose used in these studies, α-TEA- α-T3EA- or γ-T3-anti-tumor effects were not correlated with anti-angiogenic actions.

To address the discrepancy between cell culture and animal tumor efficacy studies, the tissue concentration of each compound was analyzed. Not surprisingly, α-forms of natural vitamin E or derivatives were retained in the liver, whereas γ-T3 concentration in the liver was 8 fold lower than α-T3. γ-T3EA was not detected in the liver, suggesting that γ-T3EA may not be taken up or retained by the tumor due to rapid metabolism in the liver. Although tumor levels of α-T3EA were detected as high as α-TEA, the tumor suppressive effect was not different from α-TEA, implying that the degree of saturation in the fatty acid tail of vitamin E derivatives may not impact anti-tumor efficacy *in vivo*.

Notably, our study showed that natural vitamin E form, γ-T3, exhibited significant attenuation in tumor growth; in fact as much as, α-TEA at the supplemental dose (0.625 mg/mouse/day) employed while α-T3 did not. This suggests that anticancer efficacy of α-T3 is less effective than γ-T3 as previously suggested by Yu e*t al.* based on the apoptogenic activity of each form of tocotrienol in human breast cancer cell lines (91) and by *Constantinou et al*. as reported for human prostate cancer cell lines in cell culture (87). A previous study by MacAnally *et al*. demonstrated that dietary delivery of δ-T3 at a dose of 250 mg/kg diet reduced the mean weight of melanomas by 50% compared to

the control group in a syngeneic mouse model (33). In our study, γ-T3 at a dose of 250 mg/kg diet reduced mammary tumor burden by 35%. Although we didn't test δ-T3 *in vivo*, it is possible that δ-T3 might exhibit a better efficacy than γ-T3 *in vivo*, since cell proliferation suppressive effects of δ-T3 is reported as the most potent of all eight natural forms of vitamin E in prostate cancer cells in cell culture (87).

In summary, these findings demonstrate that redox-silent modification of both α-tocopherol and tocotrienols function effectively as anticancer agents. The rapid metabolism of γ-form of natural tocotrienol or its derivative limits *in vivo* application. Further studies are needed to understand structure-function relationships among natural or synthetic vitamin Es and their derivatives, which will aid design of various vitamin E derivatives with improved bioavailability. Identifying the mechanisms of anticancer actions of different forms of vitamin E and their derivatives is another critical area to be investigated to develop more potent vitamin E derivatives possessing anticancer activities.

Chapter 3. Tocotrienols induce apoptosis in breast cancer cell lines via an endoplasmic reticulum stress dependent increase in extrinsic death receptor signaling

Tocotrienols are naturally occurring forms of vitamin E and known to possess anti-proliferative and apoptosis-inducing properties. This study focused on investigating anticancer effects of tocotrienols and the mechanisms of apoptosis induction by tocotrienols *in vivo* and *in vitro*. Dietary delivery of γ-tocotrienol (γ-T3) suppressed tumor growth in a syngeneic implantation mouse mammary cancer model by inhibiting cell proliferation and inducing apoptosis. In cell culture studies, γ-T3 inhibited colony formation of a mouse mammary cancer cell line and human breast cancer cell lines. The anti-proliferative effect of tocotrienols was correlated with an increase in apoptosis based on Annexin V assessment. Treatment of human MDA-MB-231 and MCF-7 cells with γ-T3 induced cleavage of caspases-8, -9 and -3 as well as PARP. Additional analyses showed that γ-T3 activated c-Jun NH_2-terminal kinase (JNK) and p38 MAPK, and upregulated death receptor 5 (DR5) and C/EBP homologous protein (CHOP), a biomarker of endoplasmic reticulum (ER) stress. Silencing either JNK or p38 MAPK reduced the increase in DR5 and CHOP and partially blocked γ-T3-induced apoptosis. Both DR5 and CHOP upregulation were required for γ-T3-induced apoptosis, and DR5 was transcriptionally regulated by CHOP after γ-T3 treatment. Moreover, γ-T3 increased the level of other ER stress markers. Taken together, these results suggest that

upregulation of DR5 by γ-T3 treatment is dependent on JNK and p38 MAPK activation which is mediated by ER-stress.

3.1. Introduction

Tocotrienols are highly enriched in palm oil and also found in the seed endosperm of monocots such as wheat, rice, barley, oat and rye (92). The anti-proliferative and apoptosis-inducing properties of a tocotrienol-rich fraction (TRF) extracted from palm oil or individual tocotrienol forms are well documented in cell culture studies using human breast cancer cells or mouse mammary cancer cells (reviewed by (20)). Studies evaluating tocotrienols as an anticancer agent also include other types of human cancers, such as colorectal cancer, gastric adenocarcinoma, liver cancer, lung carcinoma, pancreatic cancer, and prostate cancer (21-26).

Possible intracellular mechanisms of tocotrienol-mediated growth inhibition or apoptosis induction have been proposed. In neoplastic murine mammary epithelial cells, γ-tocotrienol (γ-T3) antagonizes phosphatidyl inositol-3 kinase (PI-3K)/Akt and nuclear factor-κB (NF-κB) signaling pathways, and also induces caspase 8 activation (28, 29). In human breast cancer cells, δ-tocotrienol-triggered apoptosis involves upregulation of transforming growth factor-β receptor II (TGF-βRII) and is mediated by TGF-β-, Fas/CD95-, and c-Jun N-terminal kinase (JNK)-signaling pathways (30). δ-Tocotrienol

also induces G0/G1 cell cycle arrest by reducing phosphorylation of retinoblastoma protein (Rb) and the loss of cyclin D1/cyclin dependent kinase 4 (CDK4) expression (31). Several *in vivo* studies also support the anticancer effect of tocotrienols alone or together with statins, the competitive inhibitors of 3-hydroxyl-3-methylglutaryl coenzyme A (HMG CoA) reductase (32, 33). Another unique property of tocotrienols is inhibition of angiogenesis which is believed to be the major therapeutic target against various human disorders including cancer, diabetic retinopathy, and rheumatoid arthritis (6, 93). Additionally, highly malignant mammary epithelial cells are more sensitive to anti-proliferative and apoptotic effects of tocotrienols; whereas, preneoplastic cells are less sensitive to the treatment effects (27). Because of the aforementioned advantages to human health, tocotrienols have gained substantial attention; however, a more complete understanding of their anticancer mechanisms of action needs to be elucidated.

The unfolded protein response (UPR) is an evolutionary conserved response triggered by disturbances in intracellular calcium homeostasis, protein secretion, redox regulation or lipid biosynthesis in the endoplasmic reticulum (ER) (52). The accumulation of unfolded protein in the ER initially induces expression of genes that restore homeostasis by enhancing protein folding capacity. ER stress also activates signal transduction pathways associated with cellular stresses including activation of mitogen-activated protein kinases (MAPKs), JNK and p38 MAPKs (53). If the UPR is persistent or excessive, the cell eventually undergoes programmed cell death, typically apoptosis (52). The C/EBP homologous protein (CHOP), also known as growth arrest- and DNA damage-inducible

gene 153 (GADD153), is a transcription factor that is upregulated at multiple levels by ER stress. CHOP directly regulates target genes including *Bcl-2, GADD34* and *ERO* whose products mediate ER stress induced apoptosis (60). ER stress can sensitize cells to tumor necrosis factor (TNF)-related apoptosis inducing ligand (TRAIL) signaling by upregulation of death receptor-5 (DR5) which enables the recruitment of adaptor proteins to trigger apoptosis upon ligand binding (94). In recent years, various cytotoxic agents used in cancer therapy that target different biological pathways have been reported to induce ER stress-mediated apoptosis. Examples include proteasome inhibitors, triterpenoid derivative, proteasome-proliferator activated receptor (PPAR) ligands, and ruthenium-derived organometallic compounds (53, 95-97).

Here, we investigated mechanisms involved in tocotrienol anticancer activities using a syngeneic mouse mammary tumor model and human breast cancer cell lines in cell culture. Dietary delivery of γ-T3 inhibited 66cl-4-GFP tumor growth in the mouse model by inhibiting cell proliferation and inducing apoptosis. Cell culture studies showed that anti-proliferative effects of tocotrienols are highly correlated with increases in apoptosis. *In vitro* analyses showed that tocotrienols trigger apoptosis via ER stress which produces an upregulation of DR5 in a CHOP dependent manner and the activation of JNK and p38 MAPK.

3.2 Materials and methods

3.2.1. Cell culture and reagents

The source and culture conditions for 66cl-4-GFP murine mammary tumor cells were previously described (79). MDA-MB-231 and MCF-7 human breast cancer cells were cultured and maintained in MEM medium as previously described (18). MDA-MB-468 cells were maintained in RPMI 1640 medium and T47D cells were maintained in DMEM high glucose medium. All human breast cancer cells were obtained from the American Type Culture Collection (ATCC). All maintenance media were supplemented with 10% fetal bovine serum (HyClone Laboratories, Logan, UT), 100 U/ml penicillin, and 100 mg/ml streptomycin. For all treatments, FBS was reduced to 2% to better mimic *in vivo* low serum exposure of these cell types. α-, γ-, and δ-tocotrienols were kindly provided by the Malaysian Palm Oil Board (Kuala Lumpur, Malaysia) and dissolved in ethanol. Salubrinal was purchased from EMD Biosciences (San Diego, CA) and desipramine, an ASMase inhibitor was purchased from Sigma-Aldrich (St. Louis, MO). Salubrinal and desipramine were dissolved in dimethyl sulfoxide (DMSO).

3.2.2. Immunohistochemistry analyses of tumor sections

Primary tumors from 5 individual mice fed with basal diet (vitamin E adjusted diet), α-T3 or γ-T3 containing diets (250 mg/kg diet) for 21 days were collected at the time of animal sacrifice and fixed in 10% formalin. Samples were processed for immunohistochemical analyses by the Histological & Tissue Processing Facility Core 3

at the University of Texas M.D. Anderson Cancer Center-Science Park Research Division (Smithville, TX) as previously describe (41, 79). Briefly, deparaffinized tumor sections (5 μm) were examined using antibody against Ki-67, a biomarker for determining active cell division and terminal deoxynucleotidyl transferase-mediated nick end labeling (TUNEL) assay for determining number of apoptotic cells. For Ki-67 analyses, three randomly chosen microscopic fields (X100) per tumor were scored. For TUNEL analyses, at least ten randomly chosen microscopic fields (X400) were scored.

3.2.3. Clonogenic assay of cells *in vitro* (colony formation assay)

Effect of tocotrienols on capacity of tumor cells to undergo unlimited division was assessed using a standard clonogenic assay (98). Cells were seeded in 6-well plates at 300 cells per well for 66cl-4-GFP and MCF-7 cells, or 200 cells per well for MDA-MB-231 cells. After 48 hrs, cells were treated with 1.25, 2.5 or 5 μM of α-T3, γ-T3 or δ-T3. Control cells were treated with the vehicle (final concentration = 0.02% ethanol). After 2 weeks, cells were fixed with 10% formalin followed by staining with 2% (w/v) crystal violet in H_2O. Colonies containing more than 50 cells were scored.

3.2.4. Cell proliferation assay (MTS assay)

Effect of tocotrienols on cell proliferation was assessed using CellTiter 96® AQueous Non-Radioactive Cell Proliferation Assay (Promega Corp., Madison, WI). MDA-MB-231 or MCF-7 cells at $5X10^3$/well and 66cl-4 cells at 10^4/well were seeded in 96-well plates. Cells were treated with a range of concentrations from 5 to 40 μM of α-T3, γ-T3

or δ-T3. Control cells were treated with the vehicle (ethanol) at a final concentration of 0.1%. After 24 hrs, viable cell number was measured following manufacturer's instructions. The percentage of viable cells at each concentration was calculated by dividing color absorbance (A490) of treated cells by that of control cells. The half maximal inhibitory concentration (IC50) was determined using Graphpad Prism software.

3.2.5. Evaluation of apoptosis (Annexin V assay)

Number of apoptotic cells after treatment was evaluated using Annexin V- Fluorescein isothiocyanate (FITC)/Propidium iodide (PI) assay or Annexin V-Phycoerythrin (PE) assay as previously described (17). Briefly, cells were collected at various time points and resuspended in Annexin V binding buffer (10 mM HEPES (pH 7.4), 150 mM NaCl, 5 mM KCl, 1 mM $MgCl_2$, 1.8 mM $CaCl_2$). Human breast cancer cells were incubated with Annexin V-FITC (Invitrogen, CA) for 8 min at room temperature, and then suspended in PI solution (50 ng/mL in PBS). For 66cl-4-GFP cells, Annexin V-PE (Invitrogen, CA) was added to the cells following 8 min incubation. Fluorescence was measured using flow cytometry (FACSCalibur, BD Biosciences, CA) and the data were analyzed using CellQuest software (FACSCalibur, BD Biosciences, San Jose, CA). The half maximal effective concentration inducing apoptosis in 50% of the cell population (EC50) was determined using Graphpad Prism software.

3.2.6. Western blot analyses

Whole cell lysates were used to analyze protein expression levels as previously described (99). Antibodies to activating transcription factor-4 (ATF4), caspase-3, CHOP, c-Jun, DR4, JNK 1/2, Histone H1, p38 MAPK, phospho-c-Jun and poly (ADP-ribose) polymerase (PARP) were purchased from Santa Cruz Biotechnology (Santa Cruz, CA). Antibodies to caspase-8, caspase-9, DR5, phospho-JNK 1/2, phospho-p38 MAPK were purchased from Cell Signaling Technology (Beverly, MA). Antibody to GAPDH was produced in house. Secondary antibodies conjugated with horseradish peroxidase included goat anti-rabbit and rabbit anti mouse IgG (Jackson Immunoresearch, Rockford, IL); and bovine anti-goat IgG (Santa Cruz Biotechnology). To quantitate the expression level, densitometric analyses were conducted using ImageJ software.

3.2.7. Gene silencing using siRNA

Small interfering RNAs targeting *CHOP, DR5, JNK1/2, p38 MAPK or acid sphingomyelinase (ASMase)* were purchased from Ambion (Austin, TX). Transient transfection with siRNAs was conducted as described elsewhere (16). A scrambled siRNA (Ambion) that targets no known mouse, rat, or human gene was used as a non-specific negative control. Transfected cells were incubated for 48 hrs before tocotrienol treatment.

3.2.8. Chromatin immunoprecipitation assay (ChIP assay)

MDA-MB-231 cells were treated with 30 μM of γ-T3 or vehicle (0.08% ethanol) for 15 hrs. Formaldehyde was added to the cell medium at a final concentration of 1% for 12 min followed by the addition of glycine (0.125M) to stop the cross-linking. Collected cells were prepared for the ChIP assay as described by Nelson *et al*. (100). The same CHOP antibody (B-3, sc-7351) used for the western blot analyses was used for immunoprecipitation. As an isotype control, normal mouse IgG_1 purchased from Santa Cruz Biotechnology was used. To detect CHOP binding sites in the DR5 promoter region, polymerase chain reaction (PCR) was conducted using the primers as described by Adbelrahim *et al.* (101).

3.2.9. Nuclear and cytoplasmic fractionation

Nuclear localization of activating transcription factor (ATF4), a transcription factor translationally activated and localized in nuclei under ER stress was analyzed (102). Cytoplasmic and nuclear fractions were prepared as described by Bijur *et al.* (103). Briefly, cells were collected after trypsinization, washed twice with phosphate buffered saline (PBS) and lysed with lysis buffer (10 mM Tris, pH 7.5, 10 mM NaCl, 3 mM MgCl2, 0.05% Nonidet P-40, 1 mM EGTA, protease inhibitor cocktail). Whole cell lysates were centrifuged at 2700 x*g* for 10 min at 4°C. The resulting pellet contained nuclear fraction and the supernatant containing the cytosol was centrifuged again at 20,000 x*g* for 15 min at 4°C. Then, the supernatant was retained as the cytosolic fraction.

The nuclear pellet was washed twice with wash buffer (10 mM PIPES, pH 6.8, 300 mM sucrose, 3 mM MgCl2, 1 mM EGTA, 25 mM NaCl, protease inhibitor cocktail). After final wash, the resuspended pellet was layered over a cushion of 1 ml sucrose buffer (1 M sucrose and protease inhibitor cocktail) and centrifuged at 2700 x*g* for 10 min at 4°C. The supernatant containing cellular debris was discarded and the pellet containing nuclei was washed once with lysis buffer. The pellet was lysed using RIPA buffer (50 mM Tris-HCl, pH 7.4, 1% NP-40, 0.25% sodium deoxycholate, 150 mM NaCl, 1 mM EDTA, protease inhibitors). Protein concentrations in the cytosolic and nuclear extracts were determined using Coomassie Brilliant Blue G-250 dye (Bio-rad, Hercules CA).

3.2.10. Quantitative real time-PCR (qRT-PCR) and reverse transcriptase PCR (RT-PCR) analyses of DR5, GRP78 and X-box binding protein (XBP-1) splice variants.

Status of messenger RNA levels for *GRP78* and *XBP-1* mRNA splice variants were assessed. Cells were collected as various time points and total RNA was purified using RNeasy mini kit following manufacturer's instructions (Qiagen Inc., Valencia, CA). Two μg of RNA from each sample was used for the reverse transcription reaction using SuperScript First Strand Synthesis System for RT-PCR (Invitrogen, Carlsbad, CA). Amplification of *GRP78* was analyzed by reverse transcriptase PCR. The primers used to detect *GRP78* were 5'-GATAATCAACCAACTGTTAC-3' (forward) and 5'-GTATCCTCTTCACCAGTTGG-3' (reverse) as described by Wang *et al* (104); and to detect *GAPDH* were 5'-ACCACAGTCCATGCCATCAC-3' (forward) and 5'-

TCCACCACCCTGTTGCTGTA-3' (reverse). The splicing of *Xbp-1* mRNA serves as an indicator of ER stress response (105). The detection of *Xbp-1* splice variants was conducted as described by Marciniak *et al.* (60). To distinguish the 448 bp spliced band from the 473 bp unspliced form, PCR products were digested with *Pst I* which cuts only in the unspliced cDNA and gives 290 and 183 bp fragments (60). For quantitative analysis of *DR5* mRNA expression, qRT-PCR was performed using SYBR® Green PCR Master Mix (Applied Biosystems Inc., Foster City, CA) following manufacturer's instructions. The primers used to detect *DR5* were 5'-TGACTCATCTCAGAAATGTC-AATTCTTA-3' (forward) and 5'-GGACACAAGAAGAAAACCTTAATG-3' (reverse)'; and to detect *GAPDH* were 5'-CCTGTTCGACAGTCAGCCG-3' (forward) and 5'-CGACCAAATCCGTTGACTCC-3' (reverse). Changes in gene expression were analyzed by comparative C_T method following ABI PRISM 7700 Sequence Detection System User Bulletin #2: Relative Quantitation of Gene Expression (P/N4303859). *GAPDH* was used for normalization of *DR5* expression.

3.2.11. Statistical analysis

Differences in number of TUNEL and Ki-67 positive cells were determined with *t-test* (two-tailed, unpaired) using Prism software version 4.0 (Graphpad, San Diego, CA). A level of $P<0.05$ was regarded as statistically significant. Student *t-test* (two-tailed, unpaired) was used to compare vehicle control versus treatment in the *in vitro* studies.

3.3. Results

3.3.1. Dietary administration of γ-T3 reduces murine mammary tumor burden and *in vivo* cell proliferation.

The anti-tumor property of dietary α-T3 or γ-T3 in comparison to the basal vitamin E (*dl*-α-tocopheryl acetate) diet was evaluated as described in Chapter 2 (Fig. 2.5). The average tumor volume of the γ-T3 diet group was significantly smaller than the basal diet group ($P<0.001$), while the α-T3 diet group exhibited no tumor growth inhibitory effect. To study the mechanism of antitumor effects of γ-T3, immunohistochemical analyses of tumor sections for Ki-67 and TUNEL labeling were analyzed as shown in Figure 3.1. Tumors from the γ-T3 diet group had 55% less Ki-67- positive cells and 386% more TUNEL positive cells compared to the basal diet group ($P=0.026$ and $P=0.077$, respectively). Tumors from the α-T3 diet group had 29% less Ki-67 positive cells and 141% more TUNEL positive cells than the basal diet group ($P=0.093$ and $P=0.340$, respectively). All together, these results indicate that γ-T3 exhibits anti-tumor activity by inhibiting tumor cell proliferation and also inducing apoptosis. α-T3 did not exhibit anticancer potential at the tested dose.

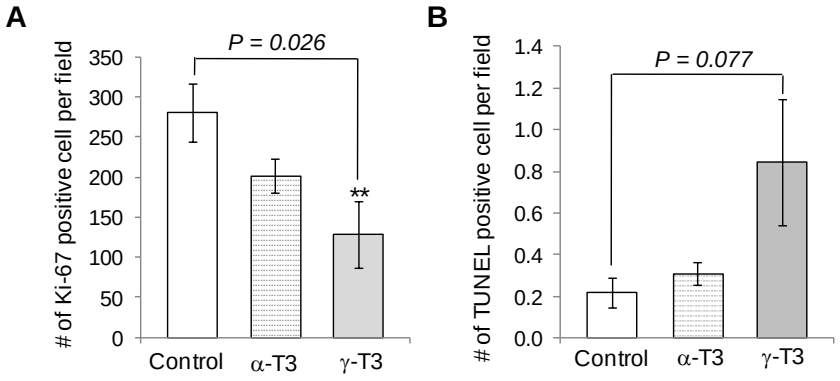

Figure 3.1. γ-T3 inhibits cell proliferation and enhances apoptosis *in vivo*. A, Immunohistochemical staining of tumors (n=5) for cell proliferation (Ki-67). Three randomly chosen microscopic fields (X100) per tumor section were scored (mean± SE). **Significant difference from control diet by *t-test* (*P<0.05*). B, Immunohistochemical staining of tumors (n=5) for apoptosis (TUNEL staining). Ten randomly chosen microscopic fields (X400) were scored (mean±SE).

3.3.2. T3s inhibit colony formation and cell proliferation by inducing apoptosis in murine mammary tumor cells and human breast cancer cells in culture.

To compare the anti-cancer activity of different tocotrienol forms in murine mammary cancer cells and human breast cancer cell lines, colony formation assays were conducted using human estrogen receptor-negative (MDA-MB-231) and positive (MCF-7) breast cancer cells along with 66cl-4-GFP cells (Figure. 3.2). In all three cell lines, δ-T3 showed the best efficacy and α-T3 exhibited the least efficacy. Although α-T3 did not reduce tumor burden *in vivo*, it did show inhibitory effects on colony formation in all three cell lines at relatively high concentrations compared to γ-T3 or δ-T3.

To investigate how the inhibitory effects of tocotrienols were being mediated, analyses of cell proliferation and apoptosis were conducted (Table 3.1). Both δ-T3 and γ-T3 strongly inhibited cell proliferation and induced apoptosis in a dose dependent manner while α-T3 did not show any anti-proliferative or apoptogenic effects on any of the cell lines after 24 hrs of treatment. Apoptosis analyses using the Annexin V assay revealed that the anti-proliferative effects of δ-T3 and γ-T3 were highly correlated with the induction of apoptosis in all three cell lines.

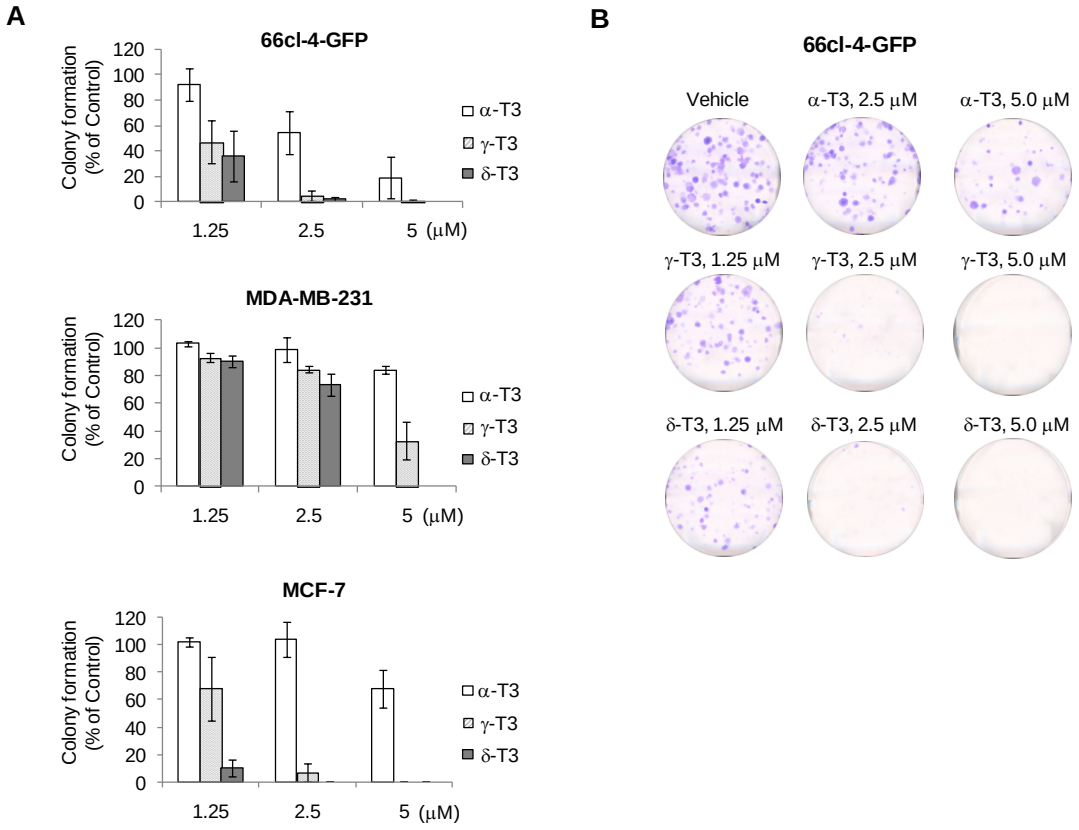

Figure 3.2. Inhibitory effects of tocotrienols on colony formation of murine mammary tumor cells and human breast cancer cells. Cells were seeded in 6-well plates (200 cells/well for MDA-MB-231 cells; 300 cells for the other cell types). After 48 hrs, cells were treated with 1.25, 2.5 and 5 μM of α-T3, γ-T3 or δ-T3. Control cells were treated with vehicle at a final concentration of 0.02% ethanol. After 2 weeks, cells were fixed with 10% formalin and stained with 2% crystal violet. Colonies containing at least 50 cells were scored. A, Colony formation data are depicted as percentage of control (mean±SD) for murine 66cl-4-GFP (top), human MDA-MB-231 (middle) and human MCF-7 cells (bottom). B, Representative examples of colonies produced by 66cl-4 GFP cells treated with various concentrations of α-, γ-, and δ-tocotrienols

Table 2. Comparison of 50% effective anti-proliferative concentration (IC50) and apoptotic concentration (EC50) of tocotrienols on mouse mammary tumor cells (66cl-4-GFP) and human breast cancer cells (MCF-7 and MDA-MB-231)

Compound	Cell proliferation inhibition[1] (IC50, μM)			Apoptosis induction[2] (EC50, μM)		
	66cl-4-GFP	MDA-MB-231	MCF-7	66cl-4-GFP	MDA-MB-231	MCF-7
α-T3	65.5	N.D.[3]	N.D.	N.D.	N.D.	N.D.
γ-T3	20.6	34.6	27.5	27.7	22.2	21.6
δ-T3	10.5	12.3	12.0	20.0	17.0	12.1

[1] Cells were treated for 24 hrs with concentrations of 5, 10, 20, 40 or 80 μM of each tocotrienol compound. Cell proliferation was measured using CellTiter 96® AQueous Non-Radioactive Cell Proliferation Assay (n=6). IC50 designates concentration producing 50% inhibition of cell proliferation.

[2] Cells were treated for 24 hrs with concentrations of 10, 20, 30 or 40 μM of each tocotrienol compound. Apoptotic cell population was analyzed using Annexin V/PI assay (n=3). EC50 designates the concentration causing 50% apoptosis.

[3] Not determined: α-T3 failed to induce inhibition of cell proliferation or apoptosis at the highest dose tested (80 μM for cell proliferation assay; and 40 μM for apoptosis analyses).

3.3.3. γ-T3 induces caspase cleavage and upregulation of JNK/c-Jun phosphorylation; as well as, increased expression of death receptor 5 (DR5).

Caspase cleavage after γ-T3 treatment of human breast cancer cells was assessed using western blot analyses. As shown in Figure. 3.3, cleaved forms of caspase-8 and -9; as well as PARP were observed after γ-T3 treatment in a dose dependent manner in both MDA-MB-231 and MCF-7 cells. Caspase 3 cleavage was observed in MDA-MB-231 cells but not in caspase 3-deficient MCF-7 cells. Similar data were observed when T47D and MDA-MB-468 were examined (data not shown), demonstrating that these responses are not cell type specific. Since the apoptotic response induced by γ-T3 was associated with cleavage of caspase 8, an initiator caspase for extrinsic death receptor signaling, next death receptors (DR) expression was examined. DR5 (L/S) protein was increased in a dose dependent manner in all four cell lines, but DR4 protein level was increased only in MDA-MB-231 and T47D cells but not in MCF-7 and MDA-MB-468 cells (Fig. 3.3.B, data not shown for T47D and MDA-MB-468). Notably, phosphorylation of JNK 1/2 and both protein levels and phosphorylation status of c-Jun were increased as DR5 expression was increased.

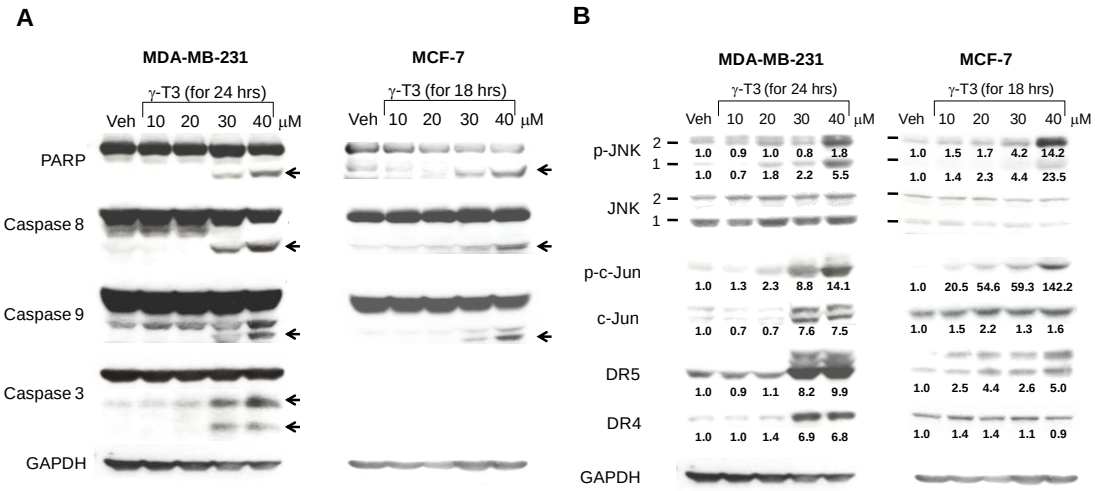

Figure 3.3. Caspases and PARP were cleaved, JNK and c-Jun were activated, and DR5 expression was increased after γ-T3 treatment in a dose-dependent manner. Cells at 2.5X10^6/plate were seeded in 100 mm plates. One day later, cells were treated with 10, 20, 30 or 40 μM of γ-T3. Control cells were treated with the vehicle at a final concentration of 0.08% ethanol. After 18 to 24 hrs, cells were collected and analyzed to detect the expression of pro-and cleaved-forms of caspase 8, caspase 9, caspase 3, and PARP (A); and p-JNK, JNK, p-cJun, cJun, DR5 (L/S) and DR4 (B) by Western blot analyses. Arrow heads in (A) indicate cleaved forms of PARP and caspases. GAPDH was used as a loading control for densitometric analyses. Numbers below p-JNK 1 and 2 represent fold change of each phosphorylated form to total JNK 1 and 2 levels respectively compared to the vehicle control. The other numbers represent the fold changes compared to the vehicle control. Data are representative of at least three independent experiments.

3.3.4. γ-T3 induced apoptosis is mediated by CCAAT/enhancer binding protein (C/EBP) homologous protein (CHOP)-mediated DR5 upregulation in human breast cancer cells.

Assessment of DR5 protein and mRNA expression at various time intervals following γ-T3 treatment showed time-dependent increases at both mRNA and protein levels (Figure 3.4.A & B). To address if DR5 was necessary for γ-T3-induced apoptosis, DR5-specific siRNA was used to knockdown DR5. Data in Figure 3.4.C show that siRNA to DR5 significantly blocked γ-T3 induced apoptosis, substantiating that DR5 plays a critical role in γ-T3-induced apoptosis. Data in Figure 3.4.D confirm the effectiveness of the knockdown in blocking γ-T3-induced apoptosis. Since it has been reported that DR5 can be transcriptionally activated by CHOP, we analyzed CHOP expression. As shown in Figure 3.5.A, the level of CHOP expression was increased in a time dependent manner. Silencing CHOP using siRNA not only inhibited apoptosis (Figure 3.5.B) but also partially suppressed the upregulation of DR5 after γ-T3 treatment (Figure 3.5.C). To determine whether DR5 transcription was directly regulated by CHOP, a ChIP assay was conducted. This assay showed that γ-T3 treatment enhanced the binding of CHOP to the DR5 promoter (Figure 3.5.D). Taken together, these data strongly suggest that CHOP is necessary for γ-T3-induction of apoptosis and that γ-T3's ability to increase DR5 protein levels is mediated at least in part by CHOP.

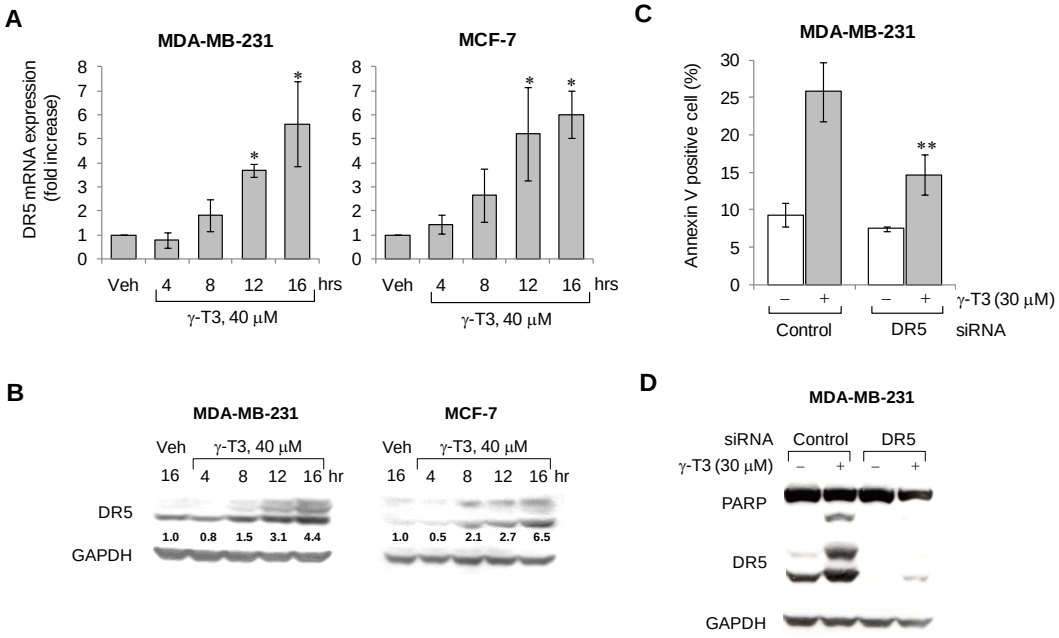

Figure 3.4. Protein and mRNA levels of DR5 were increased in a time-dependent manner after γ-T3 treatment, and siRNA against DR5 partially blocked γ-T3 induced apoptosis. A & B, Cells were treated with 40 μM of γ-T3 for indicated time points. Control cells were treated with the vehicle at a final concentration of 0.08% ethanol. Cells were collected and analyzed to detect the expression of DR5 by qRT-PCR (A); as well as, by western blot (B). Graphs in A represent fold increases in *DR5* mRNA level (mean±SD) analyzed by qRT-PCR using comparative C_T method as described in 3.2. Materials and Methods. Amplification of *GAPDH* mRNA was used as an endogenous control for the normalization. Data are representative of three independent experiments. *Statistically different from the vehicle control (*P<0.05, t-test*). The numbers in B represent the fold changes compared to the vehicle control. GAPDH was used as a loading control for densitometric analyses. C & D, MDA-MB-231 cells at $2.0X10^6$/plate were seeded in 100 mm plates. Cells were transfected with control or DR5 siRNA for 48 hrs. Then cells were treated with 30 μM of γ-T3 for 18 hrs. Cells were collected and analyzed for annexin-V labeling (C) and western blot (D) to characterize the apoptotic response (Mean±SD). Data are representative of at least three independent experiments. **Statistically different from the control siRNA + γ-T3 (*P<0.05, t-test*).

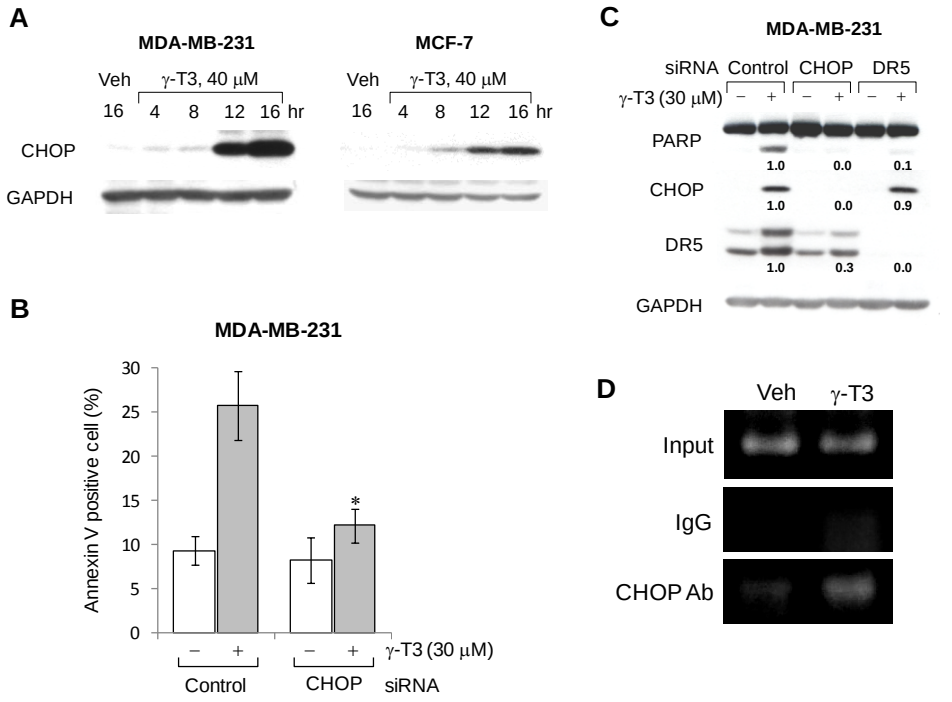

Figure 3.5. γ-T3 treatment increased CHOP expression in a time-dependent manner. Silencing CHOP partially blocked γ-T3's ability to induce apoptosis and increase DR5 protein levels. A, Cells were treated with 40 μM of γ-T3 for indicated time points. Control cells were treated with the vehicle for 16 hrs at a final concentration of 0.08% ethanol. Cells were collected and analyzed to detect the expression of CHOP by western blot. GAPDH was used as a loading control. B & C, MDA-MB-231 cells at $2.0X10^6$/plate were seeded in 100 mm plates. Cells were transfected with control, CHOP or DR5 siRNA for 48 hrs. Then cells were treated with 30 μM of γ-T3 for 18 hrs. Cells were collected and analyzed for annexin-V labeling (B) and by western blot assay (C) to characterize the apoptotic response (Mean±SD). *Statistically different from the control siRNA + γ-T3 (*$P<0.05$, t-test*). D, Direct binding of CHOP to the promoter region of DR5 was analyzed using the ChIP assay. MDA-MB-231 cells were treated with γ-T3 (30 μM) for 15 hrs and then analyzed by ChIP assay as described in 3.2. Materials and Methods. IgG served as a non-specific control in the immunoprecipitation step. Data are representative of at least three independent experiments.

3.3.5. Activation of JNK and p38 MAPK are required for the expression of CHOP and DR5, which play a critical role in γ-T3 induced apoptosis.

To further clarify the signaling pathways triggered by γ-T3, activation of JNK and p38 MAPK was analyzed. Data showed that both JNK and p38 MAPK were phosphorylated in both cell lines by 4 to 8 hrs following treatment with 40 μM γ-T3, and their activation proceeded increases in DR5 and CHOP protein levels (Figure 3.6.A). These observations raised the possibility that both JNK and p38 MAPK were playing a role in γ-T3-induced apoptosis. Silencing either JNK or p38 MAPK partially blocked apoptosis induced by γ-T3 (Figure 3.6.B & C). Interestingly, knockdown of either JNK or p38 MAPK produced decreases in DR5 and CHOP protein levels. These results suggest that JNK and p38 MAPK activation is required for the apoptotic response; as well as, is involved in the increases in DR5 and CHOP expression. Next, we examined if the activation of JNK and p38 MAPK after γ-T3 treatment is mediated by ER stress by using a chemical inhibitor, salubrinal, which specifically blocks ER stress induced apoptosis (106). Salubrinal in combination with γ-T3 protected MDA-MB-231 and MCF-7 cells from γ-T3-induced cleavage of caspase-8 and -9; as well as, PARP, suggesting that inhibition of ER stress can partially block γ-T3-mediated apoptosis (Figure 3.7.A & B). Salubrinal in combination with γ-T3 also partially blocked increases in phosphorylation status of JNK and p38 MAPK. These data suggest that the activation of JNK and p38 MAPK after γ-T3 treatment is, at least in part, mediated by ER stress.

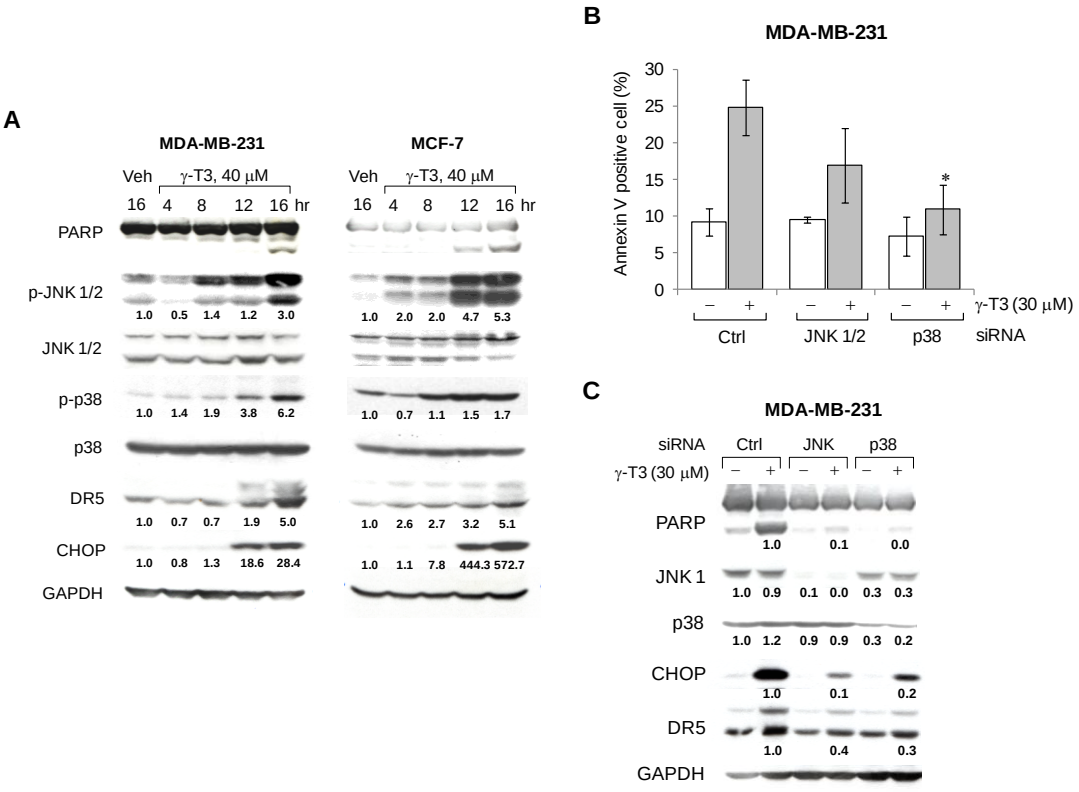

Figure 3.6. JNK and p38 MAPK were phopsphorylated by γ-T3 treatment and silencing JNK or p38 MAPK partially blocked γ-T3-induced apoptosis. A, Cells were treated with 40 μM of γ-T3 for indicated time points. Control cells were treated with the vehicle for 16 hrs at a final concentration of 0.08% ethanol. Cells were collected and analyzed to detect the expression of each protein by Western blot. Numbers below p-JNK 1/2 and p38 represent fold changes of p-JNK 1/2 and p-p38 MAPK to total JNK and p38 MAPK level compared to the vehicle control. The numbers below DR5 and CHOP represent the fold changes compared to the vehicle control. Data are representative of three independent experiments. B & C, MDA-MB-231 cells at $2.0X10^6$/plate were seeded in 100 mm plates. Cells were transfected with control, JNK 1/2 or p38 siRNA for 48 hrs. Then cells were treated with 30 μM of γ-T3 for 18 hrs. Cells were collected and analyzed by annexin V labeling (B) and western blot (C) for apoptotic response. Data are representative of 2 to 4 independent experiments. *Statistical difference from the control siRNA + γ-T3 (*$P<0.05$, *t-test*).

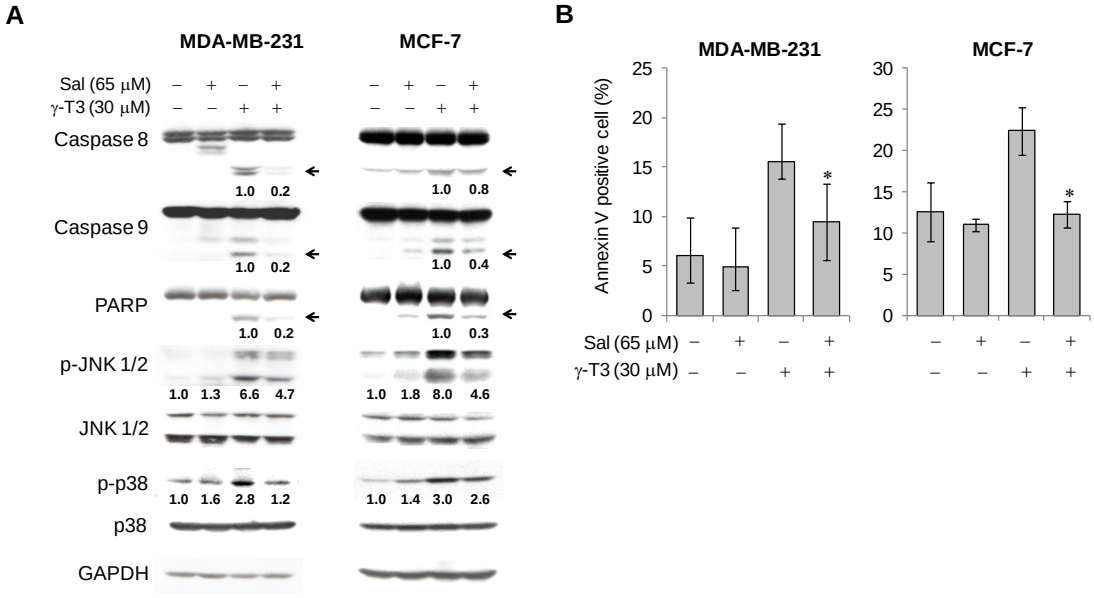

Figure 3.7. γ-T3 induced apoptosis was attenuated by ER stress inhibitor. A & B, MDA-MB-231 and MCF-7 cells at 2.5X10^6/plate were seeded in 100 mm plates. Cells were treated with DMSO or 65 μM of salubrinal combined with 30 μM of γ-T3 or ethanol (0.08%) for 18 hrs. Cells were collected and analyzed to detect the expression of each protein. GAPDH was used as a loading control. Cells were collected and analyzed by Western blot (A) and annexin V labeling (B). Data are representative of at least 3 independent experiments. *Statistical difference from the γ-T3 treatment (*$P<0.05$, *t-test*).

3.3.6. ER-stress is coupled with γ-T3-induced apoptosis in human breast cancer cells.

To further examine the involvement of ER stress in γ-T3 induced apoptosis, we analyzed several ER stress markers, ATF4, *XBP-1* splice variant and GRP78. Nuclear and cytoplasmic fractionation showed that ATF4 was localized to the nucleus as early as 4 hrs, and elevated levels of ATF4 in comparison to vehicle control were observed at all time points examined following γ-T3 treatment (Figure 3.8.A). Likewise, CHOP was also elevated in the nuclear fraction from 8 hrs after γ-T3 treatment. XBP-1 is another downstream effector and transcription factor activated upon ER stress. The splicing of *XBP-1* mRNA yields its bZIP and transactivation domain (61). After 4 to 8 hrs of γ-T3 treatment, *XBP-1* mRNA splicing was observed in both MDA-MB-231 and MCF-7 cells (Figure 3.8.B). GRP78, also known as BiP is an ER chaperon and senses the onset of the unfolded protein response (UPR). As shown in Figure 3.8.B, GRP78 expression was elevated at both mRNA and protein levels at 8 hrs of γ-T3 treatment. In order to figure out if ER stress caused by γ-T3 is a general phenomenon shared by other forms of tocotrienols, we treated MDA-MB-231 cells with δ-T3 or tocotrienol rich fraction (TRF) and analyzed the expression level of CHOP and DR5. As shown in Figure 3.8.C, both δ-T3 and TRF produced DR5 and CHOP upregulation; as well as, PARP cleavage. In comparison to γ-T3 data, these data indicate that the δ form or a mixture of T3s may activate the same apoptotic pathways as γ-T3; namely induction of ER stress and upregulation of extrinsic death receptor signaling in human breast cancer cells.

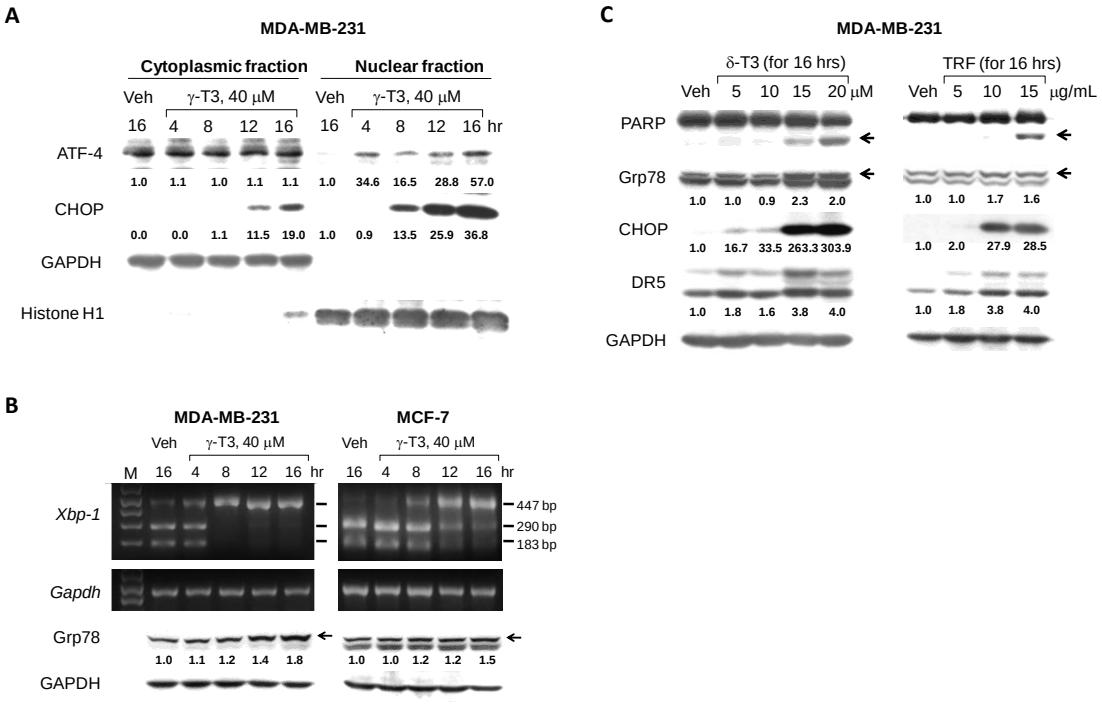

Figure 3.8. ER stress was coupled with the treatment of γ-T3. δ-T3 and TRF upregulated GRP78, CHOP and DR5. A, ATF4 expression was increased both in the cytoplasmic and nuclear fractions. MDA-MB-231 cells at $2.5X10^6$/plate were seeded in 100 mm plates. Cells were treated with 40 μM of γ-T3 for indicated time points. Cells were collected and the nuclear and cytoplasmic fractions were isolated. GAPDH and histone H1 were used for cytoplasmic and nuclear markers as well as the loading controls, respectively. B, *Xbp-1* mRNA was spliced and GRP78 was upregulated after γ-T3 treatment. MDA-MB-231 and MCF-7 cells at $2.5X10^6$/plate were seeded in 100 mm plates. Cells were treated with 40 μM of γ-T3 for indicated time points. Cells were collected and analyzed by RT-PCR. PCR products were incubated with *PstI*. Only the unspliced form of *Xbp-1* is cut by *PstI* which produces 290 and 183 bp fragments. The expression of GRP78 was analyzed by RT-PCR and Western blot analyses. The arrow head indicates the protein band specific for GRP78. C, MDA-MB-231 cells at $2.5X10^6$/plate were seeded in 100 mm plates. One day later, cells were treated with indicated concentrations of δ-T3 or tocotrienol-rich fraction (TRF). Control cells were treated with the vehicle at a final concentration of 0.08% ethanol. After 16 hrs, cells were collected and analyzed to detect the expression of GRP78, CHOP and DR5 by Western blot analyses. Arrow heads indicate cleaved form of PARP and GRP78 specific band. GAPDH was used as a loading control.

3.3.7. Inhibition of acid sphingomyelinase (ASMase) reduced apoptosis as well as ER-stress-induced increases of caspase 8 cleavage, CHOP and DR5 expression.

To identify the factor that triggers ER stress after γ-T3 treatment, the function of ASMase, an enzyme that is known to breakdown sphingomyelin in the membrane thereby releasing the second messenger ceramide, was examined. As shown in Figure 3.9.A, desipramine, an ASMase inhibitor, suppressed apoptotic responses induced by γ-T3 treatment. Silencing ASMase using siRNA reduced the cleavage of caspase 8 and PARP by γ-T3, which support the role of ASMase in γ-T3 induced apoptotic response. Interestingly, AMSase knockdown also suppressed the activation of JNK and the upregulation of GRP78, CHOP and DR5 expression (Figure 3.9.B), suggesting ASMase plays a role in triggering ER-stress after γ-T3 treatment.

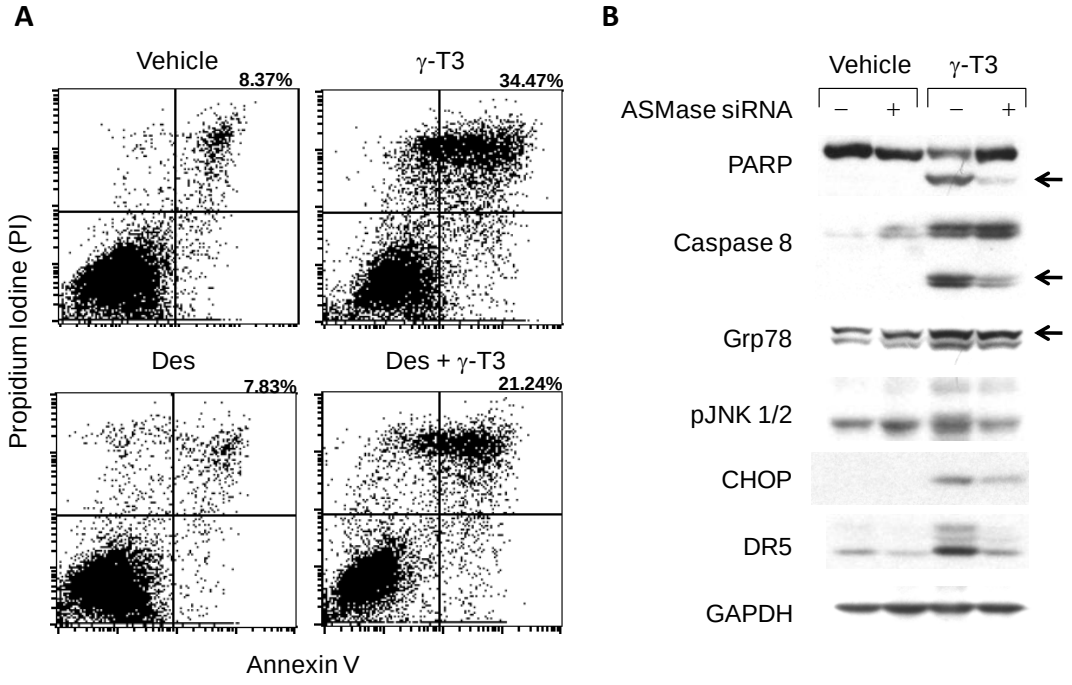

Figure 3.9. Inhibition of ASMase partially suppressed γ-T3-induced ER stress and apoptosis. A, MDA-MB-231 cells at 2.5X10^6/plate were seeded in 100 mm plates. Cells were pre-treated with DMSO or 10 μM of desipramine for 2 hrs followed by treatments with 30 μM of γ-T3 or ethanol (0.08%) for 18 hrs. Cells were collected and analyzed for the annexin V/PI labeling (Des: despipratmine). B, MDA-MB-231 cells at 2.0X10^6/plate were seeded in 100 mm plates. Cells were transfected with control or ASMase siRNA for 48 hrs. Then cells were treated with 30 μM of γ-T3 for 18 hrs. Cells were collected and analyzed by western blot. Data are representative of 2 independent experiments.

3.4. Discussion

Several studies addressing the ability of natural tocotrienols to mediate anti-carcinogenic and anti-angiogenic effects in animal models or in cells in culture have been reported (reviewed by (4)); however, the mechanisms involved in the anticancer effects of tocotrienols are not clearly understood especially in animal models. Among the reported mechanisms of action, apoptosis induction is considered to play a major role in the anti-proliferative effects of tocotrienols (107). This study was focused on understanding the molecular mechanisms of *in vivo* anticancer activity of γ-T3 in relation to its proapoptotic activities in cell culture studies. Previously, we found that γ-T3 attenuates mouse mammary tumor growth in a syngeneic animal model (described in Chapter 2). Here, based on the immunohistochemical analyses of tumor sections, we found that γ-T3 suppressed tumor growth by inhibiting cell proliferation and also by inducing apoptosis *in vivo*. In order to follow up on the anticancer mechanisms observed *in vivo*, tocotrienol effects on *in vitro* colony formation was analyzed. While the inhibitory effect of γ-T3 on cancer cell division correlated with the anti-tumor effects observed in the animal study, the inhibitory effect of α-T3 on colony formation did not match data generated in the animal study. These results suggest that anticancer efficacy of α-T3 is less effective than γ-T3 as previously suggested by Yu e*t al.* based on the apoptogenic activity of each form of tocotrienols in human breast cancer cell lines (91) and by *Constantinou et al*. as reported for human prostate cancer cell lines (87) in cell culture. A previous study by MacAnally *et al*. demonstrated that dietary delivery of δ-T3 at a dose of 250 mg/kg diet

reduced 50% of mean weight of melanomas compared to the control group in a syngeneic mouse model (33). In our previous study, γ-T3 at a dose of 250 mg/kg diet reduced mammary tumor burden by 35%. Although we did not test δ-T3 *in vivo*, it is possible that δ-T3 might exhibit a better efficacy than γ-T3 *in vivo*, since the inhibitory effect of δ-T3 on colony formation and its apoptogenic ability was the highest among α-, γ- or δ-T3 in all cell lines tested (Table 3.1 & Figure. 3.2). *Constantinou et al.* reported that δ-T3 was the most potent of all eight natural forms of vitamin E when tested on human prostate cancer cells in cell culture (87).

Data reported in previous studies showed that tocotrienols induce cell cycle arrest and apoptosis in colon and prostate cancer cells (21, 26); whereas, data reported in our study suggest that anti-proliferative effects of tocotrienols are mostly derived from apoptogenic actions; however, the possibility of the induction of cell cycle arrest by γ-T3 was not excluded. Mechanisms involved in apoptosis induced by tocotrienols in breast cancer cells have been studied using mouse +SA neoplastic mammary epithelial cells, in which caspase-8 and caspase-3 activations are required for γ-T3-induced apoptosis but no involvement of Fas signaling was detected (28, 108). In our study, we hypothesized that death receptor signaling would be involved in γ-T3 induced apoptosis based on the activation of caspase-8 and the upregulation of DR5 in the human breast cancer cells. Silencing DR5 using siRNA partially blocked γ-T3 triggered apoptosis indicating involvement of death receptor signaling. Upregulation of DR5 was observed following γ-

T3 treatment in all cells regardless of p53 status: MCF-7 cells have wild type p53, MDA-MB-231, MDA-MB-468 and T47D cells have p53 missense mutations (109). Here, we showed that DR5 expression is regulated, at least in part, by CHOP, a downstream effector protein of ER stress. CHOP-dependent activation of DR5 expression has been recently reported in different types of cancer cells treated with drugs, including lonafarnib (a farnesyltransferase inhibitor), a novel synthetic triterpenoid (methyl-2-cyano-3,12-dioxooleanan-1,9-dien-28-oate; CDDO-Me), and 2,4-dimethyl-celecoxib (a cyclo-oxygenase-2 inhibitor) (95, 108, 110). We showed that silencing CHOP reduced the increase in DR5 protein expression and decreased apoptotic responses following γ-T3 treatment. Using a chromatin immunoprecipitation assay, we further showed that CHOP directly binds to the DR5 promoter following γ-T3 treatment. This is the first report showing γ-T3 induces apoptosis via the upregulation of DR5 which is directly activated by CHOP. Furthermore, our study supports the finding of a previous gene expression study that reported increased CHOP transcript levels in tocotrienol-rich fraction (TRF) treated MDA-MB-231 and MCF-7 cells (32).

Observation of CHOP upregulation led us to further investigate the involvement of ER stress in γ-T3 induced apoptosis. We observed upregulation of ER chaperon GRP78 both in mRNA and protein, nuclear localization of ATF4 and the splicing of *XBP-1* mRNA from 4 to 8 hrs after γ-T3 treatments. Signal transduction events associated with ER stress are thought to be mediated by three ER transmembrane proteins: Ire 1, PKR-like ER kinase (PERK), and activating transcription factor 6 (ATF6) (58). The N termini of these

transducers are normally bound by ER chaperone GRP78, preventing their aggregation (52). When unfolded proteins accumulated in the ER, GRP78 binds unfolded proteins and the ER membrane proteins become dissociated from GRP78 resulting in their activation. Activation of PERK which is a Ser/Thr protein kinase results in the phosphorylation and inactivation of the eukaryotic initiation factor 2α (eIF2α) followed by translational induction of ATF4 (58). Activated ATF6, a basic leucine zipper (bZIP) containing transcription factor, induces genes with ER stress response elements (ERSE) in their promoter. *GRP78* and *XBP-1* are among the identified target genes of ATF6 (111). The other ER stress transducer, Ire-1 contains both Ser/Thr kinase domains and an endonuclease domain. Upon activation, its endonuclease activity processes *XBP-1* mRNA to generate spliced forms of *XBP-1* which encode a stable, active transcription factor (105). CHOP has been reported to be transcriptionally regulated by ATF4; as well as, XBP-1 (52), therefore our study suggests that ER stress induced by tocotrienol treatment contributes to increased expression of CHOP which plays a key role in DR5-mediated apoptosis. A recent study using mouse +SA mammary epithelial cells treated with γ-T3 showed induction of ER stress; however, unlike our study neither caspase 8 activation nor death receptor signaling was involved (112). This does not appear to be a species difference since the highly metastatic 66cl-4-GFP mouse mammary tumor cell line that we used in our *in vivo* study exhibits increased DR5 expression after γ-T3 treatment (data not shown).

We showed a time-dependent phosphorylation of JNK and p38 MAPK after γ-T3 treatment. While a marked activation of JNK was observed to occur in a time and dose-dependent manner, the activation of p38 MAPK occurred gradually 12 to 16 hrs after γ-T3 treatment. To ascertain their role in the apoptotic response, siRNA was used. Knockdown of either JNK or p38 MAPK partially blocked γ-T3-mediated apoptosis, and also reduced the upregulation of CHOP and DR5. Since CHOP is a downstream marker of ER stress, we tested if the phosphorylation of JNK and p38 MAPK was influenced by ER stress. Salubrinal is known to selectively protect cells from ER stress induced apoptosis by inhibiting the dephosphorylation of eIF2α which is phosphorylated by PERK (106). Salubrinal was capable of partially protecting the cells from γ-T3-induced apoptosis and it also partially blocked the activation of JNK and p38 MAPK. These results suggest that the activation of JNK and p38 MAPK is partially connected to ER stress mediated events. There are several reports showing that activation of JNK and/or p38 MAPK in response to ER stress is critical for inducing apoptosis (95, 96, 110). Ire-1, one of three ER stress transducers, has been shown to activate apoptosis signal-regulating kinase 1 (ASK1) which causes JNK and p38 MAPK activation (53). However, it is unclear how dephosphorylation of eIF2α by salubrinal suppressed the phosphorylation of JNK or p38 MAPK as we observed in our study. It appears that the role of JNK and p38 MAPK activation in ER stress-induced apoptosis varies in different cell types; as well as varies based on the nature of the ER stress inducer.

Finally, upregulation of Grp78, CHOP and DR5 and increased PARP cleavage were observed in cells treated with either δ-T3 or TRF suggesting that other forms of tocotrienols may trigger apoptosis coupled with ER stress which eventually activates DR5 expression in a CHOP-dependent manner. In order to understand the detailed mechanisms of how tocotrienols induce ER stress, ASMase involvement was assessed. In mouse and human T-cells, ceramide induces apoptosis mediated by ER stress in a p38 MAPK and JNK dependent fashion (110). Previous studies in our lab showed that α-tocopherol ether-linked acetic acid (α-TEA), a derivative of *R,R,R*-α-tocopherol, activates ceramide accumulation in the cell membrane, and inhibition of ceramide accumulation by a chemical inhibitor or siRNA inhibited α-TEA induced apoptosis (113). Therefore, it was of interest to see if modulation of the ceramide signaling pathway by tocotrienols initiates ER stress. Data presented here show that ASMase inhibition with either a chemical inhibitor or siRNA suppressed ER stress, caspase 8 cleavage and apoptosis induced by γ-T3. Further studies are needed to figure out the exact role of ASMase activity in γ-T3-induced apoptosis.

In conclusion, the present study showed that γ-T3 when fed in the diet suppressed mammary tumor growth *in vivo* which was correlated with decreased cell proliferation and increased apoptosis. *In vitro* data demonstrated that apoptosis triggered by tocotrienols is mediated, at least in part, by ER stress induced by ASMase action. ER stress activation of JNK and p38 MAPK followed by upregulation of DR5 in a CHOP dependent manner in human breast cancer cells in cell culture was demonstrated to be

involved in γ-T3-induced apoptosis (summarized in Figure. 3.10). Studies suggest that tocotrienols should be investigated further for their potential benefit as anticancer agents.

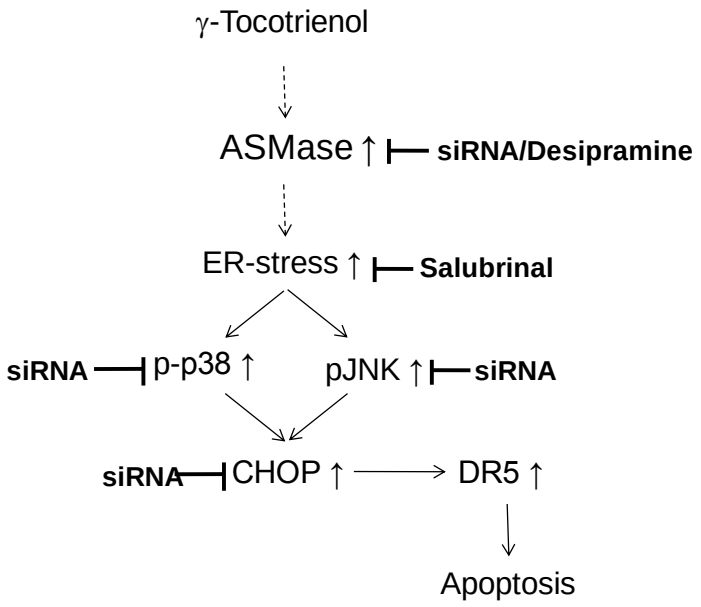

Figure 3.10. Proposed model for γ-T3 induced apoptosis mediated by ER stress. Diagram of signal transduction mediators identified and investigated in these studies. The causal nature of these mediators was established by siRNA knockdown or chemical inhibition.

Chapter 4. Investigation of γ-tocopherol as an anticancer agent in breast cancer cells and animal models.

R,R,R-γ-Tocopherol (γ-T), the major vitamin E compound consumed from food sources in the US, has been shown to have a positive correlation with lowering cancer risk in humans; however its anticancer mechanism of action is not well understood. Data presented here show that γ-tocopherol induces apoptosis and also sensitizes Tumor necrosis factor-Related Apoptosis-Inducing Ligand (TRAIL) resistant human breast cancer cells to undergo apoptosis by enhancing death receptor (DR5) expression not only at mRNA and protein levels but also by increasing cell surface expression. Cell surface increase of DR5 by γ-T triggered caspase-8 cleavage followed by increases in mitochondrial permeability, cytochrome c release and caspase-9 cleavage. In agreement with *in vitro* studies, dietary delivery of γ-T significantly suppressed the tumor growth rate of MDA-MB-231 human breast cancer cells in a *xenograft* model. In an effort to improve anti-tumorigenic potency of γ-T, we tested sesamin, a natural source human cytochrome P450 (CYP) inhibitor extracted from sesame seeds, for improving *in vivo* tissue bioavailability of γ-T. Data support that dietary supplementation with sesamin and γ-T increase liver and tumor retention of γ-T compared to single supplementation with γ-T. These data suggest that γ-T can be used singly or in combination with sesamin as a possible dietary supplementation for reducing tumor growth.

4.1. Introduction

Due to early detection followed by adjuvant therapy, breast cancer incident and mortality during past decades have decreased; however breast cancer still ranks as the second leading cause of cancer death in the US and remains the most commonly diagnosed cancer in US women (114, 115). While novel chemotherapeutics as well as early stage diagnosis and screening methods have improved breast cancer outcomes, risk-reduction and preventive strategies remain a challenge (116). Hormone-based prevention using selective estrogen receptor modulators or aromatase inhibitors have proven effective in estrogen-driven breast cancer and observational studies on lifestyle factors such as dietary fat, body weight, alcohol intake or intake of several micronutrients suggest additional targets for reducing breast cancer (115). Limited evidence is available regarding correlations between overall breast cancer risk and nutrient factors including dietary fat, carbohydrate, fruits and vegetable or micronutrients; therefore, association of breast cancer risk with individual nutrient factors requires more studies (114).

R,R,R-γ-Tocopherol (γ-T), is a vitamin E compound that shares a structural similarity and lipid-soluble antioxidant property with *R,R,R*-α-tocopherol (α-T), the predominant form of vitamin E in plasma and tissue. α-T is the most tested vitamin E form both in clinical trials and preclinical studies; however, positive correlations of α-T, synthetic α-T (*all-racemic*-α-tocopherol) or their acetate derivatives with reduction of human cancer risk has not been observed (3). Instead, studies using γ-T, the most highly consumed form of

vitamin E in the US, suggests the possibility of using γ-T as an effective chemopreventive agent in various cancers. Several clinical trials or observation studies about γ-T have been conducted. Among these, the CLUE studies best exemplify the potential chemo-preventive effect of γ-T in human prostate cancer (12, 13). In these studies, higher serum γ-T levels were associated with reduced risk of developing prostate cancer (13). In addition, previous epidemiologic studies showed that serum concentration of γ-T, but not of α-T, was relatively lower in patients with upper aerodigestive tract cancer or prostate cancer than the control subjects (117, 118). Cell culture studies using various human cancer cells have identified possible mechanisms of anticancer actions of γ-T. In human colon cancer cells, γ-T reduced DNA synthesis; decreased cyclin D1 and E expression levels; increased peroxisome proliferator activator receptor-γ (PPAR-γ) protein expression; and also induced apoptosis in a caspase-8 dependent manner (15, 119, 120). In human prostate cancer cells, reduction of cyclin D1, cell growth inhibition and the induction of apoptosis linked with interrupting *de novo* sphingolipid synthesis pathways were observed after γ-T treatment (14, 121). Although aforementioned clinical and preclinical studies strongly support possible cancer preventive or anti-proliferative effects of γ-T in prostate cancers and colorectal cancers, its application in other types of cancers remains to be investigated.

Elimination of ingested vitamin E compounds in the liver involves ϖ-hydroxylation of the phytyl side chain by cytochrome P450 enzymes (CYP)-dependent processes followed

by several steps of β-oxidation (8). In the liver, tocopherol transfer protein (TTP) discriminates between different forms of vitamin E for enrichment of α-T into nascent very low density lipoproteins (VLDL) which are subsequently transformed into low-density lipoproteins (LDL), the major carrier for α-T in blood (8). CYP3A4 and CYP4F2 are known to be the major P450 enzymes that are involved in vitamin E metabolism (8), and α-T have been shown to activate pregnane X-receptor, a nuclear receptor that induces gene expression of drug metabolizing enzymes such as CYP3A4 (10). Studies support that tissue concentrations of γ-T are limited due to CYP3A-mediated hepatic catabolism of γ-T in the liver, which may hinder the use of γ-T as a chemopreventive or an anti-cancer agent.

Data presented here demonstrated that γ-T displays anticancer effects both in cell culture studies and in a *xenograft* mouse tumor model. γ-T induced apoptosis in MDA-MB-435 and MCF-7 human breast cancer cells in a dose- and time-dependent manner in cell culture via activating death receptor 5 (DR5) signaling. Pre- or co-treatment of TRAIL-resistant human breast cancer cells with γ-T and TRAIL induced apoptosis. Dietary delivery of γ-T significantly attenuated tumor growth in a *xenograft* mouse model transplanted with MDA-MB-231-GFP human breast cancer cells. Improvement of γ-T bioavailability in tissues was observed after co-treatment of γ-T with sesamin, a natural product CYP3A inhibitor extracted from sesame oil.

4.2. Materials and Methods.

4.2.1. Cell culture and reagents

The maintenance and culture conditions for MDA-MB-435, MDA-MB-231 and MCF-7 human breast cancer cells were previously described (18, 99). All human breast cancer cells were obtained from the American Type Culture Collection (ATCC). Human mammary epithelial cells (HMEC; Cooperative Human Tissue Network, Birmingham, AL) were primary cultures of human mammary cells derived from normal mammoplasty specimens as described previously (80). For the treatment, FBS was reduced to 2% to better mimic low *in vivo* serum exposure of these cell types. α-T and γ-T were purchased from TAMA biochemical company (Tokyo, Japan) and dissolved in DMSO at 200 mM and further diluted with ethanol to 40 mM. Equivalent amount of DMSO:ethanol (1:4) were used as vehicle control. Sesamin was purchased from Cactus Botanics Ltd. (London, England). TRAIL was purchased from Alexis Biochemicals (San Diego, CA).

4.2.2. Quantification of apoptosis (Annexin V assay)

Percentage of apoptotic cells after treatment was evaluated using Annexin V- Fluorescein isothiocyanate (FITC)/Propidium iodide (PI) assay or Annexin V-Phycoerythrin (PE) assay as previously described (17). Briefly, cells were collected at indicated time points and resuspended in Annexin V binding buffer (10 mM HEPES (pH 7.4), 150 mM NaCl, 5 mM KCl, 1 mM $MgCl_2$, 1.8 mM $CaCl_2$). Cells were incubated with Annexin V-FITC (Invitrogen, CA) for 8 min at room temperature, and then suspended in PI solution (50

ng/mL in PBS). Fluorescence was measured using flow cytometry (FACSCalibur, BD Biosciences, San Jose, CA) and data were analyzed using CellQuest software (FACSCalibur, BD Biosciences). The half maximal effective concentration inducing apoptosis in 50% of the cell population (EC50) was determined using Graphpad Prism software.

4.2.3. Western blot analyses

Whole cell lysates were used to analyze protein expression levels as previously described (99). Primary antibodies used in this study were as follows: PARP (Santa Cruz Biotechnology, Santa Cruz, CA); Bid and Bax (BD Pharmingen, Rockville, MD); caspase-8 and caspase-9 (Cell Signaling Technology, Beverly, MA); DR5 (Cell Sciences, Canton, MA). The antibody to GAPDH was produced in house. Secondary antibodies conjugated with horseradish peroxidase included goat anti-rabbit and rabbit anti mouse IgG (Jackson Immunoresearch, Rockford, IL); and bovine anti-goat IgG (Santa Cruz Biotechnology). To quantitate the expression level, densitometric analyses were conducted using Scion Image Software (Scion Corporation, Frederick, MD) after normalization to glyceraldehyde-3-phosphate dehydrogenase (GAPDH) which was used as a loading control.

4.2.4. FACS analyses of cell surface expression of DR4 and DR5 and their ligand TRAIL

Cell surface expression of DR4, DR5 and TRAIL was determined using FACS analyses.

Treated or control cells were detached and washed three times with 0.5% BSA in PBS. Cells (25 μl of 8 × 106 cells/ml in 0.5% BSA in PBS) were incubated with 1 μg normal mouse IgG1 or IgG2b for 15 min at room temperature followed by incubation with phycoerythrin-conjugated antibodies to DR4, DR5 or TRAIL or phycoerythrin-conjugated isotype immunoglobulins (R&D Systems, Minneapolis, MN) for 45 min. Intensity of red fluorescence was detected using a FACSCalibur flow cytometer and data were analyzed using CellQuest software.

4.2.5. Detection of active (conformationally changed) Bax

Active (conformationally changed) Bax was detected as described previously (99). Briefly, 500 μg protein from whole cell extracts/0.5 ml was incubated overnight at 4°C with 2 μg of anti-Bax 6A7 (Sigma-Aldrich, St. Louis, MO), an antibody that specifically recognizes conformationally changed Bax, followed by reaction with 20 μl of protein G-agarose beads (Calbiochem, San Diego, CA) for 2 hours at 4°C. Protein was analyzed by SDS-PAGE followed by immunoblotting with regular anti-Bax antibody.

4.2.6. Detection of mitochondrial permeability transition

The effect of γ-T on mitochondrial membrane potential was measured using the dye JC-1 (5,5′,6,6′-tetrachloro-1,1′,3,3′ tetraethylbenzimidazolylcarbocyanine iodide/chloride; Molecular Probes, Carlsbad, CA). The JC-1 dye bearing a positive charge enters intact mitochondrial membrane due to the negative charge established by the intact mitochondrial membrane potential, accumulates as aggregates producing a red

fluorescence (122). In the absence of intact mitochondrial membrane, JC-1 accumulates in the cytoplasm as a monomeric form characterized by green fluorescence (122). Cells were collected after indicated treatment of γ-T or vehicle, incubated with JC-1 for 30 min at 37℃ followed by PBS wash. Red and green fluorescence intensity was measured using a FACSCalibur flow cytometer and data were analyzed using CellQuest software.

4.2.7. Detection of cytochrome c release from mitochondria into cytosol

A rapid and reliable technique to detect cytochrome c release during drug-induced apoptosis by FACS analyses was used (123). To detect cytochrome c release after γ-T treatment, cells were treated, collected and incubated with 100 μl digitonin (50 μg/ml in PBS with 100 μM KCl) for 5 min on ice followed by fixing the cells with 4% paraformaldehyde in PBS for 20 min at room temperature, and incubating the cells in blocking buffer (3% BSA and 0.05% saponin in PBS) for 1 h. Cells were incubated with anti-cytochrome c antibody (clone 6H2.B4, BD Pharmingen, San Diego, CA) at 1:200 in blocking buffer overnight at 4℃, washed three times with PBS, and then incubated with FITC-labeled secondary antibody in blocking buffer for 1 h at room temperature. Cytochrome c fluorescence intensity was determined using a FACSCalibur flow cytometer and data were analyzed using CellQuest software.

4.2.8. Semi-quantitative reverse transcription PCR analysis

Semi-quantitative analyses were conducted (following company instructions) to detect DR5 mRNA expression by reverse transcriptase-polymerase chain reaction (RT-PCR)

with Superscript RTase (250 U, Invitrogen) and Duplex PCR with Taq PCR Master Mix Kit (Qiagen Inc), respectively as described by Martin *et al.* (124). Primers for DR5 (478 bp) were: forward 5'-GCCTCATGGACAATGAGATAAAGGTGGCT-3' and reverse 5'-CCAAATCTCAAAGTACGCACAAACGG-3', and for β-actin (202 bp) were: forward 5'-GGCGGCACCACCATGTACCCT-3' and reverse 5'-AGGGGCCGGACTC-GTCATACT-3'. PCR conditions employed were: 94℃ for 3 min for initial denaturation, 35 cycles at 94℃ for 1 min for denaturation, 61℃ for 1 min for annealing and 72℃ for 2 min for elongation. PCR fragments were separated by electrophoresis on a 1.5% agarose gel and visualized by staining with ethidium bromide.

4.2.9. Transfection with DR5 and FADD siRNA

Cells were transiently transfected with siRNAs against DR5 or FADD (Ambion, Austin, TX) using a reverse transfection protocol following manufacturer's instructions. A negative control siRNA (Ambion, Austin, TX), which has no significant sequence similarity to any mouse, rat or human gene sequences, was used to control for any nonspecific effects on gene expression. Optimal conditions were determined using Silencer CellReady siRNA Transfection Optimization and GAPDH Kit provided by Ambion. Briefly, for each well of a 6 well plate, 9 μl transfection agent; siPORT NeoFX (Ambion, Austin, TX) was mixed with 0.5 ml serum free media (OPTI MEM-I) and incubated at room temperature for 10 min followed by addition of 2.3 μl siRNA (20 μM). The mixture of transfection agent and siRNA was incubated at room temperature for 10 min followed by mixing with 1 ml cells at 3.75×10^5/ml in culture media. Cells were

cultured for 1 day followed by replacement of the transfection media with culture media and incubating for an additional day. Transfected cells were split in 100 mm dish at 3 × 10^5 cells for 8 hrs prior to γ-T treatments for 2 days.

4.2.10. Animal study

All animal experiments were conducted according to 'Guidelines for the Humane Treatment of Animals' as designated by the University of Texas Institutional Animal Care and Use Committee. Immune compromised Nu/Nu female BALB/c mice at 6 weeks of age (approximately 20 g in weight) were purchased from Jackson Laboratories (Bar Harbor, ME).

For tumor growth rate analyses, MDA-MB-231-GFP human breast cancer cells (gift from Dr. LuZhe Sun, Department of Structural Biology, University of Texas Health Science Center at San Antonio, San Antonio, TX) in 100 μl of 50% matrigel **(**BD Biosciences, Franklin Lakes, NJ) were injected into the inguinal area at a point equal distant from the fourth and fifth nipples on the right side. About 1 wk after tumor cell injection, the mice were randomly assigned to 4 groups (10 mice/group): control, α-T, γ-T and α-T+γ-T when the tumors reached an average volume of 25 mm^3 and fed with semi-purified and tocopherol-stripped AIN-76A diets purchased from Harlan Teklad (Madison, MI). Control diet contained tocopherol-stripped purified AIN-76A diet containing 33 IU *all-rac*-α-tocopherol acetate per kg diet to meet the estimated vitamin E nutrient requirement for mice (83). To this basal (control) diet, different forms of vitamin E were added at 500

mg/kg each: thus, the combination diet contains (500 mg of α-T + 500 mg of γ-T)/kg diet**.** HPLC analyses of the actual concentrations of supplemented vitamin E forms in the diet following γ-irradiation to permit food entry into the barrier facility housing the nude mice were as follows: α-T: 378 mg/kg diet; γ-T: 358 mg/kg diet; (456 mg of α-T + 506 mg of γ-T)/kg diet. The average food intake was 3.7±0.1 g/day/mouse. With this amount of food intake, 500 mg of α-T/kg diet provided approximately 400 IU vitamin E, an amount typically found in one vitamin E soft gel capsule to an individual mouse on a daily basis based on body surface equivalency of a mouse to human (84). Tumors were measured using calipers every other day, and tumor volumes were calculated using the formula: volume (mm^3) = (width x width x length/2). Body weights were determined weekly. Animals were euthanized after 24 days of dietary treatment.

To assess the impact of sesamin on γ-T tissue availability, immune compromised Nu/Nu female BALB/c mice at 4-6 weeks of age were purchased from Jackson Laboratories (Bar Harbor, ME). A 0.72 mg β-estradiol 60 days release pellet (which is comparable to levels of estrogen in women in mid-cycle) was implanted subcutaneously between the shoulder blades of each mouse using a Trocar. After 4 days, $2X10^6$ MCF-GFP cells/mouse in 100 ml of 50% matrigel **(**BD Biosciences, Franklin Lakes, NJ) were injected into the inguinal area at a point equal distant from the fourth and fifth nipples on the right side. When the tumors were palpable, mice were randomly assigned to four groups (n=5): control, sesamin, γ-T and sesamin+γ-T groups and fed with semi-purified,

tocopherol-stripped AIN-76A diets purchased from Harlan Teklad (Madison, WI). Control diet consisted of the tocopherol-stripped purified AIN-76A diet supplemented with 60 IU *all-rac*-α-tocopherol acetate per kg diet to meet the estimated vitamin E nutrient requirement for mice (83). To this basal (control) diet, sesamin was added at 1.3 g/kg sesamin diet, γ-T was added at 250 mg/kg γ-T diet, and sesamin + γ-T was added at (1.3 g sesamin+250 mg γ-T) /kg sesamin + γ-T diet. Tumor bearing mice were fed the respective diets for 40 days. Tissues and sera were collected when animals were sacrificed.

4.2.11. Tumor immunohistochemistry

Primary tumors from 5 individual mice in each group were collected at the time of animal sacrifice and fixed in 10% formalin. Samples were processed for immunohistochemical analyses by the Histological & Tissue Processing Facility Core 3 at the University of Texas M.D. Anderson Cancer Center-Science Park Research Division (Smithville, TX) as previously describe (41, 79). Briefly, deparaffinized tumor sections (5 μm) were examined using antibody against Ki-67, a biomarker for determining active cell division and terminal deoxynucleotidyl transferase-mediated nick end labeling (TUNEL) assay for determining number of apoptotic cells. For Ki-67 analyses, 5 randomly chosen microscopic fields (X400) per tumor were scored. For TUNEL analyses, at least 15 randomly chosen microscopic fields (X400) per tumor were scored.

4.2.12. HPLC detection of vitamin E compounds in serum

Sera and tissues were snap frozen in liquid nitrogen at the time of animal sacrifice and kept in -80°C until analyzed. Lipids were extracted from each sample and different forms of tocopherols or sesamin were measured by an internal standard method using reverse-phase HPLC (high performance liquid chromatography) with fluorometric detection as described by Tirmenstein *et al.* (125). Each sample was dissolved in methanol and 40 μl of each sample was injected into a Waters 717 HPLC equipped with an autosampler. The mobile phase consisted of 96% methanol (HPLC grade; Aldrich, Milwaukee, WI), 4% water, and 0.001% glacial acetic acid. Samples were separated on a Waters spherisorb ODS-2 5u (250 x 4.6-mm) column (Alltech, Deerfield, IL). Excitation and emission wavelengths of 290 and 330 nm, respectively, were used for all determinations. Quantification of the separated compounds was performed based on the internal standard method using δ-tocotrienol as the internal standard and Millennium-32 chromatography manager software for data analyses (Waters Corp., Milford, MA).

4.2.13. Statistical analyses

Tumor growth was evaluated by transforming volumes using a logarithmic transform (base 10) and analyzed using a nested two-factor analysis of variance (ANOVA) with SPSS (SPSS Inc, Chicago, IL). Differences in tumor growth rate, number of TUNEL positive cells and Ki-67 positive cells, and serum levels of α-T and γ-T were determined using the ANOVA/Turkey's multiple comparison test and Mann-Whitney rank test with

Prism software version 4.0 (Graphpad, San Diago, CA). Tissue levels of γ-T and sesamin were compared using the student *t-test* (two-tailed, unpaired). Apoptotic data were analyzed using a one-way analyses of variance (ANOVA) followed by Tukey post hoc test or a Student *t-test* (two-tailed, unpaired). A level of $P<0.05$ was regarded as statistically significant.

4.3. Results

4.3.1. γ-T, but not α-T induced apoptosis in human breast cancer cells

The ability of tocopherols to induce apoptosis in MDA-MB-435 and MCF-7 human breast cancer cells in cell culture was evaluated using DAPI staining for visualizing DNA fragmentation, western blot assay for PARP cleavage, or Annexin V/PI assay. First, the number of cells with condensed/fragmented nuclei were observed with DAPI staining and counted following treatment with 10, 20 or 40 μM of α-T or γ-T for 3 days. As shown in Figure 4.1.A, γ-T showed a dose-dependent increase in percentage of apoptotic cells in MDA-MB-435 and MCF-7 cells but not in normal human mammary epithelial cells (HMEC); whereas α-T, the most abundant vitamin E form in human plasma and tissues, at equivalent concentrations (namely, 10-40 μM) did not induce apoptosis in any of the three cell types (Figure 4.1.A). PARP cleavage into 89 kDa fragments was observed in a dose dependent manner after γ-T treatment in both cell types (Figure 4.1.B)

and 40 μM of γ-T treatments for 2 and 3 days increased the number of annexin V positive cells in both cell lines (Figure 4.1.C), all of which confirm apoptogenic ability of γ-T in human breast cancer cells.

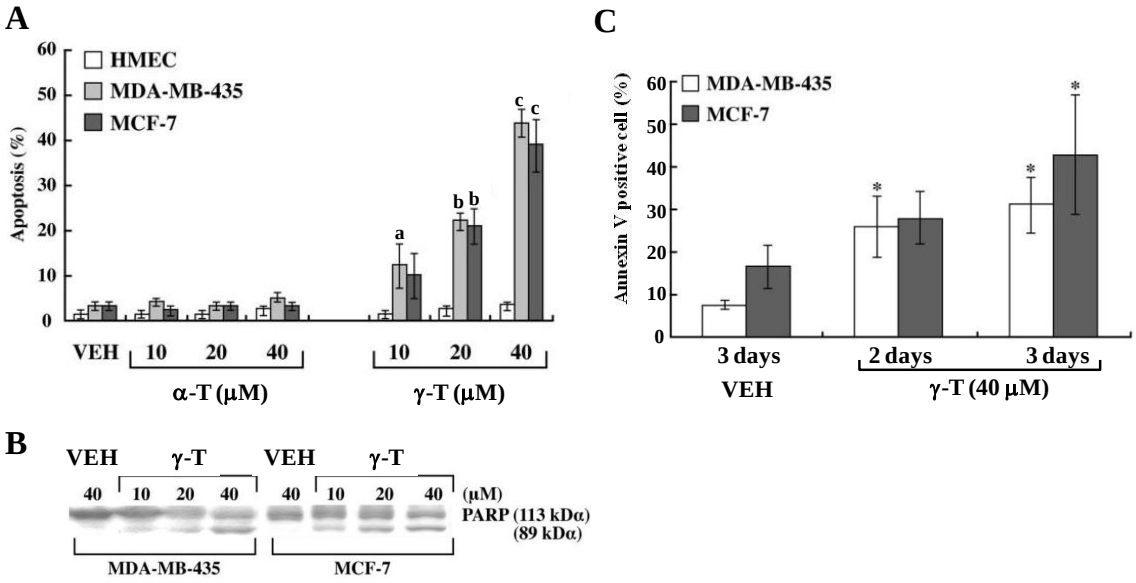

Figure 4.1. γ-T induced apoptosis in human breast cancer cells but not in HMECs. A & B, Cells were treated with 10, 20 or 40 μM of α-T or γ-T for 3 days, stained with DAPI, and percentage of apoptotic cells was determined by DAPI assay or western immunoblot analyses of PARP cleavage, respectively (a: significantly different from vehicle control; b: significantly different from vehicle control and 10 μM treatments; and c: significantly different from all treatments, $p< 0.05$). C, Cells were treated with 40 μM of γ-T for 2 and 3 days and apoptotic cell population was analyzed by FACS analyses of Annexin V positive cell. (*: significantly different from the vehicle control ($p< 0.05$). Data in A and C are represented as mean ± SD of three independent experiments. Data are adopted from Yu *et al.* (16).

4.3.2. γ-T sensitized human breast cancer cells to TRAIL induced apoptosis

Previously, HMEC and several breast cancer cell lines including MCF-7 were reported to be resistant to TRAIL induce apoptosis (126). In a preliminary study, MDA-MB-435 also showed resistance to TRAIL induced apoptosis as much as MCF-7 in comparison to TRAIL sensitive MDA-MB-231 cells (data not shown). Pre-treatment of MDA-MB-435 cells with γ-T (40 μM) for 1 day followed by treatment with 10 ng/ml of TRAIL for 2 days significantly sensitized cells to respond to TRAIL-induced apoptosis, whereas treatment of cells with 10 ng/ml of TRAIL alone did not induce apoptosis (Figure 4.2.A). Employing the same treatments to HMECs did not induce any apoptosis (Figure 4.2.A) suggesting γ-T selectively sensitized cancer cells, but not normal cells to TRAIL-induced apoptosis. This difference is likely due to the cancer cell-selective properties of TRAIL as documented previously (126). Similarly, co-treatment of γ-T at sub-apoptotic dose (20 μM) with 10 ng/ml of TRAIL for 2 days also enhanced the sensitivity of the breast cancer cells to TRAIL compared to single treatments with either γ-T or TRAIL (Figure 4.2.B).

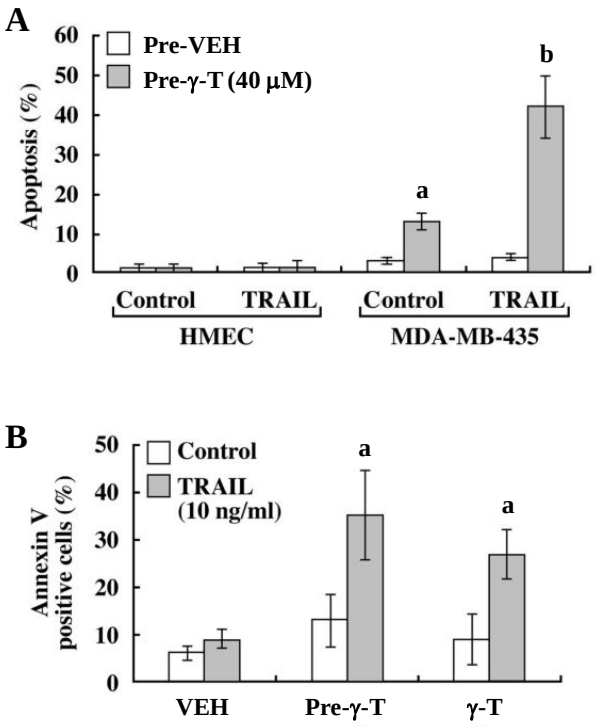

Figure 4.2. γ-T sensitized MDA-MB-435 cells to TRAIL-induced apoptosis. A, Cells were pre-treated with 40 μM of γ-T for 1 day and the treatment medium was removed followed by treatment with 10 ng/mL of TRAIL for 2 days. Cells were collected and the percentage of apoptotic cells was determined by DAPI assay (a: significantly different from vehicle control; and b: significantly different from vehicle control, γ-T alone, and TRAIL alone). B, For pre-treatment with γ-T (pre-γ-T), cells were pre-treated with 40 μM of γ-T for 1 day and the treatment medium was removed followed by treatment with 10 ng/mL of TRAIL for 2 days. For γ-T, cells were co-treated with 20 μM of γ-T + 10 ng/mL of TRAIL for 2 days. Data in A and B are represented as mean ± SD of three independent experiments. Data are adopted from Yu *et al.* (16).

4.3.3. γ-T induced increases of DR5 mRNA, protein and cell surface expression level

To figure out how γ-T reverses TRAIL-resistance in human breast cancer cells, the cell surface expression level of DR4 and DR5 and their ligand TRAIL were analyzed using specific antibodies labeled with fluorescence. As shown in Figure 4.3.A, membrane bound TRAIL or DR4 expression levels were not changed after γ-T treatment. On the other hand, DR5 expression was greatly increased in both MCF-7 and MDA-MB-231 cells. Further analyses using RT-PCR and western blot assays showed that expression of both mRNA and protein levels of DR5 were induced after γ-T treatment (Figure 4.3.B). These data suggest that DR5 expression is regulated at the transcriptional level by γ-T treatment, and translated DR5 is localized on the cell surface.

4.3.4. Silencing DR5 or Fas-associated death domain (FADD) partially blocked γ-T induced apoptosis

TRAIL binding to death receptors can initiate the subsequent recruitment of adaptor protein FADD and caspase-8 via an interaction between their death domains (DD) to form a death inducing signaling complex (DISC). To understand the role of DR5 in the apoptotic process triggered by γ-T, siRNA against either DR5 or FADD were transfected to MDA-MB-435 cells prior to γ-T treatment. Knockdown of DR5 or FADD significantly blocked γ-T-induced apoptosis in MDA-MB-435 cells (Figure 4.4.A & B). Knockdown of DR5 also restored TRAIL resistance and rendered the cells non-responsive to γ-T pre-

treatment plus TRAIL treatment (Figure 4.4.C), indicating a critical role for DR5 in γ-T's ability to sensitize breast cancer cells to TRAIL-induced apoptosis.

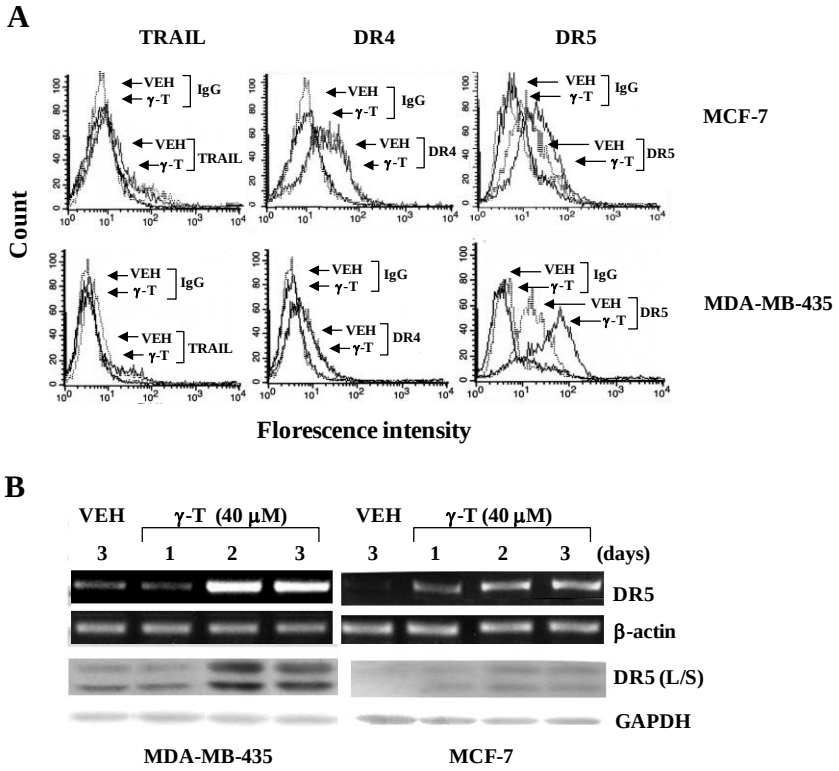

Figure 4.3. γ-T induced increases of DR5 mRNA, protein and cell surface membrane expression. A, Cells were treated with 40 μM of γ-T for 2 days and the membrane expression levels of TRAIL, DR4 and DR5 were analyzed by fluorescent antibody labeling followed by FACS analyses. B, Cells were treated at indicated time points and analyzed for DR5 mRNA level by RT-PCR (upper two panels) and protein level by western blot (lower two panels). Internal controls, β-actin for RT-PCR and GAPDH for western blot were used. All data are representative of two or more independent experiments. Data are adopted from Yu *et al*. (16).

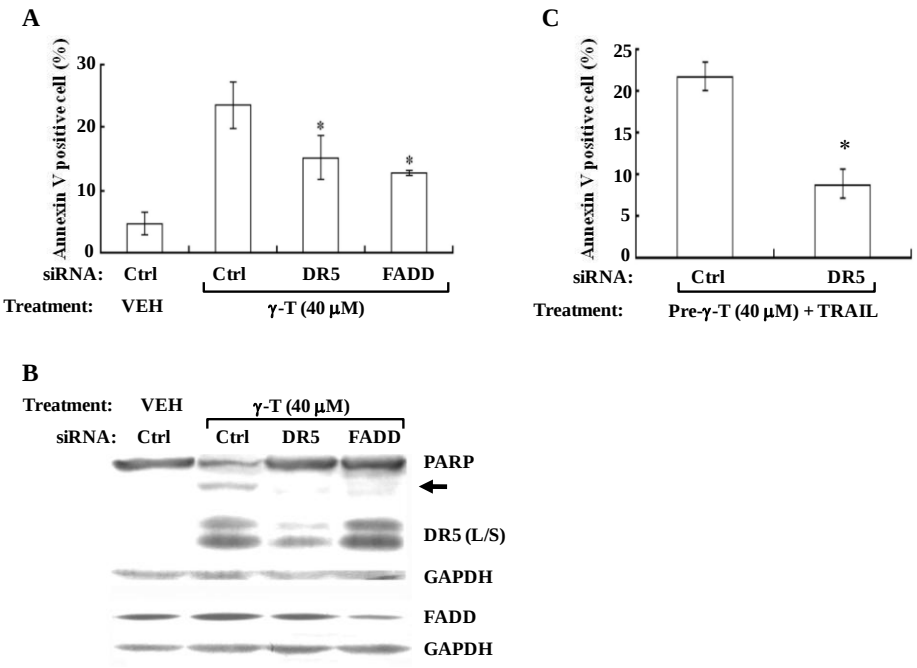

Figure 4.4. Silencing DR5 or FADD suppressed γ-T induced apoptosis. A & B, MDA-MB-435 cells were transiently transfected with siRNA targeting DR5 or FADD followed by treatment with 40 μM of γ-T for 2 days. Non-specific siRNA was used as a negative control (Ctrl). Apoptotic cells were identified using the annexin V/PI assay (A). Data are depicted as mean±SD of three independent experiments. Apoptotic response was also confirmed by checking PARP cleavage (arrow points to cleavage fragment). Knockdown of DR5 and FADD was confirmed by western blot analyses (B). C, MDA-MB-435 cells were transiently transfected with siRNA targeting DR5. Non-specific siRNA was used as a negative control (Ctrl). Transfected cells were pre-treated with γ-T (40 μM) for 1 day followed by exchange of new cell culture medium with 10 ng/ml of TRAIL for 1 day. Percentage of apoptotic cells was analyzed using the annexin V/PI assay. Data are depicted as mean±SD of two independent experiments. *Significant difference in comparison to Ctrl (P<0.05). Data are adopted from Yu *et al.* (16).

4.3.5. γ-T induced-apoptosis involved changes in mitochondrial integrity.

Since we observed DR5 and FADD involvement in γ-T induced apoptosis, we investigated downstream apoptotic signaling events. First of all, cleavage (activation) of two initiation caspases: namely, caspase-8 and -9 were analyzed using western blot. Not surprisingly, cleavages of both caspase 8 and 9 were observed after γ-T treatment in a time dependent manner (Figure 4.5.A, upper two panels). Truncation of Bid (tBid), a member of the BH3 only proapoptotic Bcl-2 family proteins as well as activation of Bax were observed upon γ-T treatment (Figure 4.5.B, lower two panels), suggesting that caspase-8 processed Bid to tBid which further activated Bax activation following treatment with γ-T. These proapoptotic Bcl-2 family proteins are well-documented for their impact on mitochondrial integrity. In this regard, we further analyzed mitochondrial potential using JC-1 which exhibits a mitochondrial potential-dependent fluorescence shift: the higher the ratio of green to red, the lower mitochondrial potential. As shown in Figure 4.5.B, cells with green signal were increased upon γ-T treatment, indicating cells lost mitochondrial potential after γ-T treatment. Cytochrome c release was also assessed using indirect immunofluorescence staining followed by FACS analysis (Figure 4.5.C). Consistently, cytochrome c release was observed in both MDA-MB-435 and MCF-7 cells after γ-T treatment. All of aforementioned data support the involvement of intrinsic mitochondria-mediated apoptosis triggered by γ-T.

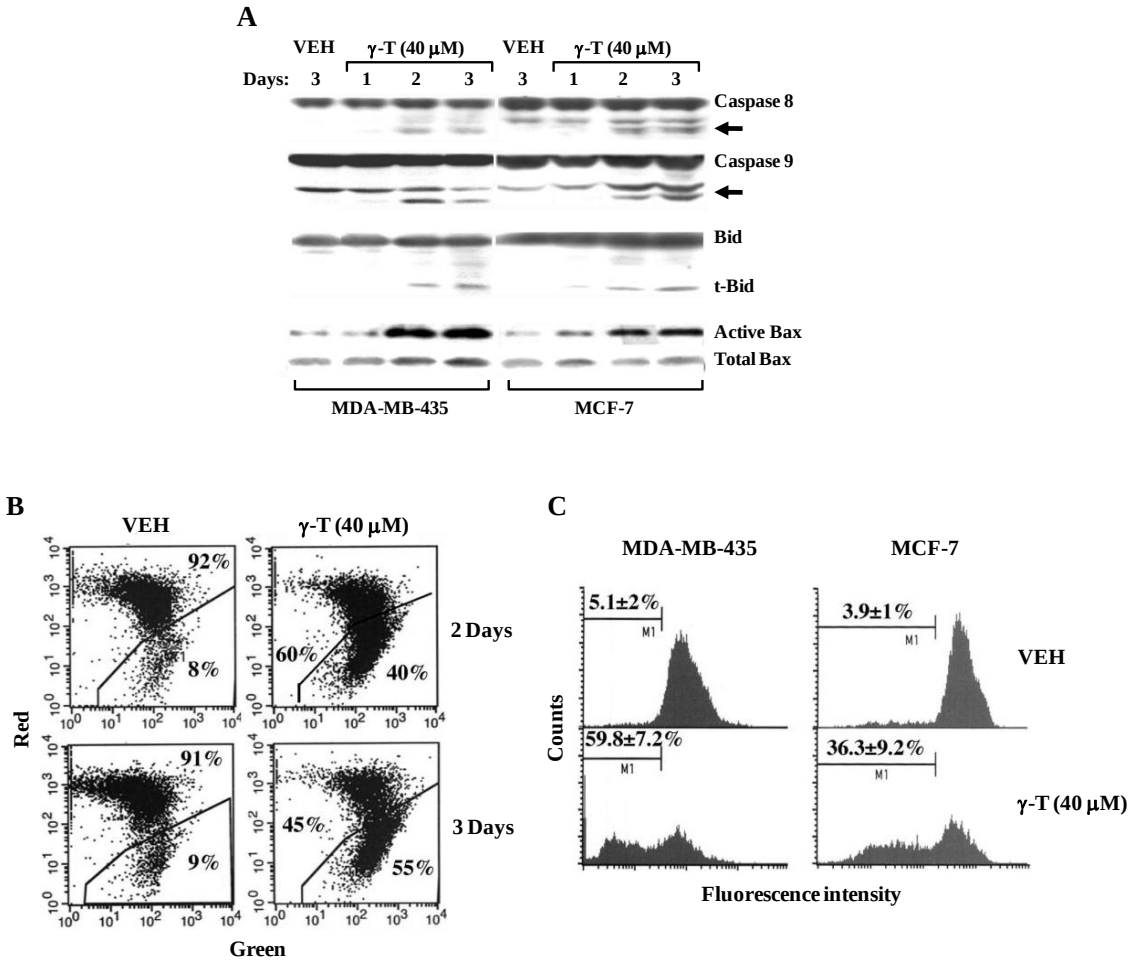

Figure 4.5. γ-T induced mitochondria dependent apoptosis. A, MDA-MB-435 cells were treated with 40 μM of γ-T for indicated time points and analyzed by western blot assays. B, Mitochondrial potential was detected using JC-1 labeling and FACS analyses after MDA-MB-435 cells were treated with 40 μM of γ-T. Decrease of mitochondrial potential was observed by the increase of cell population with loss of red and gain of green fluorescence. C, Release of cytochrome c from mitochondria was determined by indirect immunolabeling followed by FACS analyses. Numbers in graph represent percentage of cells without intact cytochrome C in mitochondria. All data were repeated twice. Data are adopted from Yu *et al.* (16).

4.3.6. γ-T significantly suppressed tumor growth in nude mice xenografted with MDA-MB-231-GFP human breast cancer cells.

Anticancer effects of dietary γ-T (500 mg of γ-T/kg diet) was tested in nude mice bearing tumors of MDA-MB-231-GFP human breast cancer cells. For comparison, basal diet (containing 33 IU all-*rac*-α-T acetate), α-T diet (500 mg of α-T/kg diet, equivalent to 400 IU/day/human) or α-T+γ-T (500 mg each compound/kg diet) were also tested. As shown in Figure 4.6.A, dietary γ-T significantly attenuated tumor growth while dietary α-T did not, suggesting γ-T, but not α-T exhibits antitumor activity, which were also correlated with in vitro cell culture studies. Interestingly, tumor suppressive effect of γ-T was blocked when co-administered with α-T, suggesting that α-T inhibits antitumor activity of γ-T as measured by reduction in tumor burden. Immunohistochemical analyses of tumor sections using TUNEL or Ki-67 labeling showed that dietary delivery of γ-T increased the number of TUNEL positive cells (P=0.03) and reduced the number of Ki-67 positive cells (P=0.06) in tumors; whereas α-T or α-T+γ-T diet groups exhibited no difference from the control diet group (Figure 4.6.B & C). These data verify that γ-T attenuated tumor growth by inducing apoptosis and inhibiting cell proliferation.

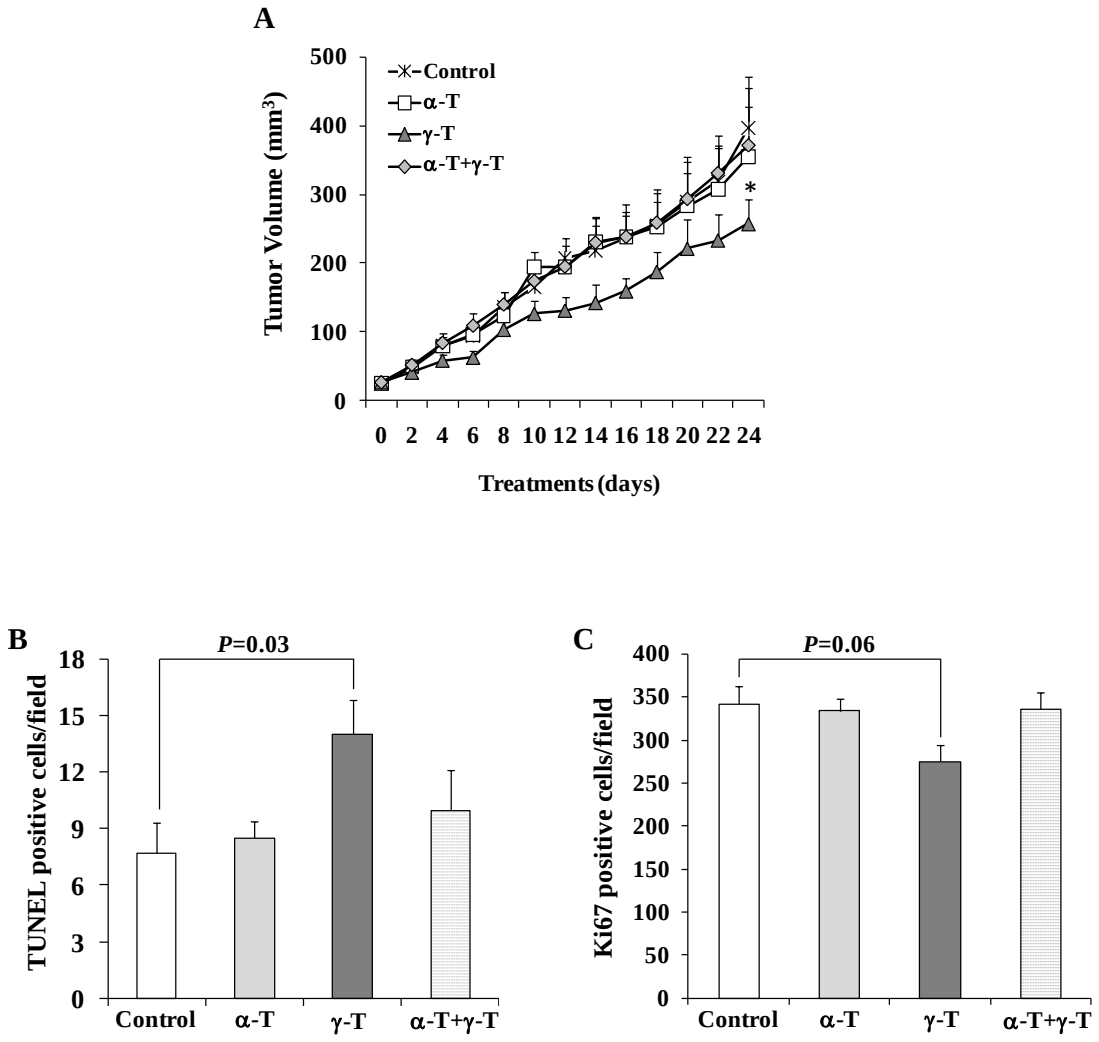

Figure 4.6. γ-T suppressed tumor growth by inducing apoptosis and inhibiting cell proliferation. A, Each supplemental diet was provided from Day 0 when MDA-MB-231-GFP tumors were palpable (approximately 25 mm^3). Tumor volumes were determined every 2 days. Data are depicted as mean±SE (n=10). *Significant difference from control diet group (P<0.05). B & C, Apoptotic cells (TUNEL positive, B) or proliferation cells (Ki-67 positive, C) in tumor section were assessed by immunohistochemical analyses. Data are depicted as mean±S.E. Data are adopted from Yu *et al*. (18).

Table 3. Serum levels of α-T and γ-T (adopted and modified from Yu *et al*. (18)).

	Serum levels [a] (μmol/L)	
Group	α-T [b]	γ-T
Control	8.5 ± 1.3	ND [c]
α-T	14.2 ± 1.7	ND
γ-T	5.7 ± 0.4	1.3 ± 0.2
α-T +γ-T	12.5 ± 1.7	ND

[a] Blood was collected at euthanasia, and the serum was harvested after blood clotted. Lipids were extracted, and levels of α-T and γ-T were analyzed by HPLC. Data are depicted as mean±S.E. (n=5).

[b] α-T levels reflect all steroisomer forms

[c] ND = not detected (below detection levels)

4.3.7. γ-T concentration in the serum was reduced by co-administration with α-T.

Levels of α-T and γ-T in mice sera were analyzed by HPLC analyses as shown in Table 4.1. Serum levels of α-T increased after dietary supplementation of α-T or α-T+γ-T in comparison to the control diet. In the case of the γ-T supplementation group, serum levels of α-T were decreased but no statistical difference was observed. Serum levels of γ-T were detected after γ-T supplementation (1.3 ± 0.2 μmol/L) which was retained approximately 10 times lower than α-T levels after same amount of α-T supplementation.

These data indicate superior stability of α-T in the serum. Notably, γ-T was not detected in the serum after γ-T + α-T supplementation.

4.3.8. γ-T concentration in tissues was enhanced by co-administration of γ-T with sesamin.

Next, we tested if co-treatment of sesamin, a natural product CYP3A inhibitor extracted from sesame oil, with γ-T in the diet enhanced the metabolic stability of γ-T. MCF-7-GFP tumor bearing nude mice were fed γ-T (250 mg/kg diet) or γ-T+sesamin (250 mg of γ-T + 1.3 g of sesamin/kg diet) supplemented diets for 40 days. HPLC analyses of γ-T concentration in serum, tumor and liver are shown in Figure 4.7. Although the serum concentration of γ-T was slightly enhanced by the combination treatment of γ-T +sesamin in comparison to γ-T supplementation alone, no significant difference was observed (P=0.29, n=5). On the other hand, γ-T retention in liver and tumor was enhanced approximately 2-fold in the γ-T +sesamin supplemented group compared to γ-T alone [P=0.005 (n=5) and P=0.07 (n=3 or 4), respectively]. These results suggest that sesamin can be used to enhance the bioavailability and thus improve anticancer activity of γ-T.

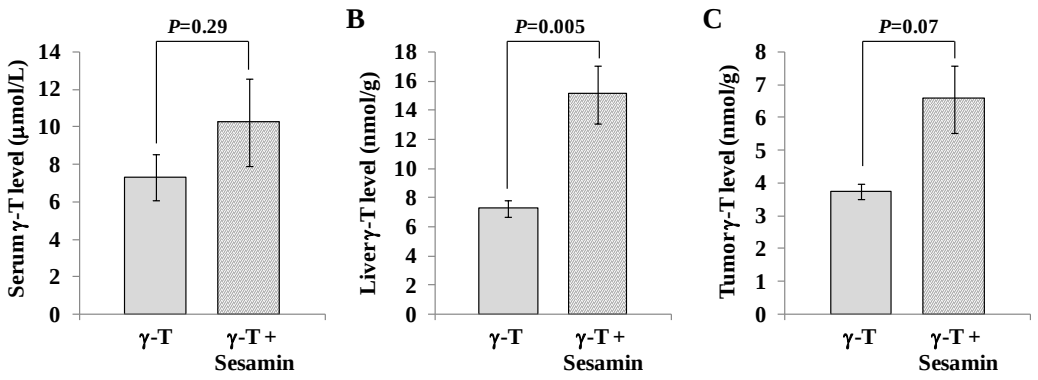

Figure 4.7. Sesamin enhanced concentration of γ-T in liver and tumor. Each supplemental diet was provided from Day 0 when MCF-7-GFP tumors were palpable (approximately 25 mm^3). On Day 40, serum (A), liver (B) or tumor (C) were collected and tissue concentration of γ-T was determined by an internal standard method using reverse-phase HPLC with fluorometric detection. Data are depicted as mean±S.E. (n=3-5).

4.4. Discussion

γ-T is the most abundant form of vitamin E in the western diet and recent research reports about its potential anticancer properties in colon and prostate cancer highlight its potential for benefiting human health. However, much remains unclear regarding mechanisms of anticancer properties of γ-T and interactions among the different forms of vitamin E found in the diet. Here, we investigated the possible application of γ-T as an adjuvant for breast cancer therapeutics by studying its effect on human breast cancer cells,

as well as in the animal *xenograft* tumor models. Data presented here showed that: 1) γ-T induced apoptosis in human breast cancer cells but not in normal epithelial cells; 2) TRAIL resistant breast cancer cells became sensitive to TRAIL-induced apoptosis after pre- or combination treatments with γ-T; 3) γ-T increased the expression of DR5 mRNA, protein, and cell surface expression levels; 4) knockdown of DR5 or FADD attenuated γ-T's apoptogenic activity as well as the ability of γ-T to sensitize TRAIL-resistant tumor cells; 5) γ-T induced mitochondria-mediated apoptosis in human breast cancer cells; 6) γ-T attenuated tumor growth in nude mice bearing MDA-MB-231 human breast cancer cells and α-T antagonized the antitumor effect of γ-T; and 7) tissue concentrations of γ-T were increased by co-treatment with sesamin, a natural product CYP3A inhibitor.

Previous studies in our lab showed that tocopherols do not induce apoptosis in human breast cancer cells under regular cell culture conditions (91). Here, we modified cell treatment conditions by reducing cell density in culture as previously proposed by Jiang *et al.* (14). This modification resulted in human breast cancer cells being induced to undergo apoptosis by γ-T but not by α-T. The proapoptotic property of γ-T has been confirmed in other types of human cancer cells (15, 127); however the mechanisms involved in γ-T triggered apoptosis have not been well defined. In prostate cancer cells, γ-T induced apoptosis via both caspase-dependent and –independent mechanisms (127) and also interrupts sphingolipid synthesis, an effect which is critical to cell death induction (14). Studies presented here demonstrate that γ-T triggers apoptosis in human breast cancer cells via activation of DR5 which is critical for γ-T-induced apoptosis as well as

for sensitization of breast cancer cells to TRAIL-induced apoptosis. Additionally, DR5 is up-regulated by γ-T at mRNA, protein and cellular membrane levels. Transcriptional regulation of DR5 has been proposed to be regulated by multiple factors including JNK, p53, NF-κB, and Myc (128-131). Increased levels of phosphorylated JNK and c-Jun have been observed after γ-T treatment of human breast cancer cells (unpublished data), suggesting JNK may be involved in transcriptional activation of DR5 by γ-T. Ongoing studies will determine if JNK/c-Jun mediates γ-T induced apoptosis and also if there is a coupling of γ-T mediated endoplasmic reticulum stress with JNK/c-Jun activation.

Activation of DR5 by γ-T seems to play a major role in restoring sensitivity to TRAIL-induced apoptosis in TRAIL-resistance cells. Agents that can increase the expression of TRAIL receptors, namely DR4 and/or DR5 have potential for clinical application in combination with TRAIL to enhance therapeutic potential of TRAIL. These agents include radiation, chemotherapeutic drugs, and natural products (108, 126, 132, 133); however, some of these agents also produce significant systemic toxicity. Therefore, it is of interest to study if γ-T can effectively sensitize cancers to TRAIL-induced apoptosis without any systemic toxicity in animal tumor models.

Based on knockdown studies of DR5 and FADD, the cleavage of caspase 8 observed after γ-T treatment is highly likely to be caused by activation of DR5 signaling. In a manner distinct from the type I mitochondria-independent apoptotic signaling pathway in which high levels of activated caspase 8 directly activate caspase 3, γ-T-mediated activation of DR5 involves caspase-8 activation followed by mitochondria-dependent

apoptotic signaling (type II) in which involves DISC formation via adaptor protein, FADD (134). This conclusion is supported by data presented in our studies showing increased levels of truncated Bid, active Bax, cytochrome C releases from mitochondria; decreased mitochondrial membrane potential; and increased caspase 9 cleavage.

Next, we evaluated the antitumor potential of dietary γ-T in comparison to α-T in nude mice xenografted with MDA-MB-231-GFP human breast cancer cells. This study confirmed our previously reported study showing oral gavage of liposomal formulated γ-T suppressed 66cl-4-GFP mouse mammary tumor growth in a syngeneic model (17). In both the *xenograft* and syngeneic tumor models, γ-T, but not α-T, attenuated tumor growth when administered by either oral gavage or dietary supplementation. Although γ-T is the most abundant form of vitamin E in the US diet, α-T is the predominant form of vitamin E detected in human serum (135). This difference in bioavailability can be explained by the superior affinity of α-T to the α-tocopherol transfer protein (α-TTP) that is expressed in the liver and responsible for preferential release of α-T from liver into the serum. The other vitamin E compounds, including γ-T, have lower binding affinity to TTP and are excreted into bile or metabolized in the liver (7). In addition to preferential binding of α-T to α-TTP, α-T is known to activate P450 enzymes that degrade and eliminate other forms of vitamin E, which also accounts for the preferential presence of α-T in serum and tissues (8, 136). Consistent with previously reported studies that demonstrated antagonistic effect of α-T on serum and tissue levels of γ-T, data presented here showed that antitumor effects of γ-T were negated by co-treatment with α-T and so

was the serum level of γ-T. Therefore, reduced bioavailability of γ-T by co-supplementation with α-T is one possible mechanism whereby α-T can antagonize γ-T antitumor action.

Sesamin is one of the major components of sesame seeds which have high nutritional value (137). It has been proposed that sesamin modifies metabolism of tocopherols; for example, γ-T level in plasma and liver of rats is increased by combination supplementation of sesamin plus γ-T in comparison to single supplementation with γ-T (138). Mechanistic studies showed that the activity of CYP3A, the major P450 family member known to metabolize vitamin E compounds in human liver is inhibited by sesamin. Thus, sesamin prevents catabolism of tocopherols thereby permitting increased retention of tocopherols in serum and tissues (139). Our data are in agreement, showing that sesamin in combination with γ-T increased tumor and liver concentrations of γ-T. Yamada *et al.* (140) showed that dietary tocotrienols protect UVB-induced skin damage and this protective effect by tocotrienols is enhanced by cotreatment with sesamin due to increased distribution of tocotrienols in the skin. Therefore, it is of interest to investigate the use of sesamin to augment anticancer actions of γ-T.

In summary, we investigated anticancer properties of γ-T in human breast cancer cells and a xenografted human breast cancer animal model. Mechanistic studies showed that γ-T triggered extrinsic death receptor mediated apoptosis signaling by increasing DR5 mRNA, protein and cell surface expression levels followed by mitochondria-dependent apoptotic signaling. γ-T suppressed MDA-MB-231-GFP tumor growth in nude mice but

the antitumor activity of γ-T was hampered by coadministration of α-T. The preferential tissue retention of α-T over γ-T could be overcome by co-administration with sesamin, which suggests that sesamin could be used to enhance anticancer benefits of γ-T.

Chapter 5. Conclusion and future directions

5.1. Conclusion

Studies in this dissertation investigated possible application of various forms of natural-source vitamin E and novel derivatives as therapeutic agents to fight breast cancer. To date, α-TEA, a redox-silent derivative of α-T, has served as the best example of a vitamin E-based anticancer agent capable of inducing apoptosis selectively in cancerous cells but not in normal cells. Based on the concept of modifying antioxidant molecule to generate apoptogenic, cancer targeting agents, we chemically modified tocotrienols, potent apoptogenic natural source vitamin E forms, to redox-silent derivatives; namely, α-T3EA and γ-T3EA. These novel compounds displayed improved apoptosis-inducing abilities and antiangiogenic activities in comparison to the parent compounds or α-TEA in cell culture studies. Although α-T3EA showed an improved tumor suppressive effect compared to α-T3 in a syngeneic mouse tumor model, no major differences in tumor suppressive effects were observed between the novel tocotrienols (α-T3EA or γ-T3EA) in comparison to either α-TEA or γ-T3. These data suggest that these redox-silencing modifications to the chroman head of the tocotrienol structure are not sufficient to dramatically augment anticancer efficacy *in vivo*, regardless of various improvements in anticancer and antiangiogenic properties observed in cell culture studies. One possible explanation of limited *in vivo* efficacy of the novel tocotrienol derivatives is the low bioavailability achieved as observed in the low liver concentration of γ-T3EA which may

result in ineffective tumor suppressive effects. Therefore, next generation of vitamin E derivatives should involve profound modifications of the chroman head or the tail of vitamin E structure to enhance metabolic stability in the liver, so that significant tissue retention and anticancer activities can be achieved.

Some natural-source vitamin E forms, especially γ-forms, were studied to better understand their mechanism of apoptogenic actions on human breast cancer cells. Data presented here demonstrated that both γ-T3 and γ-T trigger apoptosis via up-regulation of DR5 which induces caspase-8, -9 and -3 mediated apoptotic signaling events. Increase of DR5 by γ-T3 is mediated by endoplasmic reticulum (ER) stress which is coupled with JNK and p38MAPK activations followed by increase of the transcription factor CHOP which can directly bind to the promoter region of DR5 and activate DR5 gene expression. Phosphorylation of JNK was also observed in γ-T-induced apoptosis, but it is still unclear if JNK activation by γ-T treatment is coupled with ER-stress. In preclinical animal models, dietary delivery of γ-T3 and γ-T significantly attenuated the growth of tumors by inducing apoptosis and cell growth inhibition. However, anti-tumorigenic activity of γ-T was blocked by co-administration of α-T, which is in agreement with previous studies showing antagonistic effects of α-T on the serum and tissue levels of γ-T. Therefore, in order to utilize vitamin E forms demonstrating potent anticancer activity as a promising approach to target cancer, novel delivery methods designed to evade liver metabolism or

combination supplementation with agents known to inhibit metabolic enzymes need to be implemented to increase stability of these compounds.

5.2. Future directions

Previous studies testing different forms of natural-source vitamin E compounds in various types of cancer cells consistently have shown that α-forms of vitamin E compounds have the least, γ-forms have a better, and δ-forms have the best apoptogenic properties. Unfortunately, their bioavailability is known to be inversely proportional to their anticancer activities (Figure 5.1).

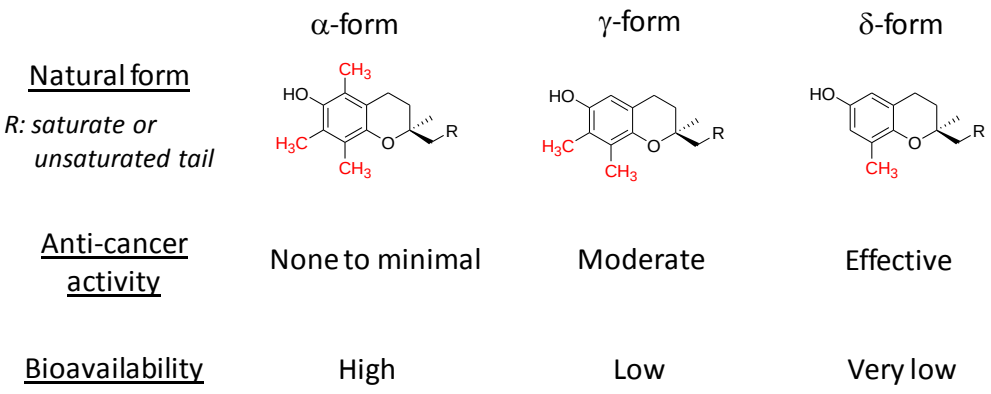

Figure 5.1. Correlation of structure, anticancer activity, and bioavailability of natural vitamin E forms.

The correlation between number of chroman head methyl groups with anticancer efficacy as well as bioavailability is striking. Reduction in number of methyl groups is predicted

to increase electronegativity on the phenolic ring and decrease the molecular size of the chroman head, suggesting that a vitamin E derivative with high electronegativity and low steric effect on the chroman head plus increased metabolic stability would be predicted to display improved anticancer properties in both *in vitro* cell culture and *in vivo* animal models.

Fluorine (F) is a small element with high electronegativity (141). Carbon-bound fluorine (C-F) often replaces carbon-bound hydrogen (C-H) in drug design strategies since F is the smallest atom that can replace H (142). Recent examination of structure-activity relationships during drug discovery and the lead compound optimization have shown that fluorinated compounds have advantageous properties in the design of small molecules. For example, introduction of fluorine atoms can increase metabolic stability of a compound by lowering the susceptibility of nearby moieties to P450 enzymatic oxidation; replacing H with F can lead to a change in the molecular conformation which may be preferable; and fluorinated compounds can have a significant increase on binding affinity of protein-ligand complexes either directly or indirectly (141, 143). In this regard, introducing fluorine into the design of new vitamin E derivatives may overcome insufficient bioavailability of some types of vitamin E compounds. As shown in Figure 5.2, several fluorinated vitamin E derivatives have been synthesized. Based on preliminary cell culture studies, compounds that contain a single fluorination and no methyl groups on the chroman head (new compounds #2 and 7 in Figure 5.2) exhibited improved apoptogenic activity in comparison to α-TEA (Figure 5.3). Another

modification that influenced the apoptogenic potential was the addition of an ether linkage between the chroman head and phytyl tail (new compounds #4, 5 and 7 in Figure 5.2). More comprehensive cell culture studies will need to be performed to explain the mechanistic aspect of these structural modifications. Anticancer efficacy studies in valid animal tumor models in conjunction with bioavailability analyses are anticipated.

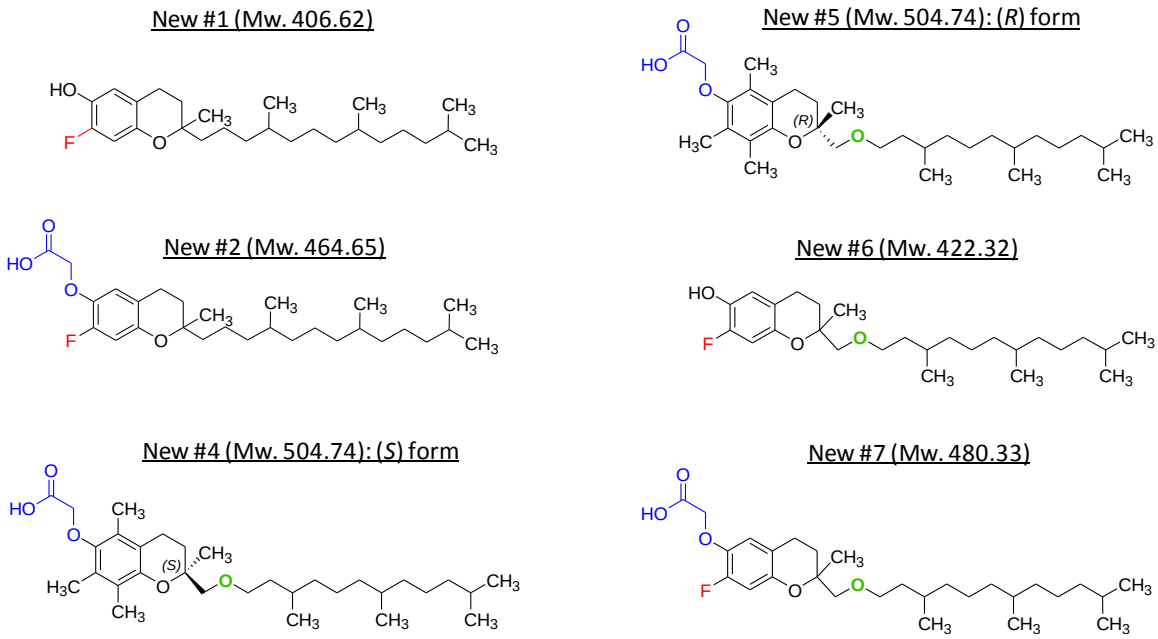

Figure 5.2. Structures and molecular weights of novel fluorinated vitamin E-related compounds and novel derivatives of α-TEA with either an *S*- or *R*-ether linked phytyl tail.

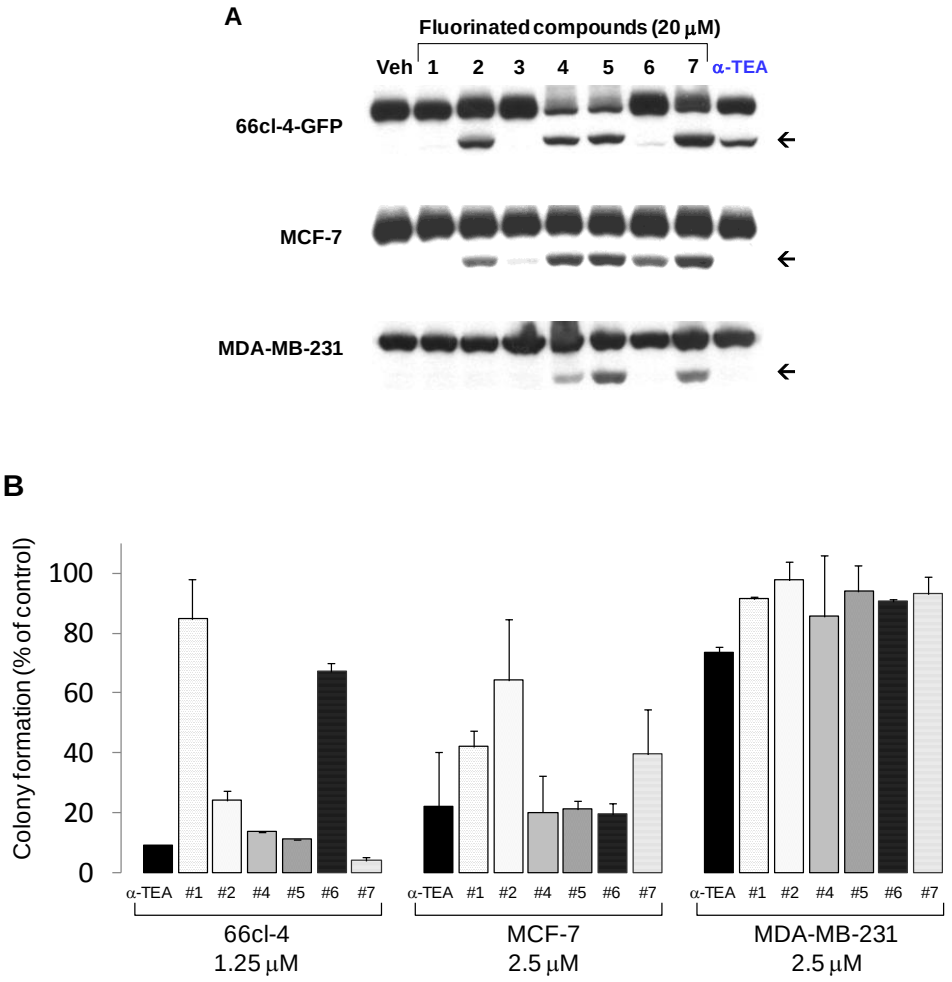

Figure 5.3. Anticancer activities of novel vitamin-E based compounds in mouse mammary tumor cells and human breast cancer cells. A, Cells were treated with 20 μM of each compound for 16 hours. Control cells were treated with the vehicle (final concentration of 0.05% ethanol). Cells were collected and PARP cleavage (indicated by arrow) were analyzed using western blot assay. Data are representative of two independent assays. B, Cells were seeded in 12-well plates at 300 cells for 66cl-4 and MCF-7 cells and 200 cells for MDA-MB-231 cells. After 48 hours, cells were treated with each compound as indicated concentrations for 2 weeks. Control cells were treated with the vehicle (final concentration of 0.02% ethanol). After 2 weeks, cells were fixed with 10% formalin followed by staining with 2% (w/v) crystal violet in H_2O. Colonies containing more than 50 cells were scored. Colony formation data are depicted as percentage of control (mean±SD, n=2-3).

Appendix 1. Anti-metastatic effect of novel vitamin E-related analogs

Fluorinated vitamin E-based compounds and novel α-TEA derivatives were synthesized and tumor-suppressive and anti-metastatic activities of these compounds were tested in a syngeneic mouse mammary tumor model using highly metastatic 66cl-4-GFP cells.

A1.1. Materials and methods

A1.1.1. Chemical reagent

Novel vitamin E-related analogs (#2, 4, 5 and 7; Figure 5.2) were chemically synthesized by Dr. Wenbin Chen.

A1.1.2. Animal study

The animal study was conducted in accordance with "Guidelines for the humane treatment of animals" as designated by the University of Texas Institutional Animal Care and Use Committee. Female BALB/c mice at 4-6 weeks of age were purchased from Jackson Laboratories (Bar Harbor, ME). The source and culture conditions for 66cl-4-GFP murine mammary tumor cells were previously described (1). 66cl-4-GFP cells were harvested and resuspended at a density of 2 x 10^5 cells/100 µl cell medium without any serum or antibiotics. Mice were injected subcutaneously with $2X10^5$ cells in the inguinal area at a point equal distant between the fourth and fifth nipples on the right side. Tumor size was measured using calipers and calculated according to the equation $V= (X^2Y)/2$, where V is the volume of each tumor, X is the smaller diameter, and Y is the larger one (1). When tumors reached an average volume of 10.7 mm^3 (day 13 after tumor cell

injection), mice were randomly assigned to 6 groups (7 or 8 animals/group): Control (vehicle control), α-TEA, #2, #4, #5 and #7. Animals were sacrificed on day 15 after treatments and tumor, heart, lung, spleen, liver and kidney were collected for measuring organ weights.

A1.1.3. Liposomal formulation and intraperitoneal (IP) injection

Each compound was formulated in liposome and lyophilized as described by Lawson *et al* (2). A dry powder of each compound was stored at -20 °C until the day of injection. Each treatment vial contained 6 to 6.25 mg of the compound. On treatment day, each vial was first brought to room temperature and the compound was dissolved in filter-sterilized water at a concentration of 3 mg/mL. Animals in each group received liposome (control) or 0.4 mg of each compound (in 130 μL) by IP injections every 4th day (on day 1, 5, 9 and 13).

A1.1.4. Determination of lung metastases

Visible lung metastases were counted after fixation in Bouin's solution as described by Giavazzi and Garofalo (3).

A1.1.5. Statistical analysis

Differences in number of treated versus control visible lung metastases and tumor/organ weights were determined by *t-test* using Prism software version 4.0 (Graphpad, San Diego, CA). A level of $P<0.05$ was regarded as statistically significant.

A1.2. Results

A1.2.1. Intraperitoneal delivery of vitamin E-related compounds had no effect on tumor growth *in vivo*

In previous cell culture studies, novel vitamin E-related compounds showed markedly improved apoptogenic activities and colony formation inhibitory effects in both murine mammary and human breast cancer cells (Figure 5.3). Here, we tested the anti-tumor efficacy of each compound in comparison to α-TEA in the 66cl-4-GFP syngeneic mouse mammary tumor transplantation model. To find the optimal dose for IP treatment, α-TEA was formulated in liposomes at various concentrations (1, 2, 4, 5, 10, and 20 mg/mL) and tested using the same animal model (n=4). Total 5 IP injections of 0.4 mg α-TEA per mouse every 4th day attenuated tumor growth by 40% in comparison to the vehicle control group (data not shown). Body weight losses of 16 and 21% in 2 out of 4 mice after the first injection were observed until day 5 after treatment initiation, but the body weights in these 2 mice recovered on day 7 after treatment initiation and remained consistent until the termination of the experiment (data not shown). Based on this pilot study, each compound was formulated in liposome and delivered by IP injection at the dose of 0.4 mg/mouse (n=7 or 8/group) every 4th day. As shown in Figure A1.1, no tumor inhibitor effect was observed in any treatments, which suggests that either the dose of each compound was not high enough or IP injection is not the best route to deliver vitamin E-related compounds to study anti-tumor activity *in vivo*. Slight weight loss was

observed after the 2nd injection of α-TEA and compound #7; however it was recovered after 2 days. No body weight differences was observed between treatments with each compound.

A1.2.2. Novel vitamin E-related compounds inhibited lung metastases *in vivo*

Visible lung metastases were counted after fixation in Bouin's solution. A reduction in the incidence of lung metastases was observed in #2 treated group compared to the control group (Table A1). Also, IP treatment of compound #5 reduced the average number of visible lung metastases observed in the metastases bearing animals compared to the vehicle treatment (Table A1). In agreement with these data, average lung weight of #2 and #5 treated groups were measured less than the control group (Figure A1.2), suggesting that compounds #2 and #5 suppressed lung metastases *in vivo.* No difference of the average organ weight between each treatment was observed except that the average kidney weight of compound #7 group was significantly reduced from the control group ($P<0.05$).

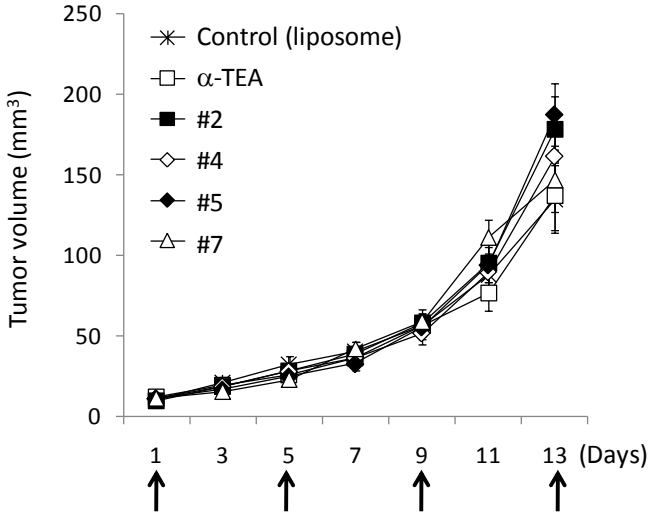

Figure A1.1. Average tumor volume (mean±SE) over time of BALB/c mice bearing 66cl-4-GFP tumor cells. Each compound was formulated in liposome and mice received liposome (control) or 0.4 mg of each compound by IP injections (↑) every 4th day. Tumor volume was measured every other day as described in Materials and Methods.

Table A1. Visible lung metastases in BALB/c mice receiving each compound formulated in liposome

Treatment groups	Number of animals with visible lung metastases/total animal number in a group [a]	Average number of visible lung metastases/animal [b]
Control	7/8	2.43 ± 0.37 (n=7)
α-TEA	6/7	2.83 ± 0.60 (n=6)
#2	4/8	3.25 ± 1.11 (n=4)
#4	7/8	2.86 ± 0.51 (n=7)
#5	5/7	1.40 ± 0.24 (n=5) [c]
#7	5/7	3.20 ± 0.49 (n=5)

[a] Visible lung metastases in all five lung lobes in each animal were counted after fixation in Bouin's solution.

[b] Data are depicted as the mean ± SE of visible lung metastases observed in the animals bearing lung metastases.

[c] Significantly different from the control (*P=0.042*, t-test).

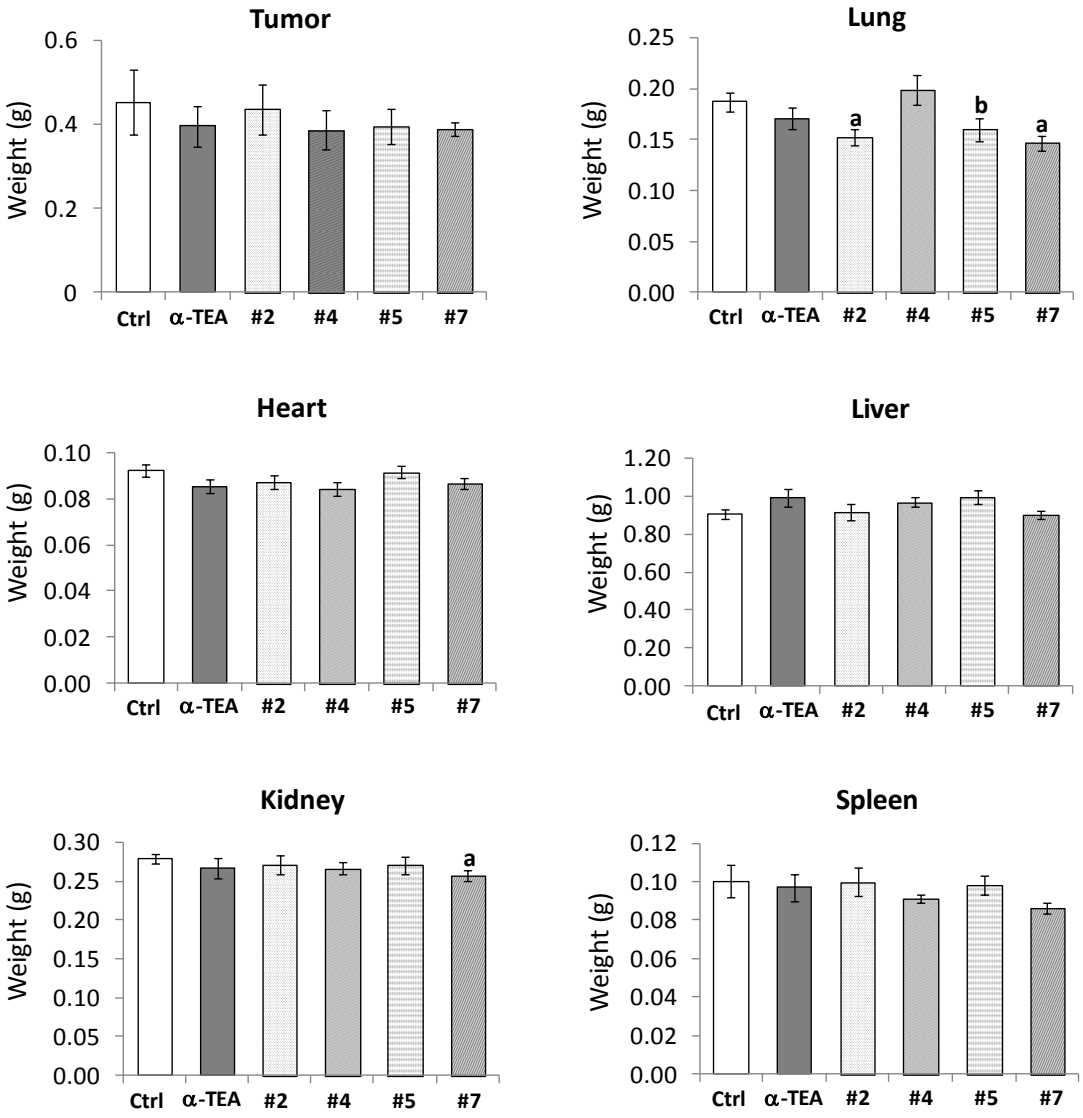

Figure A1.2. Average organ weight (mean±SE) of BALB/c mice. Each organ was collected at the time of animal sacrifice on day 15 after each treatment. [a] Significantly different from the control ($P<0.05$, t-test, n=7 or 8); [b] Marginally different from the control ($P=0.082$, t-test, n=7 or 8)

A1.3. Discussion

Our goal was to generate stronger vitamin E-related anticancer therapeutics with enhanced metabolic stability. Toward this goal, we incorporated fluorine at the chroman head and/or ether linkage between chroman head and phytyl tail of α-TEA and tested newly synthesized vitamin E-related compounds for their anticancer effects using a 66cl-4-GFP syngeneic mouse mammary tumor transplantation model. Data presented here demonstrated that: 1) intraperitoneal delivery of vitamin E-related compounds at 0.4 mg per mouse every 4th day did not display tumor inhibitory activities in a ; 2) newly synthesized compound #2 reduced the incidence of visible lung metastases; and 3) newly synthesized compound #5 reduced average number of visible lung metastases.

Due to limited amounts of newly synthesized compounds, we decided to deliver these compounds via liposomal formulations intraperitoneally. Although α-TEA has shown consistent tumor inhibitory effects in previous animal studies when delivered orally (1, 2, 4-9), intraperitoneal injections of 0.4 mg of α-TEA in liposome per mouse up to four times did not suppressed tumor growth. Instead, 100% and 75% lethality was observed after one injection of 2 and 1 mg of liposomal formulated α-TEA per mouse respectively, and severe weight loss (> 15% of body weight) was observed after one injection of 0.5 mg of liposomal formulated α-TEA per mouse in a preliminary dose response studies. These have never been observed when liposomal formulated or vesiculated α-TEA was delivered via oral routes. This may suggest that intraperitoneal route is not a proper way

of testing novel vitamin-E related compounds formulated in liposomes as attempted here. Although no tumor inhibitory effects were observed from novel compounds treatments, compounds #2 and #5 exhibited marginal inhibitory effect on lung metastases. More comprehensive cell culture studies will need to be performed to explain the mechanistic aspect of these structural modifications. Anticancer efficacy studies in a valid animal tumor model with oral routes in conjunction with bioavailability analyses are also needed to characterize the anticancer potential of these novel agents.

A1.4. References

1. Lawson KA, Anderson K, Simmons-Menchaca M, Atkinson J, Sun L, Sanders BG, Kline K (2004) Comparison of vitamin E derivatives α-TEA and VES in reduction of mouse mammary tumor burden and metastasis. *Exp Biol Med (Maywood)* 2004, 229(9): 954-963.

2. Lawon KA, Anderson K, Menchaca M, Atkinson J, Sun LZ, Knight V, Gilbert BE, Conti C, Sanders BG, Kline K (2003) Novel vitamin E analogue decreases syngeneic mouse mammary tumor burden and reduces lung metastasis. *Mol Cancer Ther* 2: 437-444.

3. Giavazzi R, Garofalo A (2001) Syngeneic Murine Metastasis Models. *Metastasis Research Protocols* 58: 223-229.

4. Yu W, Jia L, Park SK, Li J, Gopalan A, Simmons-Menchaca M, Sanders BG, Kline K (2009) Anticancer actions of natural and synthetic vitamin E forms: *RRR*-α-tocopherol blocks the anticancer actions of gamma-tocopherol. *Mol Nutr Food Res* 53(12): 1573-1581

5. Lawon KA, Anderson K, Menchaca M, Atkinson J, Sun LZ, Knight V, Gilbert BE, Conti C, Sanders BG, Kline K (2003) Novel vitamin E analogue decreases syngeneic

mouse mammary tumor burden and reduces lung metastasis. *Mol Cancer Ther* 2: 437-444.

6. Wang P, Jia L, Sanders BG, Kline K (2007) Liposomal or nanoparticle alpha-TEA reduced 66cl-4 murine mammary cancer burden and metastasis. *Drug Deliv* 14(8): 497-505.

7. Yu W, Jia L, Wang P, Lawson KA, Simmons-Menchaca M, Park SK, Sun L, Sanders BG, Kline K (2008) In vitro and in vivo evaluation of anticancer actions of natural and synthetic vitamin E forms. *Mol Nutr Food Res* 52(4): 447-456.

8. Jia L, Yu W, Wang P, Sanders BG, Kline K (2008) In vivo and in vitro studies of anticanceractions of a-TEA for human prostate cancer cells. *Prostate* 68: 849-860.

9. Latimer P, Menchaca M, Snyder RM, Yu W, Gilbert BE, Sanders BG, Kline K (2009) Aerosol delivery of liposomal formulated paclitaxel and vitamin E analog reduces murine mammary tumor burden and metastases. *Exp Biol Med (Maywood)* 234(10): 1244-1252.

Appendix 2. α-TEA improves obesity-induced glucose intolerance and insulin insensitivity

Obesity is highly associated with the development of various chronic diseases such as cardiovascular diseases, type 2 diabetes, hypertension, stroke, dyslipidemia and some cancers (1). One common feature of obesity-related complications is obesity-induced adipose tissue inflammation (2; 3) characterized by abnormal production of adipokines, free fatty acids (FFA), and proinflammatory cytokines including tumor necrosis factor-α (TNF-α), monocyte chemoattractant protein 1 (MCP-1), and interleukin 6 (IL-6) (4; 5). These proinflammatory signals involve intracellular signaling pathways, such as nuclear factor kappa light-chain enhancer of activated B cells (NF-κB) system (4). Increased production of proinflammatory cytokines and FFA by adipose tissue contributes to macrophage infiltration into adipose tissue, thereby exacerbating chronic inflammation and eventually impairing insulin action in peripheral tissues, such as fat and skeletal muscle (6).

α-TEA, an *R,R,R*-α-tocopherol derivative possessing pleiotropic anticancer activities, has shown to modulate AMP-activated protein kinase (AMPK) activity, a sensor and regulator of cellular energy balance (unpublished data). Activation of AMPK is involved in glucose transport and fatty acid oxidation which result in improvement of glucose homeostasis and breakdown of stored fat (7). Studies using antidiabetic agents have shown that insulin-sensitizing action of these agents requires AMPK activation in

peripheral tissues (8). Notably, AMPK activation in macrophages can downregulate proinflammatory responses and also improve insulin sensitivity in adipocytes, suggesting that AMPK is a potential target for the treatment of inflammation associated disorders (9). Here, we investigated the possible application of α-TEA for the prevention of obesity related complications using mouse macrophages and adipocytes in cell culture; as well as, dietary administration of α-TEA in a diet-induced obese (DIO) mouse model.

A2.1. Materials and methods

A2.1.1. Cell culture and reagents

Mouse macrophages (RAW264.7) and fibroblasts (3T3-L1) were purchased from the American Type Culture Collection (ATCC). RAW264.7 cells were cultured and maintained in Gibco® RPMI 1640 medium (Invitrogen, Carlsbad, CA) supplemented with 10% (v/v) fetal bovine serum (HyClone, Logan, UT), 100 μg/mL streptomycin, and 100 units/mL penicillin. 3T3-L1 cells were cultured and maintained in Dulbecco's modified Eagle's medium (DMEM) high glucose medium (Invitrogen) supplemented with 10% (v/v) bovine calf serum (Gemini Bio-Products, West Sacramento, CA), 100 μg/mL streptomycin, and 100 units/mL penicillin following manufacturer's instructions. Curcumin (C1386), dexamethasone (DEX, D4902), 3-isobutyl-1-methyl-xanthine (IBMX, I7018) and insulin (INS, I6634) were purchased from Sigma-Aldrich (St. Louis, MO).

Recombinant mouse tumor necrosis factor-α (TNF-α) was purchased from R&D Systems (Minneapolis, MN).

A.2.1.2. Cell viability assay (MTS assay)

Effect of α-TEA on cell proliferation was assessed in RAW264.7 macrophages in cell culture. Cells at $5X10^3$/well were seeded in 96-well plates. Cells were treated with a range of concentrations of α-TEA (1.25 to 40 μM). Control cells were treated with the vehicle (ethanol) at a final concentration of 0.1 %. After 48 hrs, viable cells were measured using CellTiter 96® AQueous Non-Radioactive Cell Proliferation Assay kit (Promega, Corp., Madison, WI) following manufacturer's instructions. The percentage of viable cells at each concentration was calculated by dividing color absorbance (A290) of treated cells by that of control cells.

A.2.1.3. 3T3-L1 adipocyte differentiation and TNF-α treatment

To differentiate 3T3-L1 fibroblasts into adipocytes, 4 days post-confluent 3T3-L1 cells were treated with 10 μ/mL INS, 1 μM DEX and 0.5 mM IBMX for 72 hrs. Cells were maintained in adipocyte maturation medium containing 10 μg/mL INS in complete medium. Media were changed every 2-3 days (10). To induce inflammatory cytokine genes, differentiated adipocytes (Day 6 after differentiation) were treated with TNF-α (20 ng/mL) for 2 days (11).

A.2.1.4. Western blot analyses

Whole cell lysates were used to analyze protein expression levels as previously described (12). Antibodies to poly (ADP-ribose) polymerase (PARP) and NF-κB p65 were purchased from Santa Cruz Biotechnology (Santa Cruz, CA). Antibodies to inhibitor of NF-κB (IκB)-α, AMPKα, phospho-AMPK (p-AMPK) α, and phosphor-acetyl-CoA carboxylase (p-ACC) were purchased from Cell Signaling Technology (Beverly, MA). Secondary antibodies conjugated with horseradish peroxidase included goat anti-rabbit and rabbit-anti-mouse IgG (Jackson Immuoresearch, Rockford, IL).

A.2.1.5. Quantitative real time-PCR (qRT-PCR) analyses of inflammatory cytokines

Changes in messenger RNA levels for inflammatory cytokines in 3T3-L1 adipocytes after TNF-α treatment were assessed. Cells were differentiated for 6 days and treated with TNF-α in combination with 0.01% ethanol or 20 and 40μM α-TEA for 48 hrs. Cells were then collected and total RNA was purified using RNeasy mini kit following manufacturer's instructions (Qiagen Inc. Valencia, CA). Two μg of RNA from each sample was used for the reverse transcription reaction using SuperScript First Strand Synthesis System for RT-PCR (Invitrogen, Carlsbad, CA). Quantitative analyses of each gene using specific primers (Table A2) were performed with 1 μL cDNA using SYBR® Green PCR Master Mix (Applied Biosystems Inc., Forster City, CA) following manufacturer's instructions. Each primer set was used at a concentration of 2 μM in a final reaction volume of 20 μL. Changes in gene expression were analyzed by

comparative C_T method following ABI PRISM 7700 Sequence Detection System User Bulletin #2: Relative Quantitation of Gene Expression (P/N4304859). The *36B4* gene (ribosomal acid phosphoprotein P0) was used for internal control to normalize target gene expression (13).

Table A2. Primers used for quantitative real-time PCR

Genes	Forward primers (5'→ 3')	Reverse primers (5' → 3')	References
COX-2	TGGGGTGATGAGCAACTATT	AAGGAGCTCTGGGTCAAACT	(14)
MCP-1	GCCCACTCACCTGCTGCTACT	CCTTGCTCGTCCTCATCCTCTTGT	(15)
IL-6	AGTTGCCTTCTTGGGACTGA	CAGAATTGCCATTGCACAAC	(14)
36B4	GGCCCTGCACTCTCGCTTTC	TGCCAGGACGCGCTTGT	(13)

A2.1.6. Diet-induced obese (DIO) mouse model

The animal study was conducted in accordance with "Guidelines for the humane treatment of animals" as designated by the University of Texas Institutional Animal Care and Use Committee. Female C57BL/6 mice at 4-6 weeks of age were purchased from Jackson Laboratories (Bar Harbor, ME). Mice were acclimated for 10 days and randomly divided into 5 groups (10 animals/group). Each group received corresponding diet for 91 days and all diets were purchased from Research Diets (New Brunswick, NJ). Group 1 received rodent lean control diet (10% total kcal% from fat, D12450B), group 2 received

high fat diet (60% total kcal% from fat, Diet D12492), group 3 received high fat diet containing α-TEA (Diet D12492+500 mg alpha-TEA/kg diet), group 4 received high fat diet containing curcumin (Diet D12492+500 mg curcumin/kg diet), and group 5 received high fat diet containing both curcumin and α-TEA (Diet D12492+500 mg curcumin and 500 mg alpha-TEA/kg diet). Body weights and food intake were monitored every 3-4 days. The fat tissue mass was determined using quantitative magnetic resonance (Echo Medical Systems, Houston, TX) on Days 34, 69 and 89.

A2.1.7. Glucose tolerance and insulin sensitivity tests

On day 80, tail-tip blood was collected to measure fasting glucose level of overnight (approximately 16 hrs) fasted-animals using Accu-Chek Compact Plus glucometer (Roche, Basel, Switzerland). Then to determine glucose tolerace, mice were injected with 20% glucose intraperitoneally (2 g/kg) and thereafter the blood glucose levels were measured at 15, 30, 60 and 120 min. As an indication of insulin sensitivity, the homeostasis model assessment (HOMA) was used as described by Hong *et al.* (16). Briefly, on the day of animal sacrifice (Day 91), overnight fasting glucose level was measured as described above. Blood was collected from heart puncture after CO2 asphyxiation. Serum insulin was measured using Insulin (mouse) Ultrasensitive ELISA kit (ALPCO, Salen, NH) following manufacturer's instructions. HOMA-IR values were calculated using the formula below:

$$\text{HOMA IR} = \frac{\text{fasting insulin } (\mu g/mL) \times \text{fasting glucose } (mmol/L)}{22.5}$$

A2.1.8. Statistical analyses

Differences in *in vitro* gene expression, body weight, fat mass, glucose tolerance test, HOMA, and organ weights were determined with *t-test*. A level of $P<0.05$ was regarded as statistically significant.

A2.2. Results

A2.2.1. α-TEA reduced NK-κB expression and induced apoptosis in RAW264.2 mouse macrophages

Effects of α-TEA on inflammation were tested using RAW264.2 mouse macrophages. Treatment of α-TEA inhibited macrophage cell viability and also induced apoptosis based on PARP cleavages in a dose dependent manner (Figure A2.1.A & B). Decreased expression of NF-κB p65 was also observed by α-TEA treatment (Figure A2.1.B).

A2.2.2. α-TEA induced AMPK activation and reduced inflammatory factors in TNF-α-activated adipocytes.

Next, α-TEA effects on AMPK signaling were tested in 3T3-L1 adipocytes. As shown in Figure A2.2.A, phosphorylation of AMPK as well as ACC, a target of AMPK, was increased by α-TEA treatment, suggesting that AMPK is activated by α-TEA in adipocytes. In addition, NF-κB p65 protein level was decreased while IκB protein level

was increased in 3T3-L1 adipocytes following α-TEA treatment. To further determine the role of α-TEA in inflammation, TNF-α was added to the 3T3-L1 adipocytes to trigger inflammatory signaling. As shown in Figure A2.2.B, C & D, addition of TNF-α markedly increased mRNA levels of *IL-6*, *COX-2* and *MCP-1*, whereas co-treatment with TNF-α+α-TEA significantly suppressed the gene activation of these inflammatory biomarkers, suggesting that α-TEA may be beneficial in preventing obesity associated inflammation.

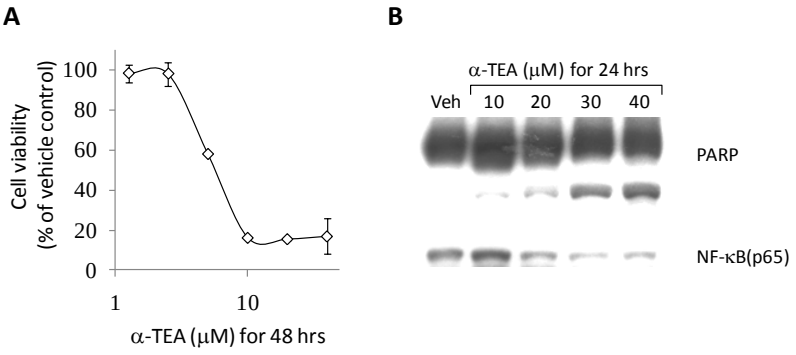

Figure A2.1. α-TEA inhibited cell proliferation (A) and induced apoptosis in RAW264.7 macrophages (B). A, Cells were treated with 1.25, 2.5, 5, 10, 20 and 40 μM α-TEA for 48 hrs and the cell viability was measured as described in A2.2. Materials and methods. Data are depicted as mean±SD of triplicate plates. B, Cells were treated with indicated concentration of α-TEA for 24 hrs and PARP cleavage and NF-κB p65 expression were analyzed by western blot assay.

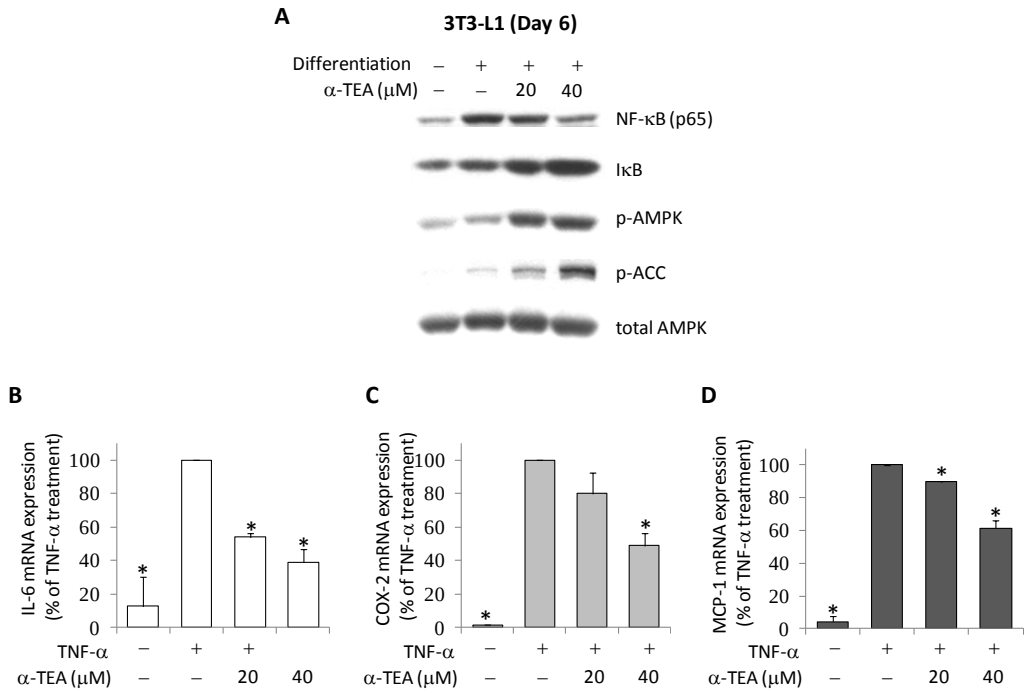

Figure A2.2. α-TEA activates AMPK pathway, downregulates NK-κB expression, as well as suppresses inflammatory factor expression after TNF-α stimulation. A, 3T3-L1 cells were induced to differentiate for 6 days in the presence or absence (vehicle, 0.01% ethanol) of α-TEA at indicated concentrations. Cell lysates were used for western blot analyses. B, C, & D, 3T3-L1 cells were induced to differentiate into adipocytes for 6 days, and then treated with 20 ng/mL TNF-α in combination with 0.01% ethanol or 20 and 40 μM α-TEA for 48 hrs. Cells were collected and analyzed to detect the expression of *IL-6*, *COX-2*, and *MCP-1* by qRT-PCR using comparative C_T method. Graphs in B, C & D represent percentage of gene expression in comparison to TNF-α single treatment. Data represent two or three independent experiments (mean±SD). *Statistically different from the TNF-α single treatment (*P<0.05, t-test*).

A2.2.3. α-TEA did not affect body weight or fat mass in diet-induced obese mice.

Based on cell culture studies showing that α-TEA suppressed NF-κB expression and the mRNA expression of inflammatory cytokines in adipocytes, we hypothesized that α-TEA will inhibit obesity-induced inflammation. To test this hypothesis, we used a diet-induce obese mouse (DIO) model. Female C57BL6 mice were fed a high-fat diet for 90 days with or without α-TEA (500 mg/kg diet). Curcumin which has been shown to inhibit adipogenesis and body weight gain in the same animal model served as a positive control (17). As shown in Figure A2.3, α-TEA did not affect weight gain or fat mass in DIO mice. Curcumin slightly decreased body weight and fat mass compared to the high fat-diet fed control group, but no statistically significant differences were observed.

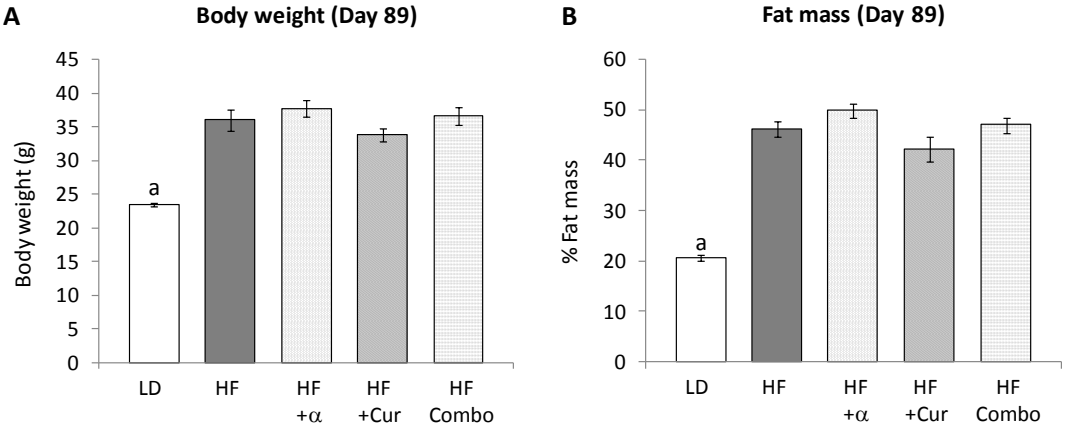

Figure A2.3. Average body weight (A) and fat mass composition (B) of C57BL6 female mice. Data represent mean±SE (n=10) for each group: LD (lean control diet); HF (high fat diet); HF+α (high fat diet + 500 mg α-TEA/kg diet); HF+Cur (high fat diet + 500 mg curcumin/kg diet); and HF Combo (high fat diet + 500 mg α-TEA + 500 mg curcmumin/kg diet). [a] Significant difference from the high fat diet group ($P<0.05$, t-test).

A2.2.4. α-TEA improved obesity-associated glycemic status and insulin sensitivity in the DIO model.

We determined if 500 ppm α-TEA in diet could improve glycemic status in DIO mice. On day 80, mice received a glucose tolerance test for evaluating glycemic status. As shown in Figure A2.4.A & B, all treatments including α-TEA, curcumin and combination of α-TEA+curcumin significantly improved glucose tolerance in C56BL6 DIO mice. Improved insulin sensitivity was only demonstrated in α-TEA group by HOMA-IR value but not in the other groups; however, no statistically significant difference was observed between HF and HF+α-TEA.

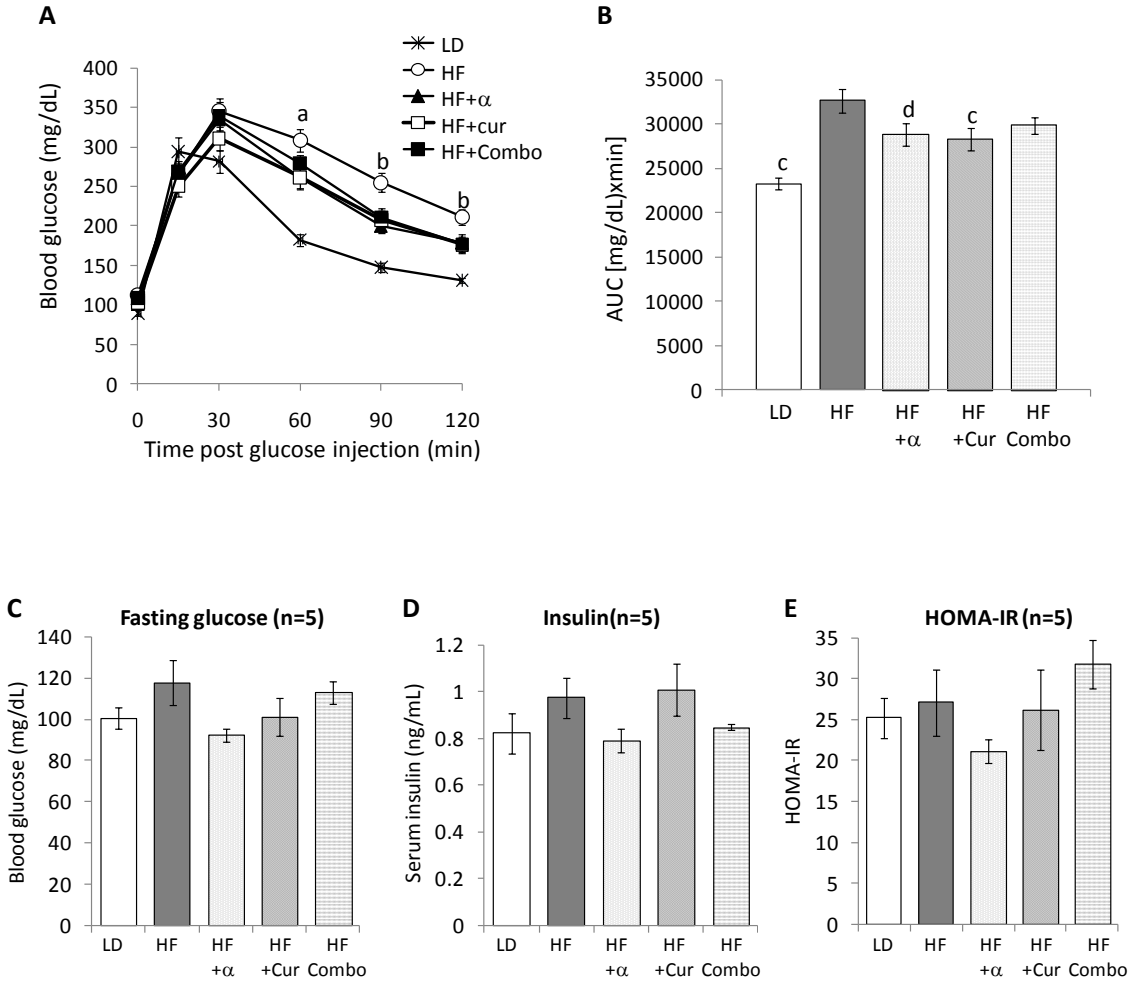

Figure A2.4. Effects of α-TEA on glucose tolerance and insulin sensitivity in DIO mice. A & B, On day 80 after feeding designated diets, mice were fasted overnight and injected with 20% glucose intraperitoneally (2 g/kg). Thereafter, the blood glucose levels were measured at indicated time points (A). The area under the curve from 0 to 120 min (mg/dL X min) was calculated for each group (B). Data represent mean±SE (n=10). [a] Significant difference from all groups except HF+Combo (*P<0.05, t-test*); [b] Significant difference from all groups (*P<0.05, t-test*); [c] Significant difference from HF group (*P<0.05, t-test*); and [d] Significant difference from HF group (*P=0.0512, t-test*). C, D & E, On day 91, mice were sacrificed after overnight fasting and the blood was collected and measured for glucose level and serum insulin level. HOMA-IR was calculated as described in A2.2. Materials and methods. Data represent mean±SE (n=5).

A2.3. Discussion

Our goal was to examine the possibility that α-TEA, a chemopreventive agent that can activate AMPK might impact obesity related disorders. Toward this goal, we tested α-TEA effects on mouse macrophages and adipocytes in cell culture; as well as in a diet-induced obese (DIO) mouse model. Data presented here demonstrated that: 1) α-TEA inhibited proliferation, induced apoptosis and reduced NF-κB expression in RAW264.7 murine macrophages in cell culture; 2) α-TEA caused activation of AMPK, decreased NF-κB expression and increased IκB expression in 3T3-L1 adipocytes in cell culture; and 3) 500 ppm α-TEA in diet did not affect body weight or fat mass; however, α-TEA did improve glucose and insulin sensitivity in DIO mice.

Although the mechanism(s) of how α-TEA improved glycemic status in DIO animal is not clear, it is possible that α-TEA prevents insulin resistance by inhibiting TNF-α stimulation of proinflammatory signals based on cell culture studies using 3T3-L1 adipocytes. Further tissue analyses from the DIO mouse study are needed to gain further mechanistic insights, and dose-dependent efficacy studies using DIO mice, *ob*/*ob* obese or *db*/*db* diabetic mouse models are also needed to confirm preventive or therapeutic effects of α-TEA on obesity related complications.

A2.4. References

1. Must A, Spadano J, Coakley EH, Field AE, Colditz G, Dietz WH (1999) The disease burden associated with overweight and obesity. *JAMA* 282(16):1523-1529.

2. Ferrante AW Jr. (2007) Obesity-induced inflammation: a metabolic dialogue in the language of inflammation. *J Intern Med* 262(4): 408-414.

3. Chakrabarti SK, Cole BK, Wen Y, Keller SR, Nadler JL (2009) 12/15-lipoxygenase products induce inflammation and impair insulin signaling in 3T3-L1 adipocytes. *Obesity (Silver Spring)* 17(9): 1657-1663.

4. Bastard JP, Maachi M, Lagathu C, Kim MJ, Caron M, Vidal H, Capeau J, Feve B (2006) Recent advances in the relationship between obesity, inflammation, and insulin resistance. *Eur Cytokine Netw* 17(1): 4-12.

5. Nieto-Vazquez I, Fernández-Veledo S, Krämer DK, Vila-Bedmar R, Garcia-Guerra L, Lorenzo M (2008) Insulin resistance associated to obesity: the link TNF-α. *Arch Physiol Biochem* 114(3): 183-194.

6. Strissel KJ, Stancheva Z, Miyoshi H, Perfield JW, DeFuria J, Jick Z, Greenberg AS, Obin MS (2007) Adipocyte death, adipose tissue remodeling, and obesity complications. *Diabetes* 56(12): 2910-2918.

7. Misra P (2008) AMP activated protein kinase: a next generation target for total metabolic control. *Expert Opin Ther Targets* 12(1): 91-100.

8. Greenberg AS, Obin MS (2006) Obesity and the role of adipose tissue in inflammation and metabolism. *Am J Clin Nutr*. 83(2): 461S-465S.

9. Jeong HW, Hsu KC, Lee JW, Ham M, Huh JY, Shin HJ, Kim WS, Kim JB (2009) Berberine suppresses proinflammatory responses through AMPK activation in macrophages. *Am J Physiol Endocrinol Metab* 296(4): E955-964.

10. Moon HS, Chung CS, Lee HG, Kim TG, Choi YJ, Cho CS (2007) Inhibitory effect of (-)-epigallocatechin-3-gallate on lipid accumulation of 3T3-L1 cells. *Obesity (Silver Spring)* 15(11): 2571-2582.

11. Ahn J, Lee H, Kim S, Ha T (2007) Resveratrol inhibits TNF-alpha-induced changes of adipokines in 3T3-L1 adipocytes. *Biochem Biophys Res Commun* 364(4): 972-977.

12. Yu W, Sanders BG, Kline K (2003) *RRR*-α-tocopheryl succinate-induced apoptosis of human breast cancer cells involves Bax translocation to mitochondria. *Cancer Res* 63: 2483-2491.

13. Ito A, Suganami T, Miyamoto Y, Yoshimasa Y, Takeya M, Kamei Y, Ogawa Y. (2007) Role of MAPK phosphatase-1 in the induction of monocyte chemoattractant protein-1 during the course of adipocyte hypertrophy. *J Biol Chem* 282(35): 25445-52.

14. Gonzales AM, Orlando RA (2008) Curcumin and resveratrol inhibit nuclear factor-kappaB-mediated cytokine expression in adipocytes. *Nutr Metab (Lond)* 5(17): 1-13.

15. Fasshauer M, Klein J, Kralisch S, Klier M, Lossner U, Bluher M, Paschke R (2004) Monocyte chemoattractant protein 1 expression is stimulated by growth hormone and interleukin-6 in 3T3-L1 adipocytes. *Biochem Biophys Res Commun* 317(2): 598-604.

16. Hong J, Holcomb VB, Tekle SA, Fan B, Núñez NP (2010) Alcohol consumption promotes mammary tumor growth and insulin sensitivity. *Cancer Lett* 294(2): 229-35.

17. Ejaz A, Wu D, Kwan P, Meydani M (2009) Curcumin inhibits adipogenesis in 3T3-L1 adipocytes and angiogenesis and obesity in C57/BL mice. *J Nutr* 139 (5): 919-925.

Bibliography

1. Min KC. (2007) Structure and Function of alpha-tocopherol transfer protein: implications for vitamin E metabolism and AVED. *Vitam Horm* 76: 24-40.

2. Mustacich DJ, Bruno RS, Traber MG. (2007) Vitamin E. *Vitam Horm* 76: 1-21.

3. Kline K, Lawson KA, Yu W, Sanders BG. (2007) Vitamin E and cancer. *Vitam Horm* 76: 436-454.

4. Sen CK, Khanna S, Rink C, Roy S. (2007) Tocotrienol: The emerging face of natural vitamin E. *Vitam Horm* 76: 203-261.

5. Inokuchi H, Hirokane H, Tsuzuki T, Nakagawa K, Igarashi M, Miyazawa T. (2003) Anti-angiogenic activity of tocotrienol. *Biosci Biotechnol Biochem* 67(7): 1623-1627.

6. Nakagawa K, Shibata A, Yamashita S, Tsuzuki T, Kariya J, Oikawa S, Miyazawa T. (2007) In vivo angiogenesis is suppressed by unsaturated vitamin E, tocotrienol. *J Nutr* 137: 1938-1943.

7. Galli F, Cristina Polidori M, Stahl W, Mecocci P, Kelly FJ. (2007) Vitamin E biotransformation in humans. *Vitam Horm* 76: 264-277.

8. Stocker A. (2004) Molecular mechanisms of vitamin E transport. *Ann N Y Acad Sci* 1031: 44-59.

9. Khanna S, Patel V, Rink C, Roy S, Sen CK. (2005) Delivery of orally supplemented α-tocotrienol to vital organs of rats and tocopherol-transport protein deficient mice. *Free Radic Biol Med* 39(10): 1310-1319.

10. Brigelius-Flohé R. (2005) Induction of drug metabolizing enzymes by vitamin E. *J Plant Physiol* 162(7): 797-802.

11. Lippman SM, Klein EA, Goodman PJ *et al.* (2009) Effect of selenium and vitamin E on risk of prostate cancer and other cancers: the selenium and vitamin E cancer prevention trail (SELECT). *JAMA* 301(1): 39-51.

12. Hensley K, Benaksas EJ, Bolli R, Comp P, Grammas P, Hamdheydari L, Mou S, Pye QN, Stoddard MF, Wallis G, Williamson KS, West M, Wechter WJ, Floyd

RA.(2004) New perspectives on vitamin E: γ-tocopherol and carboxyelthylhydroxy-chroman metabolites in biology and medicine. *Free Radic Biol Med* 36(1): 1-15.

13. Huang HY, Alberg AJ, Norkus EP, Hoffman SC, Comstock GW, Helzlsouer KJ. (2003) Prospective study of antioxidant micronutrients in the blood and the risk of developing prostate cancer. *Am J Epidemiol* 157(4): 335-344.

14. Jiang Q, Wong J, Fyrst H, Saba JD, Ames BN. (2004) γ-Tocopherol or combinations of vitamin E forms induce cell death in human prostate cancer cells by interrupting sphingolipid synthesis.. *Proc Natl Acad Sci U S A* 101(51): 17825-17830.

15. Campbell SE, Stone WL, Lee S, Whaley S, Yang H, Qui M, Goforth P, Sherman D, McHaffie D, Krishnan K.(2006) Comparative effects of *RRR*-α- and *RRR*-γ-tocopherol on proliferation and apoptosis in human colon cancer cell lines. *BMC Cancer* 6(13): 1-14.

16. Yu W, Park SK, Jia L, Tiwary R, Scott WW, Li J, Wang P, Simmons-Menchaca M, Sanders BG, Kline K. (2008) *RRR*-γ-tocopherol induces human breast cancer cells to undergo apoptosis via death receptor 5 (DR5)-mediated apoptotic signaling. *Cancer Lett* 259(2): 165-176.

17. Yu W, Jia L, Wang P, Lawson KA, Simmons-Menchaca M, Park SK, Sun L, Sanders BG, Kline K. (2008) In vitro and in vivo evaluation of anticancer actions of natural and synthetic vitamin E forms. *Mol Nutr Food Res* 52(4): 447-456.

18. Yu W, Jia L, Park SK, Li J, Gopalan A, Simmons-Menchaca M, Sanders BG, Kline K.(2009) Anticancer actions of natural and synthetic vitamin E forms: *RRR*-α-tocopherol blocks the anticancer actions of γ-tocopherol. *Mol Nutr Food Res* 53(12): 1573-1581.

19. Guthrie N, Gapor A, Chambers AF, Carroll KK. (1997) Inhibition of proliferation of estrogen receptor-negative MDA-MB-435 and -positive MCF-7 human breast cancer cells by palm oil tocotrienols and tamoxifen, alone and in combination. *J Nutr*127(3): 5445-5485.

20. Nesaretnam K. (2008) Multitargeted therapy of cancer by tocotrienols. *Cancer Lett* 269: 388-395.

21. Xu WL, Liu JR, Liu HK, Qi GY, Sun XR, Sun WG, Chen BQ . (2009) Inhibition of proliferation and induction of apoptosis by γ-tocotrienol in human colon carcinoma HT-29 cells. *Nutrition* 25(5): 555-566.

22. Sun W, Xu W, Liu H, Liu J, Wang Q, Zhou J, Dong F, Chen B. (2009) γ-Tocotrienol induces mitochondria-mediated apoptosis in human gastric adenocarcinoma SGC-7901 cells. *J Nutr Biochem* 20(4): 276-284.

23. Sakai M, Okabe M, Tachibana H, Yamada K. (2006) Apoptosis induction by γ-tocotrienol in human hepatoma Hep3G cells. *J Nutr Biochem* 17(10): 672-676.

24. Wada S, Satomi Y, Murakoshi M, Noguchi N, Yoshikawa T, Noshino H.(2005) Tumor suppressive effects of torotrienol in vivo and in vitro. *Cancer Lett* 229: 181-191.

25. Hussein D, Mo H. (2009) δ-Tocotrienol-mediated suppression of the proliferation of human PANC-1, mIA-PaCa-2 and BxPC-3 pancreatic carcinoma cells. *Pancreas* 38(4): e124-136.

26. Srivastava JK, Gupta S. 2006, Tocotrienol-rich fraction of palm oil induces cell cycle arrest and apoptosis selectively in human prostate cancer cells. *Biochem Biophys Res Commun* 346(2): 447-453.

27. McIntyre BS, Briski KP, Gapor A, Sylvester PW. (2000) Antiproliferative and apoptotic effects of tocopherols and tocotrienols on preneoplastic and neoplastic mouse mammary epithelial cells. *Exp Biol Med (Maywood)* 224(4): 292-301.

28. Shah S, Gapor A, Sylvester PW. (2003) Role of caspase-8 activation in mediating vitamin E-induced apoptosis in murine mammary cancer cells. *Nutr Cancer* 45(2): 236-246.

29. Shah JS, Sylvester PW (2004) γ-Tocotrienol inhibits neoplastic mammary epithelial cell proliferation by decreasing Akt and nuclear factor kB activity. *Exp Biol Med (Maywood)* 230: 235-241.

30. Shun MC, Yu W, Gapor A, Parsons R, Atkinson J, Sanders BG, Kline K. (2004) Pro-apoptotic mechanisms of action of a novel vitamin E analog (α-TEA) and a naturally occurring form of vitamin E (delta-tocotrienol) in MDA-MB-435 human breast cancer cells. *Nutr Cancer* 48(1): 95-105.

31. Elangovan S, Hsieh TC, Wu JM. (2008) Growth inhibition of human MDA-MB-231 breast cancer cells by delta-tocotrienol is associated with loss of cyclin D1/CDK4 expression and accompanying changes in the state of phosphorylation of the retinoblastoma tumor suppressor gene product. *Anticancer Res* 28(5A): 2641-2647.

32. Nesaretnam K, Ambra R, Selvaduray R, Radhakrishnam A, Reinamm K, Razak G, Virgili F. (2004) Tocotrienol-rich fraction from palm oil affects gene expression in tumors resulting from MCF-7 cell inoculation in athymic mice. *Lipids* 39(5): 459-467.

33. McAnally JA, Gupta J, Sodhani S, Bravo L, Mo H. (2007) Tocotrienols potentiate lovastatin-mediated growth suppression in vitro and in vivo. *Exp Biol Med (Maywood)* 232(4): 523-531.

34. Netscher T. (2007) Synthesis of vitamin E. *Vitam Horm* 76: 155-202.

35. Harris PL, Ludwig MI. (1949) Vitamin E potency of alpha-tocopherol and α-tocopherol esters. *J Biol Chem* 180: 611-615.

36. Cheeseman KH, Holley AE, Kelly FJ, Wasil M, Hughes L, Burton G. (1995) Biokinetics in humans of *RRR*-α-tocopherol: the free phenol, acetate ester, and succinate ester forms of vitamin E. *Free Rad Biol Med* 19(5): 591-598.

37. Tomasetti M, Neuzil J. (2007) Vitamin E analogues and immune response in cancer treatment. *Vitam Horm* 76: 463-491.

38. Anderson K, Simmons-Menchaca M, Lawson KA, Atkinson J, Sanders BG and Kline K. (2004) Differential response of human ovarian cancer cells to induction of apoptosis by vitamin E succinate and vitamin E analogue. *Cancer Res* 64: 4263-4269.

39. Hahn T, Szabo L, Gold M, Ramanathapuram L, Hurley LH, Akporiaye ET. (2006) Dietary administration of the proapoptotic vitamin E analogue α-tocopheryl-oxyacetic acid inhibits metastatic murine breast cancer. *Cancer Res* 66(19): 9374-9378.

40. Lawon KA, Anderson K, Menchaca M, Atkinson J, Sun LZ, Knight V, Gilbert BE, Conti C, Sanders BG, Kline K. (2003) Novel vitamin E analogue decreases

syngeneic mouse mammary tumor burden and reduces lung metastasis. *Mol Cancer Ther* 2: 437-444.

41. Zhang S, Lawson KA, Simmons-menchaca M, Sun LZ, Sanders BG, Kline K. (2004) Vitamin E analog α-TEA and celecoxib alone and together reduce human MDA-MB-435-FL-GFP brast cancer burden and metastasis in nude mice. *Breast Cancer Res Treat* 87: 111-121.

42. Jia L, Yu W, Wang P, Sanders BG, Kline K. (2008) In vivo and in vitro studies of anticacner actions of α-TEA for human prostate cancer cells. *Prostate* 68: 849-860.

43. Anderson K, Lawson KA, Simmons-Menchaca M, Sun LZ, Sanders BG, Kline K. (2004) α-TEA plus cisplatin reduces human cisplatin-resistant ovarian cancer cell tumor burden and metastasis. *Exp Biol Med (Maywood)* 229(11): 1169-1176.

44. Riedel SB, Fischer SM, Sanders BG, Kline K. (2008) Vitamin E analog, α-tocopherol ether-linked acetic acid analog, alone and in combination with celecoxib, reduces multiplicity of ultraviolet-induced skin cancers in mice. *Anticancer Drugs* 19(2): 175-181.

45. Lawson KA, Anderson K, Snyder RM, Simmons-Menchaca M, Atkinson J, Sun LZ, Bandyopadhyay A, Knight V, Gilbert BE, Sanders BG, Kline K. (2004) Novel vitamin E analogue and 9-nitro-camptothecin administered as liposome aerosols decrease syngeneic mouse mammary tumor burden and inhibit metastasis. *Cancer Chemother Pharmacol* 54(5): 421-431.

46. Latimer P, Menchaca M, Snyder RM, Yu W, Gilbert BE, Sanders BG, Kline K. (2009) Aerosol delivery of liposomal formulated paclitaxel and vitamin E analog reduces murine mammary tumor burden and metastases. *Exp Biol Med (Maywood)* 234(10): 1244-1252.

47. Wang P, Jia L, Sanders BG, Kline K. (2007) Liposomal or nanoparticle α-TEA reduced 66cl-4 murine mammary cancer burden and metastasis. *Drug Deliv* 14(8): 497-505.

48. Yu W, Shun MC, Anderson K, Chen H, Sanders BG, Kline K. (2006) α-TEA inhibits survival and enhances death pathways in cisplatin sensitive and resistant human ovarian cancer cells. *Apoptosis* 11(10): 1813-1823.

49. Shun MC, Yu W, Park SK, Sanders BG, Kline K.(2010) Downregulation of Epidermal Growth Factor Receptor Expression Contributes to α-TEA's Proapoptotic Effects in Human Ovarian Cancer Cell Lines. *J Oncol* Article ID 824571 Epub: 1-11.

50. Jia L, Yu W, Wang P, Li J, Sanders BG, Kline K. (2008) Critical roles for JNK, c-Jun, and Fas/FasL-Signaling in vitamin E analog-induced apoptosis in human prostate cancer cells. *Prostate* 68(4): 427-4441.

51. Wang P, Yu W, Hu Z, Jia L, Iyer VR, Sanders BG, Kline K. (2008) Involvement of JNK/p73/NOXA in vitamin E analog-induced apoptosis of human breast cancer cells. *Mol Carcinog* 47(6): 436-445.

52. Xu C, Bailly-Maitre B, Reed JC. (2005) Endoplasmic reticulum stress: cell life and death decisions. *J Clin Invest* 115(10): 2656-2564.

53. Kim I, Xu W, Reed JC. (2008) Cell death and endoplasmic reticulum stress: disease relevance and therapeutic opportinities. *Nat Rev Drug Discov* 7(12): 1013-1030.

54. Healy SJ, Gorman AM, Mousavi-Shafaei P, Gupta S, Samali A. (2009) Targeting the endoplasmic reticulum-stress response as an anticancer strategy. *Eur J Pharmacol* 625: 234-246.

55. Raven JF, Koromilas AE. (2008) PERK and PKR: old kinases learn new tricks. *Cell Cycle* 7(9): 1146-1150.

56. Ron D, Walter P. (2007) Signal integration in the endoplasmic reticulum unfolded protein response. *Nat Rev Mol Cell Biol* 8(7): 519-529.

57. Takeda K, Noguchi T, Naguro I, Ichijo H. (2008) Apoptosis signal-regulating kinase 1 in stress and immune response. *Annu Rev Pharmacol Toxicol* 48: 199-225.

58. Szegezdi E, Logue SE, Gorman AM, Samali A. (2006) Mediators of endoplasmic reticulum stress-induced apoptosis. *EMBO Rep* 7(9): 880-885.

59. Koong AC, Chauhan V, Romero-Ramirez L. (2006) Targeting XBP-1 as a novel anti-cancer strategy. *Cancer Biol Ther* 5(7): 756-759.

60. Marciniak SJ, Yun CY, Oyadomari S, Novoa I, Zhang Y, Jungreis R, Nagata K, Harding HP, Ron D. (2004) CHOP induces death by promoting protein synthesis and oxidation in the stressed endoplasmic reticulum. *Genes Dev* 18(24): 3066-3077.

61. Oyadomari S, Mori M. (2004) Roles of CHOP/GADD153 in endoplasmic reticulum stress. *Cell Death Differ* 11(4): 381-389.

62. Gotoh T, Oyadomari S, Mori K, Mori M. (2002) Nitric oxide-induced apoptosis in RAW 264.7 macrophages is mediated by endoplasmic reticulum stress pathway involving ATF6 and CHOP. *J Biol Chem* 277(14): 12343-12350.

63. Oyadomari S, Koizumi A, Takeda K, Gotoh T, Akira S, Araki E, Mori M. (2002) Targeted disruption of the Chop gene delays endoplasmic reticulum stress-mediated diabetes. *J Clin Invest* 109(4): 525-532.

64. McCullough KD, Martindale JL, Klotz LO, Aw TY, Holbrook NJ. (2001) Gadd153 sensitizes cells to endoplasmic reticulum stress by down-regulating Bcl2 and perturbing the cellular redox state. *Mol Cell Biol* 21(4): 1249-1259.

65. Puthalakath H, O'Reilly LA, Gunn P, Lee L, Kelly PN, Huntington ND, Hughes PD, Michalak EM, McKimm-Breschkin J, Motoyama N, Gotoh T, Akira S, Bouillet P, Strasser A. (2007) ER stress triggers apoptosis by activating BH3-only protein Bim. *Cell* 129(7): 1337-1349 .

66. Nagata S. (1997) Apoptosis by death factor. *Cell* 88(3): 355-365.

67. Elmore S. (2007) Apoptosis: a review of programmed cell death. *Toxicol Pathol* 35(4): 495-576.

68. Shepard BD, Badley AD. (2009) The biology of TRAIL and the role of TRAIL-based therapeutics in infectious diseases. *Anti-Infect Agents Med Chem* 8: 87-101.

69. Reed JC. (2006) Drug insight: cancer therapy strategies based on restoration of endogenous cell death mechanisms. *Nat Clin Pract Oncol* 3(7): 388-398.

70. Li J, Yuan J. (2008) Caspases in apoptosis and beyond. *Oncogene* 27: 6194–6206.

71. Mahmood Z, Shukla Y. (2010) Death receptors: targets for cancer therapy. *Exp Cell Res* 316(6): 887-899.

72. Kurokawa M, Kornbluth S. (2009) Caspases and kinases in a death grip. *Cell* 138(5): 838-854.

73. Kimberley FC, Screaton GR. (2004) Following a TRAIL: update on a ligand and its five receptors. *Cell Res* 14(5): 359-372.

74. Mérino D, Lalaoui N, Morizot A, Solary E, Micheau O. (2007) TRAIL in cancer therapy: present and future challenges. *Expert Opin Ther Targets* 11(10): 1299-1314.

75. Mahalingam D, Szegezdi E, Keane M, Jong S, Samali A. (2009) TRAIL receptor signalling and modulation: Are we on the right TRAIL? *Cancer Treat Rev* 35(3): 280-288.

76. Zhang Y, Zhang B. (2008) TRAIL resistance of breast cancer cells is associated with constitutive endocytosis of deaht receptors 4 and 5. *Mol Cancer Res* 6(12): 1861-1871.

77. Kim K, Fisher MJ, Xu SQ, el-Deiry WS. (2000) Molecular determinants of response to TRAIL in killing of normal and cancer cells. *Clin Cancer Res* 6(2): 335-346.

78. Festuccia C, Gravina GL, D'Alessandro AM, Millimaggi D, Di Rocco C, Dolo V, Ricevuto E, Vicentini C, Bologna M. (2008) Downmodulation of dimethyl transferase activity enhances tumor necrosis factor-related apoptosis-inducing ligand-induced apoptosis in prostate cancer cells. *Int J Oncol* 33(2): 381-388.

79. Lawson KA, Anderson K, Simmons-Menchaca M, Atkinson J, Sun L, Sanders BG, Kline K (2004) Comparison of vitamin E derivatives α-TEA and VES in reduction of mouse mammary tumor burden and metastasis. *Exp Biol Med (Maywood)* 229(9): 954-963.

80. Yu W, Israel K, Liao QY, Aldaz CM, Sanders BG, Kline K. (1999) Vitamin E succinate (VES) induces Fas sensitivity in human breast cancer cells: role for Mr 43,000 Fas in VES-triggered apoptosis. *Cancer Res* 59(4): 953-961.

81. Staton CA, Stribbling SM, Tazzyman S, Hughes R, Brown NJ, Lewis CE. (2004) Current methods for assaying angiogenesis in vitro and in vivo. *Int J Exp Path* 85: 233-248.

82. Yamagishi S, Yonekura H, Yamamoto Y, Katsuno K, Sato F, Mita I, Ooka H, Satozawa N, Kawakami T, Nomura M, Yamamoto H. (1997) Advanced glycation end products-driven angiogenesis in vitro. *J of Biol Chem* 272(13): 8723–8730.

83. Subcommittee on laboratory animal nutrition, committee on animal nutrition, board on agriculture, and national research council. (1995) Nutrient Requirements of

Laboratory Animals (4th revised edition). National Academy Press. Washington DC.

84. Derelanko MJ (2000) Toxicologist's Pocket Handbook. Boca Raton, FL : CRC Press, p16.

85. Vlahovic G, Ponce AM, Rabbani Z, Salahuddin FK, Zgonjanin L, Spasojevic I, Vujaskovic Z, Dewhirst MW. (2005) Treatment with Imatinib improves drug delivery and efficacy in NSCLC xenografts. *Br J Cancer* 97: 735-740.

86. Birringer M, EyTina JH, Salvatore BA, Neuzil J. (2003) Vitamin E analogues as inducers of apoptosis: structure-function relation. *Br J Cancer* 88(12): 1948-1955.

87. Constantinou C, Hyatt JA, Vraka PS, Papas A, Papas KA, Neophytou C, Hadjivassiliou V, Constantinou AI. (2009) Induction of caspase-independent programmed cell death by vitamin E natural homologs and synthetic derivatives. *Nutr Cancer* 61(6): 864-874.

88. Ferrara N, Kerbel RS. (2005) Angiogenesis as a therapeutic target. *Nature* 438(7070): 967-974.

89. Auerbach R, Lewis R, Shinners B, Kubai L, Akhtar N. (2003) Angiogenesis assays: a critical overview. *Clin Chem* 49(1): 32-40.

90. Dong LF, Swettenham E, Eliasson J, Wang XF, Gold M, Medunic Y, Stantic M, Low P, Prochazka L, Witting PK, Turanek J, Akporiaye ET, Ralph SJ, Neuzil J. (2007) Vitamin E analogues inhibit angiogenesis by selective induction of apoptosis in proliferating endothelial cells: the role of oxidative stress. *Cancer Res* 67(23): 11906-11913.

91. Yu W, Simmons-Manchaca M, Gapor A, Sanders BG, Kline K. (1999) Induction of apoptosis in human breast cancer cells by tocopherols and tocotrienols. *Nut Cancer* 33(1): 26-32.

92. Das S, Nesaretnam K, Das DK. (2007) Tocotrienols in cardioprotection. *Vitam Horm* 76: 419-433.

93. Inokuchi H, Hirokane H, Tsuzuki T, Nakagawa K, Igarashi M, Miyazawa T. (2003) Anti-angiogenic activity of tocotrienol. *Biosci Biotechnol Biochem* 67(7): 1623-1627.

94. Yamaguchi H, Wang HG . (2004) CHOP is involved in endoplasmic reticulum stress-induced apoptosis by enhancing DR5 expression in human carcinoma cells. *J Biol Chem* 279(44): 45495-45502.

95. Zou W, Yue P, Khuri FR, Sun SY. (2008) Coupling of endoplasmic reticulum stress to CDDO-Me-induced upregulation of death receptor 5 via a CHOP-dependent mechanism involving JNK activation. *Cancer Res* 68(8): 7484-7492.

96. Zang C, Liu H, Bertz J, Possinger K, Koeffler PK, Elstner E, Eucker J. (2009) Induction of endoplasmic reticulum stress response by TZD19, a novel dual ligand for peroxisome proliferator-activated receptor α/γ, in human breast cancer cells. *Mol Cancer Ther* 8(8): 2296-2306.

97. Meng X, Leyva ML, Jenny M, Gross I, Benosman S, Fricker B, Harlepp S, Hébraud P, Boos A, Wlosik P, Bischoff P, Sirlin C, Pfeffer M, Loeffler JP, Gaiddon C. (2009) A ruthenium-containing organometallic compound reduces tumor growth through induction of the endoplasmic reticulum stress gene CHOP. *Cancer Res* 69(13): 5458-5466.

98. Franken NA, Rodermond HM, Stap J, Haveman J, Van Bree C. (2006) Clonogenic assay of cells in vitro. *Nature Protocols* 1(5): 2315~2319.

99. Yu W, Sanders BG, Kline K. (2003) *RRR*-α-tocopheryl succinate-induced apoptosis of human breast cancer cells involves Bax translocation to mitochondria. *Cancer Res* 63: 2483-2491.

100. Nelson JD, Denisenko O, Bomsztyk K. (2006) Protocol for the fast chromatin immunoprecipitation (ChIP) method. *Nature Protocols* 1(1): 179-185.

101. Abdelrahim M, Newman K, Vanderlaag K, Samudio I, Safe S. (2006) 3,3'-Diindolylmethane (DIM) and its derivatives induce apoptosis in pancreatic cancer cells through endoplasmic reticulum stress-dependent upregulation of DR5. *Carcinogenesis* 27(4): 717-728.

102. Jiang H-Y, Wek SA, McGrath BC, Lu D, Hai T, Harding HP, Wang X, Ron D, Cavener DR, Wek RC. (2004) Activating transcription factor 3 is integral to the eukaryotic initiation factor 2 kinase stress response. *Mol Cell Biol* 24(3): 1365-1377.

103. Bijur GN, Jope RS. (2001) Proapoptotic stimuli induce nuclear accumulation of glycogen synthase kinase-3. . *J Biol Chem* 276(40): 37436-37442.

104. Wang Q,He Z, Zhang J, Wang Y, Wang T, Tong S, Wang L, Wang S, Chen Y. (2005) Overexpression of endoplasmic reticulum molecular chaperone GRP94 and GRP78 in human lung cancer tissues and its significance. *Cancer Detect Prev* 29(6): 544-551.

105. Calfon M, Zeng H, Urano F, Till JH, Hubbard SR, Harding HP, Clark SG, Ron D. (2002) IRE1 couples endoplasmic reticulum load to secretory capacity by processing the XBP-1 mRNA. *Nature* 415: 92-96.

106. Boyce M, Bryant KF, Jousse C, Long K, Harding HP, Scheuner D, Kaufman RJ, Ma D, Coen DM, Ron D, Yuan J. (2005) A selective inhibitor of eIF2a dephosphorylation protects cells from ER stress. *Science* 307: 935-939.

107. Miyazawa T, Shibata A, Sookwong P, Kawakami Y, Eitsuka T, Asai A, Oikawa S, Nakagawa K. (2009) Antiangiogenic and anticancer potential of unsaturated vitamin E (tocotrienol). *J Nut Biochem* 20: 79-86.

108. Ishibashi M, Ohtsuki T. (2008) Studies on search for bioactive natural products targeting TRAIL signaling leading to tumor cell apoptosis. *Med Res Rev* 28(5): 688-714.

109. Wasielewski M, Elstrodt F, Klijn JG, Berns EM, Schutte M . (2006) Thirteen new p53 gene mutants identified among 41 human breast cancer cell lines. *Breast Cancer Res Treat* 99: 97–101.

110. Chen CL, Lin CF, Chang WT, Huang WC, Teng CF, Lin YS. (2008) Ceramide induces p38 MAPK and JNK activation through a mechanism involving a thioredoxin-interacting protein-mediated pathway. *Blood* 111(8): 4365-4374.

111. Yoshida H, Haze K, Yanagi H, Yura T, Mori K. (1998) Identification of the cis-acting endoplasmic reticulum stress response element responsible for transcriptional induction of mammalian glucose-regulated proteins. *J Biol Chem* 273(50): 33741-33749.

112. Wali VB, Bachawal SV, Sylvester PW. (2009) Endoplasmic reticulum stress mediates -tocotrienol-induced apoptosis in mammary tumor cells. *Apoptosis* 14: 1366-1377.

113. Li J, Yu W, Tiwary R, Park SK, Xiong A, Sanders BG, Kline K. (2010) α-TEA induced death receptor dependent apoptosis involves activation of acid

sphingomyelinase and elevated ceramide-enriched cell surface membranes. *Submitted.*

114. Mahoney MC, Bevers T, Linos E, Willett WC. (2008) Opportunities and strategies for breast cancer prevention through risk reduction. *CA Cancer J Clin* 58: 347-371.

115. Chlebowski RT. (2002) Breast cancer risk reduction: strategies for women at increased risk. *Annu Rev Med* 53: 519-540.

116. Brody JG, Rudel RA, Michels KB, Moysich KB, Bernstein L, Attfield KR, Gray S. (2007) Environmental pollutants, diet, physical activity, body size, and breast cancer: where do we stand in research to identify opportunities for prevention? *Cancer* 109(12): 2627-2634.

117. Nomura AM, Ziegler RG, Stemmermann GN, Chyou PH, Craft NE. (1997) Serum micronutrients and upper aerodigestive tract cancer. Cancer *Epidemiol Biomarkers Prev* 6(6): 407-412.

118. Nomura AM, Stemmermann GN, Lee J, Craft NE. (1997) Serum micronutrients and prostate cancer in Japanese Americans in Hawaii. *Cancer Epidemiol Biomarkers Prev* 6(7): 489-491.

119. Gysin R, Azzi A, Visarius T. (2002) γ-Tocopherol inhibits human cancer cell cycle progression and cell proliferation by down-regulation of cyclins. *FASEB J* 16(14): 1952-1954.

120. Campbell SE, Stone WL, Whaley SG, Qui M, Krishnan K. (2003) γ-Tocopherol upregulates peroxisome proliferator activated receptor (PPAR)-γ expression in SW 480 human colon cancer cell lines. *BMC Cancer* 3(25): 1-13.

121. Galli F, Stabile AM, Betti M, Conte C, Pistilli A, Rende M, Floridi A, Azzi A. (2004) The effect of α- and γ-tocopherol and their carboxyethyl hydroxychroman metabolites on prostate cancer cell proliferation. *Arch Biochem Biophys* 423(1): 97-102.

122. Cossarizza A, Baccarani-Contri M, Kalashnikova G, Franceschi C.(1993) A new method for the cytofluorimetric analysis of mitochondrial membrane potential using the J-aggregate forming lipophilic cation 5,5',6,6'-tetrachloro-1,1',3,3'-tetraethyl-benzimidazolcarbocyanine iodide (JC-1). *Biochem Biophys Res Commun* 197(1): 40-45.

123. Waterhouse NJ, Trapani JA. (2003) A new quantitative assay for cytochrome c release in apoptotic cells. *Cell Death Differ* 10(7): 853-857.

124. Martin JH, Potthoff A, Ledig S, Cornberg M, Jandl O, Manns MP, Kubicka S, Flemming P, Athmann C, Beil W, Wagner S. (2004) Effect of H. pylori on the expression of TRAIL, FasL and their receptor subtypes in human gastric epithelial cells and their role in apoptosis. *Helicobacter* 9(5): 371-386.

125. Tirmenstein MA, Watson BW, Haar NC, Fariss MW. (1998) Sensitive method for measuring tissue alpha-tocopherol and alpha-tocopheryloxybutyric acid by high-performance liquid chromatography with fluorometric detection. *J Chromatogr B Biomed Sci Appl* 707(1-2):308-11

126. Keane MM, Ettenberg SA, Nau MM, Russell EK, Lipkowitz S. (1999) Chemotherapy augments TRAIL-induced apoptosis in breast cell lines. *Cancer Res* 59(3): 734-741.

127. Jiang Q, Wong J, Ames BN. (2004) γ-Tocopherol induces apoptosis in androgen-responsive LNCaP prostate cancer cells via caspase-dependent and independent mechanisms. *Ann N Y Acad Sci* 1031: 399-400.

128. Zou W, Liu X, Yue P, Zhou Z, Sporn MB, Lotan R, Khuri FR, Sun SY. (2004) c-Jun NH2-terminal kinase-mediated up-regulation of death receptor 5 contributes to induction of apoptosis by the novel synthetic triterpenoid methyl-2-cyano-3,12-dioxooleana-1, 9-dien-28-oate in human lung cancer cells. *Cancer Res* 64(30): 7570-7578.

129. Takimoto R, El-Deiry WS. (2000) Wild-type p53 transactivates the KILLER/DR5 gene through an intronic sequence-specific DNA-binding site. *Oncogene* 19(14): 1735-1743.

130. Shetty S, Graham BA, Brown JG, Hu X, Vegh-Yarema N, Harding G, Paul JT, Gibson SB. (2005) Transcription factor NF-kappaB differentially regulates death receptor 5 expression involving histone deacetylase 1. *Mol Cell Biol* 25(13): 5404-5416.

131. Wang Y, Engels IH, Knee DA, Nasoff M, Deveraux QL, Quon KC. (2004) Synthetic lethal targeting of MYC by activation of the DR5 death receptor pathway. *Cancer Cell* 5(5): 501-512.

132. Singh TR, Shankar S, Chen X, Asim M, Srivastava RK. (2003) Synergistic interactions of chemotherapeutic drugs and tumor necrosis factor-related apoptosis-inducing ligand/Apo-2 ligand on apoptosis and on regression of breast carcinoma in vivo. *Cancer Res* 63(17): 5390-5400.

133. Shankar S, Singh TR, Chen X, Thakkar H, Firnin J, Srivastava RK. (2004) The sequential treatment with ionizing radiation followed by TRAIL/Apo-2L reduces tumor growth and induces apoptosis of breast tumor xenografts in nude mice. *Int J Oncol* 24(5): 1133-1140.

134. Ozören N, El-Deiry WS. (2003) Cell surface death receptor signaling in normal and cancer cells. *Semin Cancer Biol* 13(2): 135-147.

135. Traber MG. (2007) Vitamin E regulatory mechanisms. *Annu Rev Nutr* 27: 347-362.

136. Blatt DH, Leonard SW, Traber MG. (2001) Vitamin E kinetics and the function of tocopherol regulatory proteins. *Nutrition* 17(10): 799-805.

137. Kamal-Eldin A, Pettersson D, Appelqvist LA. (1995) Sesamin (a compound from sesame oil) increases tocopherol levels in rats fed ad libitum. *Lipids* 30(6): 499-505.

138. Yamashita K, Nohara Y, Katayama K, Namiki M.(1992) Sesame seed lignans and γ-tocopherol act synergistically to produce vitamin E activity in rats. *J Nutr* 122(12): 2440-2446.

139. Parker RS, Sontag TJ, Swanson JE. (2000) Cytochrome P450 3A-dependent metabolism of tocopherols and inhibition by sesamin. *Biochem Biophys Res Commun* 277(3): 531-534.

140. Yamada Y, Obayashi M, Ishikawa T, Kiso Y, Ono Y, Yamashita K. (2008) Dietary tocotrienol reduces UVB-induced skin damage and sesamin enhances tocotrienol effects in hairless mice. *J Nutr Sci Vitaminol* 54(2): 117-123.

141. Böhm HJ, Banner D, Bendels S, Kansy M, Kuhn B, Müller K, Obst-Sander U, Stahl M. (2004) Fluorine in medicinal chemistry. *Chembiochem* 5(5): 637-643.

142. Kirk KL. (2006) Selective Fluorination in Drug Design and Development: An Overview of Biochemical Rationales. *Curr Top Med Chem* 6(14): 1529-1543.

143. Müller K, Faeh C, Diederich F. (2007) Fluorine in pharmaceuticals: looking beyond intuition. *Science* 317(5846): 1881-1886.

Vita

Sook Kyung Park was born in Seoul, South Korea in 1973 to Sung Un Park and Ok Kum Kim. In 1996, she graduated Summa Cum Laude with Bachelor of Science in Life Science from Sogang University where she stayed for her graduate study under the supervision of Dr. Won-Sun Kim in Life Science department. After she received Master of Science degree in 1998, she worked as a research associate under the direction of Dr. Young-Ik Lee in Korea Research Institute of Bioscience and Biotechnology, the governmental research institute dedicated to biotechnology research in South Korea. She published 3 research papers during this time. From September 1999 to July 2004, she worked as a research scientist at the Toxicology Center in R&D Park of LG Life Science Ltd., a R&D-centered pharmaceutical company. She worked with Drs. Hyun-Ju Yim and Sang-Kyun Lee for *in vivo* efficacy and safety evaluation of drug candidates and participated in 5 patent applications of anti-obesity drug candidates. In September 2005, she began her pre-doctoral graduate career at the Institute of Cellular and Molecular Biology, University of Texas at Austin. She worked with Drs. Bob G Sanders and Kimberly Kline as a graduate research assistant and also taught undergraduate microbiology lab course as a teaching assistant.

Email address: park.sookkyung@gmail.com

This dissertation was typed by Sook Kyung Park